Integrative approach to interpret DYRK1A variants, leading to a frequent neurodevelopmental disorder

Jeremie Courraud, Eric Chater-Diehl, Benjamin Durand, Marie Vincent, Maria del Mar Muniz Moreno, Imène Boujelbene, Nathalie Drouot, Lauréline Genschik, Elise Schaefer, Mathilde Nizon, et al.

Integrative approach to interpret DYRK1A variants, leading to a frequent neurodevelopmental disorder

Jeremie Courraud[1,2,3,4], Eric Chater-Diehl[5], Benjamin Durand[1,2,3,4], Marie Vincent[6], Maria del Mar Muniz Moreno[1,2,3,4], Imène Boujelbene[1,2,3,4,7], Nathalie Drouot[1,2,3,4], Loréline Genschik[1,2,3,4], Elise Schaefer[8], Mathilde Nizon[6], Bénédicte Gerard[7], Marc Abramowicz[9], Benjamin Cogné[6], Lucas Bronicki[10], Lydie Burglen[11], Magalie Barth[12], Perrine Charles[13], Estelle Colin[12], Christine Coubes[14], Albert David[6], Bruno Delobel[15], Florence Demurger[16], Sandrine Passemard[17], Anne-Sophie Denommé[18], Laurence Faivre[18], Claire Feger[7], Mélanie Fradin[20], Christine Francannet[21], David Genevieve[14], Alice Goldenberg[22], Anne-Marie Guerrot[22], Bertrand Isidor[6], Katrine M. Johannesen[24,25], Boris Keren[13], Maria Kibæk[23], Paul Kuentz[18], Michele Mathieu-Dramard[26], Bénédicte Demeer[26], Julia Metreau[27], Rikke Steensbjerre Møller[24,25], Sébastien Moutton[18], Laurent Pasquier[20], Kristina Pilekær Sørensen[23], Laurence Perrin[28], Mathilde Renaud[29], Pascale Saugier[22], Marlene Rio[30], Joane Svane[23], Julien Thevenon[31], Frederic Tran Mau Them[18], Cathrine Elisabeth Tronhjem[23], Antonio Vitobello[18], Valerie Layet[32], Stéphane Auvin[33], Khaoula Khachnaoui[34], Marie-Christine Birling[35], Severine Drunat[36], Allan Bayat[23], Christèle Dubourg[37], Salima El Chehadeh[7], Christina Fagerberg[23], Cyril Mignot[12], Michel Guipponi[9], Thierry Bienvenu[38], Yann Herault[1,2,3,4], Julie Thompson[39], Marjolaine Willems[14], Jean-Louis Mandel[1,2,3,4], Rosanna Weksberg[5,40,41,42,43], *Amélie Piton[1,2,3,4,7,44]

AFFILIATIONS

[1] Institut de Génétique et de Biologie Moléculaire et Cellulaire, Illkirch 67400, France

[2] Centre National de la Recherche Scientifique, UMR7104, Illkirch 67400, France

[3] Institut National de la Santé et de la Recherche Médicale, U964, Illkirch 67400, France

[4] Université de Strasbourg, Illkirch 67400, France

[5] Genetics and Genome Biology, The Hospital for Sick Children, Toronto, ON M5G 1X8, Canada

[6] Service de Génétique Médicale, CHU de Nantes & Inserm, CNRS, Université de Nantes, l'institut du thorax, 44000 Nantes, France

[7] Unité de Génétique Moléculaire, IGMA, Hôpitaux Universitaire de Strasbourg, Strasbourg, France

[8] Service de Génétique Médicale, IGMA, Hôpitaux Universitaires de Strasbourg, Strasbourg, France

[9] Service of Genetic Medicine, University Hospitals of Geneva, Geneva, Switzerland

[10] Department of Genetics, CHEO, Ottawa, ON, Canada.

[11] Centre de référence des malformations et maladies congénitales du cervelet et Département de génétique et embryologie médicale, APHP, Sorbonne Université, Hôpital Armand Trousseau, 75012 Paris, France

[12] Pediatrics & Biochemistry and Genetics, Department, Angers Hospital, Angers, France.

[13] Genetic Department, University Hospital Pitié-Salpêtrière, AP-HP, Paris, France

[14] Département de Génétique Médicale maladies rares et médecine personnalisée, Centre de Référence Maladies Rares Anomalies du Développement, Hôpital Arnaud de Villeneuve, Université Montpellier, France

[15] Centre de Génétique Chromosomique, GHICL, Hôpital Saint Vincent de Paul, Lille, France

[16] Service de Génétique, CH Bretagne Atlantique- Vannes

[17] Département de Génétique, Hôpital Universitaire Robert Debré, APHP, Paris, France.

[18] Centre de Génétique et Centre de Référence Anomalies du développement et Syndromes malformatifs, Hôpital d'Enfants and INSERM UMR1231 GAD, FHU TRANSLAD, CHU de Dijon, Dijon, France

[19] Unité Fonctionnelle d'Innovation en Diagnostique Génomique des Maladies Rares, Pôle de Biologie, FHU-TRANSLAD, CHU Dijon Bourgogne, F-21000, Dijon, France

[20] Centre de Référence Maladies Rares, Unité Fonctionnelle de Génétique Médicale, CHU, Rennes, France

[21] Service de Génétique médicale, CHU de Clermont-Ferrand, Clermont-Ferrand, France

[22] Normandie Univ, UNIROUEN, Inserm U1245 and Rouen University Hospital, Department of Genetics and Reference Center for Developmental Disorders , F 76000, Normandy Center for Genomic and Personalized Medicine, Rouen, France

[23] Department of Clinical Genetics, Odense Denmark Hospital, Odense University Hospital, Odense, Denmark

[24]Department of Epilepsy Genetics and Personalized Treatment, The Danish Epilepsy Centre, Dianalund, Denmark

[25]Institute for Regional Health Services, University of Southern Denmark, Odense Denmark

[26] Service de Génétique Clinique, Centre de référence maladies rares, CHU d'Amiens-site Sud, Amiens, France

[27]APHP, Service de neurologie pédiatrique, Hôpital Universitaire Bicetre, Le Kremlin-Bicetre, France

[28]Department of Genetics, Robert Debré Hospital, AP-HP, Paris, France

[29] Service de Génétique Clinique et de Neurologie, Hôpital Brabois Enfants, Nancy, France

[30] Department of medical genetics and reference centre for rare intellectual disabilities. INSERM UMR 1163, Paris Descartes-Sorbonne Paris Cité University, Imagine Institute, Necker Enfants Malades Hospital, Paris, France

[31]Department of Genetics and Reproduction, Centre Hospitalo-Universitaire Grenoble-Alpes, Grenoble, France
[32] Consultations de génétique, Groupe Hospitalier du Havre, Le Havre, France
[33] Center for rare epilepsies & epilepsy unit Robert-Debré Hospital, APHP, & INSERM NeuroDiderot, Université de Paris, Paris, France
[34] Université Côte d'Azur, Inserm U1081, CNRS UMR7284, IRCAN, CHU de Nice, Nice, France
[35] ICS, Mouse Clinical Institute, Illkirch-Graffenstaden, France
[36] Département de Génétique, Hôpital Universitaire Robert Debré, Paris
[37] Laboratoire de Génétique Moléculaire, CHU Pontchaillou, UMR 6290 CNRS, IGDR, Faculté de Médecine, Université de Rennes 1, Rennes, France
[38] Molecular Genetics Laboratory, Cochin Hospital, APHP.Centre-Université de Paris, and INSERM UMR 1266, Institut de Psychiatrie et de Neurosciences de Paris, 75014 Paris, France
[39] Complex Systems and Translational Bioinformatics (CSTB), ICube laboratory - CNRS, Fédération de Médecine Translationnelle de Strasbourg (FMTS), University of Strasbourg, Strasbourg, France
[40] Division of Clinical and Metabolic Genetics, The Hospital for Sick Children, Toronto, Ontario, M5G 1X8, Canada
[41] Department of Molecular Genetics, University of Toronto, Toronto, Ontario, M5S 1A1, Canada-RBW
[42] Department of Pediatrics, University of Toronto, Toronto, ON, Canada
[43] Institute of Medical Science, School of Graduate Studies, University of Toronto, Toronto, Ontario, Canada
[44] Institut Universitaire de France

The authors declare no conflict of interest.

*Address for correspondence and material request:

Amélie Piton, PhD

Laboratoire "Mécanismes génétiques des maladies neurodéveloppementales", IGBMC, Illkirch, France

Tel : +33369551652

E-mail: piton@igbmc.fr

Competing interests

None.

ABSTRACT

PURPOSE: *DYRK1A* syndrome is among the most frequent monogenic forms of intellectual disability (ID). We refined the molecular and clinical description of this disorder and developed tools to improve interpretation of missense variants, which remains a major challenge in human genetics.
METHODS: We reported clinical and molecular data for fifty individuals with ID harboring *DYRK1A* variants and developed i) a specific *DYRK1A* clinical score, ii) amino acid conservation data generated from one hundred of DYRK1A sequences across different taxa, iii) *in vitro* overexpression assays to study level, cellular localization, and kinase activity of DYRK1A mutant proteins, and iv) a specific blood DNA methylation signature.
RESULTS: This integrative approach was successful to reclassify several variants as pathogenic. However, we questioned the involvement of some others, such as p.Thr588Asn, still reported as likely pathogenic, and showed it does not cause an obvious phenotype in mice.
CONCLUSION: Our study demonstrated the need for caution when interpreting variants in *DYRK1A*, even those occurring *de novo*. The tools developed will be useful to interpret accurately the variants identified in the future in this gene.

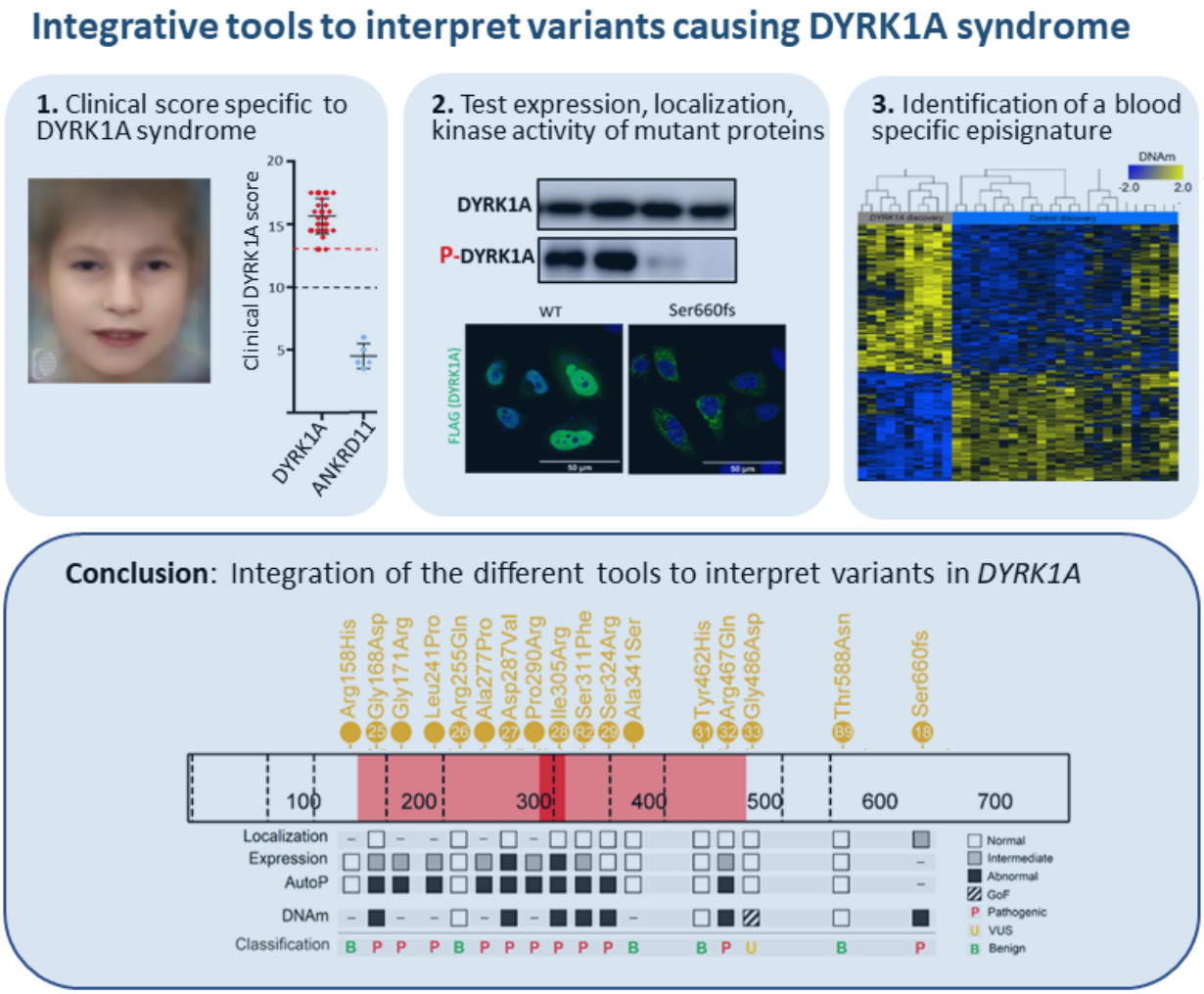

INTRODUCTION

Intellectual disability (ID) and autism spectrum disorder (ASD) are two highly heterogeneous groups of neurodevelopmental disorders (NDD) with substantial genetic contributions which overlap strongly both at the clinical and genetic levels. More than one thousand genes have been implicated in monogenic forms of NDD, with an important contribution of autosomal dominant forms caused by *de novo* variants [1]. One of these genes, *DYRK1A (dual-specificity-tyrosine-phosphorylation-regulated-kinase-1A)*[2], located on chromosome 21, is among the genes the most frequently mutated in individuals with ID [1].

The first *DYRK1A* disruptions were identified in individuals with intrauterine growth restriction (IUGR), primary microcephaly and epilepsy [3]. Few years later, the first frameshift variant was described in a patient with similar features [4]. The clinical spectrum associated with *DYRK1A* pathogenic variants (*MRD7 for Mental Retardation 7* in OMIM*)* was further refined with the publication of additional patients, presenting suggestive facial dysmorphism, severe speech impairment and feeding difficulty, while epilepsy and prenatal microcephaly were not always present [5–9]. Pathogenic variants were also identified in cohorts of individuals with ASD [10], but all have ID [11]. The *DYRK1A* gene encodes a dual tyrosine-serine/threonine (Tyr-Ser/Thr) kinase composed of a central catalytic domain including Tyrosine-321, involved in DYRK1A activation by autophosphorylation [12], two nuclear localization signal sequence (NLS), and additional functional domains. *DYRK1A* is ubiquitously expressed during embryonic development and in adult tissues. Its location is both cytoplasmic and nuclear and varies by cell type and stage of development [13]. By the

number and diversity of its proposed protein targets, DYRK1A regulates numerous cellular functions (reviews [14,15]), among them the MAPT (Tau) protein phosphorylated by DYRK1A on its Thr212 position [16].

High Throughput Sequencing (HTS) has revolutionized the identification of genetic variants for diagnostic applications but a major challenge remains in the interpretation of the vast number of variants, especially for highly heterogeneous disease such ID. A combination of genetic, clinical and functional approaches, summarized by the American College of Medical Genetics and the Association for Molecular Pathology (ACMG/AMP), are commonly used to interpret these variants [17]. A significant proportion of the variants, especially the missense variants, remain classified as variants of unknown significance (VUS, according to ACMG/AMP) after the primary analysis. For autosomal dominant diseases with complete penetrance such as *DYRK1A* syndrome, the *de novo* occurrence of a variant is a strong but not absolute argument for pathogenicity, and the parents' genotype is not always available. Clinical observations are useful but could also lead to misinterpretation, as numerous ID-associated manifestations are unspecific. Many tools have been developed to predict *in silico* the pathogenicity of missense variants but they remain predictions and protein-specific functional tests are useful to confirm variants effect. DNA methylation (DNAm) is also a powerful tool to test variant pathogenicity in disorders associated with epigenetic regulatory genes. We discovered that pathogenic variants in these genes can exhibit disorder-specific DNAm signatures comprised of consistent, multilocus DNAm alterations in peripheral blood, useful for classifying variants in these genes as pathogenic or benign [18–21]. DYRK1A has numerous targets, and while it is not well-described as an epigenetic regulator, it has been shown to phosphorylate histone H3 and histone acetyltransferase proteins [22,23]. Therefore, we hypothesized that pathogenic variants in *DYRK1A* might generate a specific DNAm signature in blood.

We reviewed the clinical signs present in 34 individuals never reported and carrying deletions or clearly pathogenic variants in *DYRK1A* to refine the clinical spectrum of *DYRK1A* syndrome. Based on these data, we developed a score to help to recognize affected individuals and to interpret variants (reverse phenotyping). In parallel, we developed *in silico* and *in vitro* approaches to assess variant effects on DYRK1A function. Finally, we defined a DNAm signature specific to *DYRK1A* syndrome in patient blood. We used this multifaceted approach to interpret 17 variants identified in patients with ID/NDD and demonstrated its efficiency in optimizing accurate interpretation of variants.

METHODS

Patients and molecular analysis

Variants in *DYRK1A* (NM_001396.4) were identified during routine genetic analyses in individuals referred to clinical genetic services for intellectual disability in France, Denmark and Switzerland: CGH-array, *DYRK1A* coding regions sanger sequencing, targeted next generation sequencing of ID genes (TES)[24–26], trio or simplex clinical exome sequencing (CES) or exome sequencing (ES), and confirmed by an additional method. Combined Annotation Dependent Depletion (CADD) and Nnsplice were used to predict the effect of missense and splice variants respectively. Fibroblasts were established from skin biopsies for Ind #1, #11, #22, #24, Bronicki#9 and Bronicki#10 and cultivated as previously described [27]. Paxgene blood samples were collected for Ind #9, #18, #19 and #30. mRNA extraction, RNA sequencing, RT-PCR or qPCR (primers available on request) were performed as previously described [28].

Phenotypic analysis and clinical scoring

Clinical information and photographs were provided by the referring clinicians for the 44 individuals reported here (**Table S1**) as well as for six individuals previously published (individuals Bronicki#2, #3, #8, #9 and #10 and Ruaud#2)[6,7](n=50 individuals in total). Based on the most frequent signs and the morphometric characteristics presented by the 34 individuals with truncating variants in *DYRK1A*, a clinical score out of 20 was established (DYRK1A_I, n=21 individuals with photographs available **Table S2**). Clinical scores were calculated for this initial cohort plus a second cohort (replication cohort, DYRK1A_R, n=13) with individuals already described in previous publications [5–7] by experienced clinical geneticists, as well as for individuals with other frequent monogenic forms of ID, caused by pathogenic variants in *DDX3X* (n=5), *ANKRD11* (n=5), *ARID1B* (n=8), *KMT2A* (n=6), *MED13L* (n=5), *SHANK3* (n=6) or *TCF4* (n=6) genes.

Definition of sets of missense variants and conservation analysis

To evaluate which tools are pertinent to predict effect of missense variants on the DYRK1A protein, we used different sets of variants : 1) variants presumed to be benign (negative N-set, n=115) including missense variants reported "benign" in ClinVar plus variants found more than once in GnomAD (november 2019 release), 2) variants reported as "pathogenic"/"likely pathogenic" in Clinvar (positive P-set, n=16), and 3) other variants reported here, in literature, or as VUS in Clinvar (test T-set, n=44)(**Table S3**). 123 orthologous sequences of human DYRK1A were extracted from the OrthoInspector database version 3.0. and a multiple sequence alignment (MSA) was constructed using the Clustal Omega software. The MSA was then manually refined to correct local alignment errors using the Jalview MSA editor [29]. The refined MSA was used as input to the PROBE software[30], in order to identify conserved regions in the sequences. The sequences in the MSA were divided into five separate clades: Vertebrates, Metazoans, Protists, Plants and Fungi.

In vitro analysis of variant effect on DYRK1A protein

DYRK1A expression plasmids (addgene #101770, Huen lab) were generated from the pMH-SFB-*DYRK1A* vector containing the N-terminal FLAG-tagged human *DYRK1A* cDNA sequence (NM_001396.4). Variant sequences were obtained by site-directed mutagenesis as described[31]. Antibodies used are listed in **Supplementary Methods**. HeLa, HEK293 and COS1 cells were maintained and transfected for 24h with *DYRK1A* plasmids (for immunoflurorescence) or *DYRK1A* plasmids plus pEGFP-N1 plasmid (for Western Blot) as previously done [31,32]. For autophosphorylation analysis and DCFA7 (WDR68) interaction, proteins were extracted from transfected HEK293 cells and immunoprecipitated with anti-FLAG antibody as described[31]. Phosphorylated Tyr321 DYRK1A was visualized as described [33] and normalized by the level of total DYRK1A protein. Kinase activity was investigated by co-transfecting *DYRK1A* and *MAPT* plasmids (MAPT_OHu28029C_pcDNA3.1(+)-C-HA, geneScript) in HEK293 cells, adapted from [34]. The level of DYRK1A, MAPT and pMAPT (Thr212) proteins were normalized with GAPDH.

DNA methylation signature

Methylation analysis was performed using blood DNA from individuals with *DYRK1A* LoF variants (n=16), split into signature discovery (n=10) and validation (n=6) cohorts, based primarily on whether age at time of blood collection was available, and age- and sex-matched neurotypical controls (n=24). Whole blood DNA samples were prepared, hybridized to the Illumina Infinium Human MethylationEPIC BeadChip

and analyzed as previously described [20], a total of n=774,590 probes were analyzed for differential methylation. Standard quality control metrics showed good data quality for all samples except Ind#20. Briefly, *limma* regression with covariates age, sex, and five predicted blood cell types identified a DNAm signature with a Benjamini-Hochberg adjusted *p*-value<0.05 and 10% methylation difference. Next, we developed a support vector machine (SVM) model with linear kernel trained on including non-redundant CpG sites [20] using the methylation values for the discovery cases vs. controls. The model generated scores ranging between 0 and 1 for tested samples, classifying samples as "positive" (score>0.5) or "negative" (score<0.5). Additional neurotypical controls (n=94) and *DYRK1A* LoF validation samples (n=6) were scored to test model specificity and sensitivity respectively, and samples with pathogenic *KMT2A* (n=8) and *ARID1B* (n=4) variants and *DYRK1A* missense and distal frameshift (n=11) variants were tested.

RESULTS

Identification of genetic variants in DYRK1A in individuals with ID

We collected molecular and clinical information from 50 individuals with ID (44 never reported and six previously reported[6,7]) carrying a variant in *DYRK1A* identified in clinical and diagnostic laboratories: structural variants deleting or interrupting *DYRK1A* and recurrent or novel nonsense, frameshift, splice and missense variants (**Table 1, Figure S1**). When blood or fibroblast samples were available, we characterized the consequences of these variants on *DYRK1A* mRNA by RNA-sequencing and RT-qPCR (**Figure S2, Supplementary Text**). For one variant, c.1978del, occurring in the last exon of the gene (**Ind #18**), the mutant transcripts escape to nonsense mRNA mediated decay (NMD) and result in a truncated protein p.Ser660fs (or p.Ser660Profs*43) retaining its entire kinase domain (**Figure S2F**). The variants occurred *de novo* in most of the cases (36/44), one was inherited from a mosaic father and parental DNA was not available for the seven others.

Clinical manifestations in individuals with pathogenic variants in DYRK1A and definition of a clinical score

We reviewed the clinical manifestations of the patients with truncating variants, except p.(Ser660fs)(**Table S1, Supplementary text).** Recurrent features include, consistently with what was reported [5,6,8,11]: moderate to severe ID, prenatal or postnatal progressive microcephaly, major speech impairment, feeding difficulties, seizures and especially history of febrile seizures, autistic traits and anxiety, delayed gross motor development with unstable gait, brain MRI abnormalities including dilated ventricles and corpus callosum hypoplasia and recurrent facial features (**Figure 1A, Figure S3).** We found genital abnormalies as reported [35] but no obvious renal anomalies**.** We noted the importance of skin manifestations and especially atopic dermatitis. We used recurrent features to establish a "DYRK1A- clinical score" (CS_{DYRK1A}) on a 20 point scale (**Figure 1A**), which aims to reflect specificity rather than severity of the phenotype. High scores, ranging from 13 to 18.5 (mean=15.5), were obtained for the individuals having a pathogenic variant in *DYRK1A* described here (DYRK1A_I) or previously (DYRK1A_R) **(Table S2**, **Figure 1B)**. The threshold of CS_{DYRK1A} >=13 appears to be discriminant between individuals with LoF variants in *DYRK1A* (all $\geq$13) and individuals suffering from another form of ID (all<13) and is considered as "highly suggestive" (13>CS_{DYRK1A}>10: "intermediate"; CS_{DYRK1A}<10:"poorly evocative"). A clinical score on 15 points without photograph is less discriminative (**Figure S4**).

In silico analysis of missense variant effects

We evaluated the discriminative power of the CADD score, commonly used in medical genetics [36] to interpret missense variants in *DYRK1A*. If a significant difference in the CADD score distribution is observed between the "benign" variants (N-set, see **Methods**) and those reported as "pathogenic" (P-set, see **Methods**)(p-value<0.0001), a substantial proportion of the N-set variants still have a CADD score above thresholds (20 or 25) usually used to define pathogenicity **(Figure S5A)**. This could be explained by the high degree of amino acid conservation of DYRK1A among vertebrates, and this could lead to over-interpretation of pathogenicity. We performed sequence alignment with orthologs from different taxon (**Figure S6)** and confirmed that using sequences from vertebrates only is not efficient to classify missense variants, as one third of the N-set variants affect amino acids conserved in all species (**Figure S5B**, V=100%). Considering conservation parameters going beyond vertebrates appears more discriminant (13/16 P-set and 1/115 N-set variants are conserved in 100% of vertebrates, 90% of metazoan and 80% of other animals) (**Figure S5B**).

In vitro characterization of consequences of missense variants on DYRK1A protein

In order to test the consequences of the missense variants *in vitro*, we overexpressed wild-type (WT) and mutant DYRK1A proteins in three different cell lines (HEK293, HeLa, COS1) including a truncating pathogenic variant Arg413fs and a benign missense variant from gnomAD, Ala341Ser. A significant and drastic decrease in DYRK1A protein level (**Figure 2A**), due to a reduction of protein stability (**Figure S7A**), was observed for the truncating Arg413fs and missense Asp287Val, Ser311Phe, Arg467Gln, Gly168Asp and Ile305Arg variants in each cell type. None of the variants affects DYRK1A interaction with DCAF7 (WDR68) (**Figure S7B**). To be active, DYRK1A has to undergo an autophosphorylation on Tyrosine 321 [12]. To measure the level of active DYRK1A protein, we detected phospho-DYRK1A (Tyr321) by immunoprecipitation followed by immunoblot using anti-phospho-HIPK2, as previously described [33](**Figure 2B**). We confirmed that the three variants previously tested (Asp287Val, Ser311Phe and Arg467Gln) abolish autophosphorylation [33,37], as do the Gly168Ap and Ile305Arg variants. The Ser324Arg DYRK1A variant showed only residual autophosphorylation. No effect on autophosphorylation was observed for Arg255Gln, Tyr462His, Gly486Asp and Thr588Asn. No effect was detected either for the Glu366Asp amino acid change, but the analysis of patient's blood mRNA showed that this variant (c.1098G>T) affects splicing leading to a deletion of 49 amino acids p.Ile318_Glu366del (**Figure S2G**). We used this strategy to test additional variants reported in databases and showed that Arg158His, affecting a highly conserved amino acid position but reported twice in GnomAD, does not affect DYRK1A protein. Ala277Pro, reported as pathogenic in ClinVar, as well as Gly171Arg, Leu241Pro and Pro290Arg, reported initially as VUS in ClinVar, affect both DYRK1A level and autophosphorylation (**Figure S8A-B, Table S3, Figure S5B**). None of the missense variants appears to affect DYRK1A cellular localization, contrary to Arg413fs variant or changes in NLS domains (**Supplementary Text, Figure S8C**). However, we observed an aggregation of DYRK1A proteins with the distal frameshift variant Ser660fs (**Figure 2C)**, preventing a correct measure of the protein and autophosphorylation levels.

Identification of a DNAm signature associated with DYRK1A pathogenic variants

To determine if *DYRK1A* is associated with specific changes in genome-wide DNA methylation (DNAm) in blood, we used methylation array analysis. We compared DNAm in blood for a subset (*discovery*) of our cohort carrying pathogenic LoF variants in *DYRK1A* with age- and sex-matched neurotypical controls and identified n=402 differentially methylated CpG sites corresponding to 165 RefSeq genes (**Table S4, Figure 3A-B**). The sensibility and specificity of the score (0-1) derived from this signature

was validated using additional individuals with *DYRK1A* truncating variants (*validation*), additional controls and individuals with pathogenic variants in other genes (**Table S5; Figure 3C**). Next, we scored the samples with missense variants and found that six classified positively (p.Asp287Val, p.Ser311Phe, p.Arg467Gln, p.Gly168Asp, p.Ile305Arg and p.Ser324Arg) and three negatively (p.Arg255Gln, p.Tyr462His, p.Thr588Asn) (**Figure 3B-C, Table S5, Figure S9**). The sample with the distal frameshift variant p.Ser660fs classified as DNAm positive, with a high score (0.92). The sample with the p.Gly486Asp variant clustered out from both *DYRK1A* cases and controls and its methylation profile was even opposite to *DYRK1A* LoF cases (increased methylation at sites decreased in LoF cases and vice versa, **Figure S9, S11**), suggesting this variant might have a gain-of-function (GoF) effect. A notable feature of these GoF CpG sites is that they tended to cluster together, as for instance in the *HIST1H3E* promoter (**Table S4**).

Integration of the different tools to reclassify variants

We integrated the clinical score, *in silico* predictions, functional assays results and DNAm score to evaluate the pathogenicity of the variants and reclassify them according to ACMG/AMP categories (**Figure 4, Table S6**). We found that variants p.Gly168Asp, p.Asp287Val, p.Ile305Arg, p.Ser311Phe and p.Arg467Gln, identified in individuals with intermediate to high CS_{DYRK1A} scores, led to reduced protein level as well as an absence of autophosphorylation activity, which was previously described for three of them [33,37]. All classified as DNAm-positive, definitively supporting their pathogenicity. For the p.Ser324Arg variant, identified *de novo* in a patient with an intermediate CS_{DYRK1A} score, we observed only a slight decrease of DYRK1A stability and a partial decrease of its autophosphorylation ability. The binary nature of the DNAm signature, showing a positive score, definitively supports its pathogenic effect.

The p.Arg255Gln and p.Tyr462His variants were identified in individuals with low CS_{DYRK1A} score, they had relatively high CADD score (24 and 29.6) but affect amino acids not highly conserved. They had no effect on protein level, autophosphorylation and cellular localization of DYRK1A and classified DNAm-negative, and were therefore both considered as likely benign. While parental DNA was not available to test the inheritance of p.Arg255Gln, the variant p.Tyr462His occurred *de novo*. This individual has an affected brother who does not carry the variant, and exome sequencing of the whole family failed to identify additional promising variants, even taken into account the possibility of two different origins for the brothers. This remains puzzling and WGS is ongoing for both to go further. Another *de novo* variant affecting the same position p.Tyr462Cys was identified in a girl with mild developmental delay, hypotonia and hypermobility without facial dysmorphia, who finally obtained another molecular diagnosis (personal communication Sander Stegmann, Maastricht University Medical Center). The p.Thr588Asn variant, previously reported as likely pathogenic[6], affects a mildly conserved amino acid and appears to have no effect on mRNA or protein level and function, as described by others [33,37]. To go further, we tested the ability of the mutant Thr588Asn DYRK1A to phosphorylate MAPT on its Thr212 and confirmed it does not affect its kinase activity (**Figure S10**). Moreover, a knock-in mouse model generated for Thr588Asn failed to present any decrease of kinase activity and any obvious behavioral phenotype (**Supplementary Text, Figure S12**). In addition, if this variant was not reported in gnomAD, two other amino acid changes are reported at the same position: p.Thr588Pro, (44 times including once at the homozygote state) and p.Thr588Ala (once). All these arguments plus the fact that the patient's DNAm signature was negative were convincing enough to reclassify this variant as likely benign. The fact that it occurred *de novo* in a girl with a high CS_{DYRK1A} (15.5/20) remains puzzling, while no additional promising variants were identified in trio-exome sequencing data and no positive classification was found using ~20 DNAm signatures available. However, the girl also presents additional manifestations unusual for *DYRK1A* syndrome such as truncal obesity.

Only one sample showed a DNAm profile different from both controls and individuals with DYRK1A syndrome (**Figure 3A, Figure S9 and S11**). This individual has a low $CS_{DYRK1A,}$ presenting relative macrocephaly and ASD without ID and carries a *de novo* p.Gly486Asp variant. This variant was previously reported in another individual with NDD [38], but it was not possible to obtain DNA, clinical or inheritance information. No significant change in protein and autophosphorylation level was observed for this variant and analysis of MAPT Thr212 phosphorylation failed to confirm the potential GoF effect (**Figure S10**).

We characterized the consequences of a distal frameshift *de novo* variant, p.Ser660fs. Its overexpression leads to cytoplasmic aggregation of DYRK1A, which makes it difficult to quantify the real effect on protein level, autophosphorylation or kinase activity (**Figure S8 and S10**). However, its DNAm overlaps those of other individuals with truncating variants located further upstream in the protein, confirming its pathogenic effect (**Figure S9**). To test if these aggregations could be driven by the novel C-terminal extension added by the frameshift variant (43 amino acids), we introduced nonsense variants at the same position (Ser660* and Ser661*). As no aggregate was detected (**Figure 2C & S8D**), we concluded that the C-terminal extension is responsible for the self-aggregation of the mutant DYRK1A protein. Interestingly, the two truncating variants Ser660* and Ser661* did not affect DYRK1A level, localization or autophosphorylation (**Figure S8A-B).**

DISCUSSION

Here we report clinical manifestations of 34 novel patients with clear loss-of-function (LoF) variants in *DYRK1A*, refining the clinical spectrum associated with *DYRK1A* syndrome. We used recurrent signs present in individuals to establish a clinical score, which may seem outdated in the era of pangenomic approaches but is in fact very useful to interpret variants of unknown significance identified by these approaches. Indeed, here we demonstrated that the combination of clinical data together with *in silico* and *in vitro* observations are essential to interpret variants accurately.

Since *DYRK1A* is a highly conserved gene in vertebrates, we assumed that *in silico* predictive tools using conservation calculated mainly from vertebrates might overestimate the potential pathogenicity of missense variants. We showed that deeper conservation analyses using additional taxa are useful to improve the predictions for missense variants. However, *in silico* analyses have their limitations, and functional assays are essential to assess variant effect conclusively. We therefore tested the effect of 17 variants and showed that ten of them decreased both DYRK1A protein level and DYRK1A autophosphorylation level. The remaining variants showed no effect on protein function (**Figure 4**). However, the absence of effects observed during series of functional tests does not totally exclude a potential effect.

Over the past five years, several studies have found patients with specific monogenic disorders involving genes encoding epigenetic regulatory proteins are associated with DNAm signatures in blood. The advantage of such signatures is the high rate of clear classification (positive/pathogenic vs negative/benign) they provide for variants. Considering the potential role played by DYRK1A in epigenetic regulation [22,23,39], we tested whether *DYRK1A* LoF leads to such a DNAm profil and identified a *DYRK1A* DNAm signature with high sensitivity and specificity (**Figure 3**). We undertook this work in whole-blood (as most signature work is done) due its clinically availability and *in silico* tools to account for cell proportion differences. We expect many of these changes to be blood-specific in patients with DYRK1A pathogenic variants. However, enough DNAm changes may overlap other tissues for the blood signature to have cross-tissue utility for variant classification, as we found for fibroblasts in Sotos Syndrome[18]. The combination of clinical score (CS_{DYRK1A}), *in silico* predictions, functional assays and DNAm signature allow to reclassify ten missense

variants as pathogenic. Three variants were considered as likely benign: a variant located in the catalytic domain whose inheritance was unknown, p.Arg255Gln, and two *de novo* variants located at the end or outside of this domain: p.Tyr462His and p.Thr588Asn.

Still based on methylation data, we suspected a gain-of-function (GoF) effect for another *de novo* variant located outside the catalytic domain: p.Gly486Asp. We have already shown that DNAm profiles at gene-specific signature sites provide a functional readout of each variants effect, GoF activity. Indeed, in previous work, we found the same pattern for a patient with a missense variant in *EZH2,* typically associated with Weaver syndrome. The patient, presenting undergrowth rather than overgrowth characteristic of Weaver syndrome, had an opposite DNAm profile to *EZH2* cases relative to controls and carried a missense variant which was demonstrated to increase EZH2 activity [19]. In our case, we could not confirm the putative GoF effect of Gly486Asp by measuring MAPT-Thr212 phosphorylation. Arranz et al. observed on the contrary an increase of DYRK1A kinase activity [37] for this variant, but they reported significant increase for five additional variants, including one present four times in GnomAD (Arg528Trp), which might question the sensitivity of the test.

We identified a *de novo* distal frameshift variant in the last exon of *DYRK1A* leading to DYRK1A aggregation *in vitro*, which needs to be confirmed *in vivo*. Interestingly, nonsense changes introduced at this position (aa660 and 661) lead to the expression of a protein which seems to be stable, does not aggregate, and maintains its autophosphorylation capacity and ability to phosphorylate MAPT (**Figure 2C, S8C-D, S10**). Therefore, we think that distal truncating variants should be interpreted with caution, especially when they escape to NMD. Three additional such distal variants are reported in individuals with ID/NDD in ClinVar/literature (**Table S8**) for which DNAm analysis on blood samples would be interesting to perform.

In conclusion, we developed a combination of tools efficient to interpret variants identified in *DYRK1A*. We showed that missense variants located outside and inside the catalytic domain as well as variants leading to distal premature stop codon are not necessarily pathogenic. These results illustrate that variants in *DYRK1A*, as well as in other NDD causative genes, should be interpreted with caution, even if they occur *de novo*. In the future, we recommend performing DNAm analysis if blood DNA sample is available or, if not, *in vitro* testing of variant effect on DYRK1A autophosphorylation.

DATA AVAILABILITY

Variants were submitted to ClinVar or to Decipher database (as indicated in Table 1). Additional data are available upon request.

ACKNOWLEDGEMENTS

The authors would like to thank the families for their participation and support. The authors also thank the Agence de Biomédecine, Fondation APLM, Fondation Maladies Rares and Fondation Jérome Lejeune for financial support. We also thank the Centre National de Génotypage, the diagnostic laboratories of Hôpitaux Universitaire de Strasbourg (HUS), clinical genetic residents, the GenomEast sequencing and the molecular biology platforms of IGBMC.

CONFLICTS OF INTEREST

None

ETHICS DECLARATION

Individuals were referred by clinical geneticists for genetic testings as part of routine clinical care. All patients enrolled and/or their legal representative have signed informed consent for research use and authorization for publication, including for photograph publication for those included in **Figure S3**. All the institutions received local IRB approval to use these data in research purpose. The main IRB approval was obtained from the Ethics Committee of the Strasbourg University Hospital (CCPPRB). For experiments performed in animal, they were all done in compliance with the ARRIVE Guidelines and were non-invasive procedures approved by Com'Eth, the local ethic committee.

WEB RESSOURCES

The URLs for online tools and data presented herein are:
CADD: https://cadd.gs.washington.edu/
ClinVar: http://www.ncbi.nlm.nih.gov/clinvar/
Clustal Omega: https://www.ebi.ac.uk/Tools/msa/clustalo/
dbSNP: http://www.ncbi.nlm.nih.gov/projects/SNP/
Decipher: https://decipher.sanger.ac.uk/
GnomAD*:* http://gnomad.broadinstitute.org/
Integrative Genomics Viewer (IGV): http://www.broadinstitute.org/igv/
Mutation Nomenclature: http://www.hgvs.org/mutnomen/recs.html
Nnsplice: https://www.fruitfly.org/seq_tools/splice.html
OMIM: http://www.omim/org/
UCSC: http://genome.ucsc.edu/
CADD score: https://cadd.gs.washington.edu/
OrthoInspector database: https://www.lbgi.fr/orthoinspectorv3/databases

BIBLIOGRAPHY

1. Deciphering Developmental Disorders Study. Prevalence and architecture of de novo mutations in developmental disorders. *Nature*. 2017;542(7642):433-438. doi:10.1038/nature21062
2. Gonzalez-Mantilla AJ, Moreno-De-Luca A, Ledbetter DH, Martin CL. A Cross-Disorder Method to Identify Novel Candidate Genes for Developmental Brain Disorders. *JAMA Psychiatry*. 2016;73(3):275-283. doi:10.1001/jamapsychiatry.2015.2692
3. Møller RS, Kübart S, Hoeltzenbein M, et al. Truncation of the Down syndrome candidate gene DYRK1A in two unrelated patients with microcephaly. *Am J Hum Genet*. 2008;82(5):1165-1170. doi:10.1016/j.ajhg.2008.03.001
4. Courcet J-B, Faivre L, Malzac P, et al. The DYRK1A gene is a cause of syndromic intellectual disability with severe microcephaly and epilepsy. *J Med Genet*. 2012;49(12):731-736. doi:10.1136/jmedgenet-2012-101251
5. van Bon BWM, Coe BP, Bernier R, et al. Disruptive de novo mutations of DYRK1A lead to a syndromic form of autism and ID. *Mol Psychiatry*. 2016;21(1):126-132. doi:10.1038/mp.2015.5
6. Bronicki LM, Redin C, Drunat S, et al. Ten new cases further delineate the syndromic intellectual disability phenotype caused by mutations in DYRK1A. *Eur J Hum Genet*. 2015;23(11):1482-1487. doi:10.1038/ejhg.2015.29
7. Ruaud L, Mignot C, Guët A, et al. DYRK1A mutations in two unrelated patients. *Eur J Med Genet*. 2015;58(3):168-174. doi:10.1016/j.ejmg.2014.12.014
8. Ji J, Lee H, Argiropoulos B, et al. DYRK1A haploinsufficiency causes a new recognizable syndrome with microcephaly, intellectual disability, speech impairment, and distinct facies. *Eur J Hum Genet*. 2015;23(11):1473-1481. doi:10.1038/ejhg.2015.71
9. Meissner LE, Macnamara EF, D'Souza P, et al. DYRK1A pathogenic variants in two patients with syndromic intellectual disability and a review of the literature. *Mol Genet Genomic Med*. Published online November 7, 2020:e1544. doi:10.1002/mgg3.1544
10. O'Roak BJ, Vives L, Fu W, et al. Multiplex targeted sequencing identifies recurrently mutated genes in autism spectrum disorders. *Science*. 2012;338(6114):1619-1622. doi:10.1126/science.1227764
11. Earl RK, Turner TN, Mefford HC, et al. Clinical phenotype of ASD-associated DYRK1A haploinsufficiency. *Mol Autism*. 2017;8:54. doi:10.1186/s13229-017-0173-5
12. Himpel S, Panzer P, Eirmbter K, et al. Identification of the autophosphorylation sites and characterization of their effects in the protein kinase DYRK1A. *Biochem J*. 2001;359(Pt 3):497-505. doi:10.1042/0264-6021:3590497

13. Hämmerle B, Elizalde C, Tejedor FJ. The spatio-temporal and subcellular expression of the candidate Down syndrome gene Mnb/Dyrk1A in the developing mouse brain suggests distinct sequential roles in neuronal development. *Eur J Neurosci*. 2008;27(5):1061-1074. doi:10.1111/j.1460-9568.2008.06092.x
14. Tejedor FJ, Hämmerle B. MNB/DYRK1A as a multiple regulator of neuronal development. *FEBS J*. 2011;278(2):223-235. doi:10.1111/j.1742-4658.2010.07954.x
15. Duchon A, Herault Y. DYRK1A, a Dosage-Sensitive Gene Involved in Neurodevelopmental Disorders, Is a Target for Drug Development in Down Syndrome. *Front Behav Neurosci*. 2016;10:104. doi:10.3389/fnbeh.2016.00104
16. Woods YL, Cohen P, Becker W, et al. The kinase DYRK phosphorylates protein-synthesis initiation factor eIF2Bepsilon at Ser539 and the microtubule-associated protein tau at Thr212: potential role for DYRK as a glycogen synthase kinase 3-priming kinase. *Biochem J*. 2001;355(Pt 3):609-615. doi:10.1042/bj3550609
17. Richards S, Aziz N, Bale S, et al. Standards and guidelines for the interpretation of sequence variants: a joint consensus recommendation of the American College of Medical Genetics and Genomics and the Association for Molecular Pathology. *Genet Med*. 2015;17(5):405-424. doi:10.1038/gim.2015.30
18. Choufani S, Cytrynbaum C, Chung BHY, et al. NSD1 mutations generate a genome-wide DNA methylation signature. *Nat Commun*. 2015;6:10207. doi:10.1038/ncomms10207
19. Choufani S, Gibson WT, Turinsky AL, et al. DNA Methylation Signature for EZH2 Functionally Classifies Sequence Variants in Three PRC2 Complex Genes. *Am J Hum Genet*. 2020;106(5):596-610. doi:10.1016/j.ajhg.2020.03.008
20. Chater-Diehl E, Ejaz R, Cytrynbaum C, et al. New insights into DNA methylation signatures: SMARCA2 variants in Nicolaides-Baraitser syndrome. *BMC Med Genomics*. 2019;12(1):105. doi:10.1186/s12920-019-0555-y
21. Aref-Eshghi E, Bend EG, Colaiacovo S, et al. Diagnostic Utility of Genome-wide DNA Methylation Testing in Genetically Unsolved Individuals with Suspected Hereditary Conditions. *Am J Hum Genet*. 2019;104(4):685-700. doi:10.1016/j.ajhg.2019.03.008
22. Jang SM, Azebi S, Soubigou G, Muchardt C. DYRK1A phoshorylates histone H3 to differentially regulate the binding of HP1 isoforms and antagonize HP1-mediated transcriptional repression. *EMBO Rep*. 2014;15(6):686-694. doi:10.15252/embr.201338356
23. Li S, Xu C, Fu Y, et al. DYRK1A interacts with histone acetyl transferase p300 and CBP and localizes to enhancers. *Nucleic Acids Res*. 2018;46(21):11202-11213. doi:10.1093/nar/gky754
24. Redin C, Gérard B, Lauer J, et al. Efficient strategy for the molecular diagnosis of intellectual disability using targeted high-throughput sequencing. *J Med Genet*. 2014;51(11):724-736. doi:10.1136/jmedgenet-2014-102554
25. Carion N, Briand A, Cuisset L, Pacot L, Afenjar A, Bienvenu T. Loss of the KH1 domain of FMR1 in humans due to a synonymous variant causes global developmental retardation. *Gene*. 2020;753:144793. doi:10.1016/j.gene.2020.144793
26. Nasser H, Vera L, Elmaleh-Bergès M, et al. CDK5RAP2 primary microcephaly is associated with hypothalamic, retinal and cochlear developmental defects. *J Med Genet*. 2020;57(6):389-399. doi:10.1136/jmedgenet-2019-106474
27. Balak C, Benard M, Schaefer E, et al. Rare De Novo Missense Variants in RNA Helicase DDX6 Cause Intellectual Disability and Dysmorphic Features and Lead to P-Body Defects and RNA Dysregulation. *Am J Hum Genet*. 2019;105(3):509-525. doi:10.1016/j.ajhg.2019.07.010
28. Quartier A, Chatrousse L, Redin C, et al. Genes and Pathways Regulated by Androgens in Human Neural Cells, Potential Candidates for the Male Excess in Autism Spectrum Disorder. *Biol Psychiatry*. Published online January 9, 2018. doi:10.1016/j.biopsych.2018.01.002
29. Waterhouse AM, Procter JB, Martin DMA, Clamp M, Barton GJ. Jalview Version 2--a multiple sequence alignment editor and analysis workbench. *Bioinformatics*. 2009;25(9):1189-1191. doi:10.1093/bioinformatics/btp033
30. Kress A, Lecompte O, Poch O, Thompson JD. PROBE: analysis and visualization of protein block-level evolution. *Bioinformatics*. 2018;34(19):3390-3392. doi:10.1093/bioinformatics/bty367
31. Mattioli F, Isidor B, Abdul-Rahman O, et al. Clinical and functional characterization of recurrent missense variants implicated in THOC6-related intellectual disability. *Hum Mol Genet*. 2019;28(6):952-960. doi:10.1093/hmg/ddy391
32. Quartier A, Courraud J, Thi Ha T, et al. Novel mutations in NLGN3 causing autism spectrum disorder and cognitive impairment. *Hum Mutat*. 2019;40(11):2021-2032. doi:10.1002/humu.23836
33. Widowati EW, Ernst S, Hausmann R, Müller-Newen G, Becker W. Functional characterization of DYRK1A missense variants associated with a syndromic form of intellectual deficiency and autism. *Biol Open*. 2018;7(4). doi:10.1242/bio.032862
34. Lee K-S, Choi M, Kwon D-W, et al. A novel de novo heterozygous DYRK1A mutation causes complete loss of DYRK1A function and developmental delay. *Sci Rep*. 2020;10(1):9849. doi:10.1038/s41598-020-66750-y
35. Blackburn ATM, Bekheirnia N, Uma VC, et al. DYRK1A-related intellectual disability: a syndrome associated with congenital anomalies of the kidney and urinary tract. *Genet Med*. 2019;21(12):2755-2764. doi:10.1038/s41436-019-0576-0
36. Kircher M, Witten DM, Jain P, O'Roak BJ, Cooper GM, Shendure J. A general framework for estimating the relative pathogenicity of human genetic variants. *Nat Genet*. 2014;46(3):310-315. doi:10.1038/ng.2892
37. Arranz J, Balducci E, Arató K, et al. Impaired development of neocortical circuits contributes to the neurological alterations in DYRK1A haploinsufficiency syndrome. *Neurobiol Dis*. 2019;127:210-222. doi:10.1016/j.nbd.2019.02.022
38. Dang T, Duan WY, Yu B, et al. Autism-associated Dyrk1a truncation mutants impair neuronal dendritic and spine growth and interfere with postnatal cortical development. *Mol Psychiatry*. 2018;23(3):747-758. doi:10.1038/mp.2016.253
39. Lepagnol-Bestel A-M, Zvara A, Maussion G, et al. DYRK1A interacts with the REST/NRSF-SWI/SNF chromatin remodelling complex to deregulate gene clusters involved in the neuronal phenotypic traits of Down syndrome. *Hum Mol Genet*. 2009;18(8):1405-1414. doi:10.1093/hmg/ddp047

FIGURE LEGENDS

Figure 1. Clinical score for Intellectual Disability associated to *DYRK1A* haploinsufficiency

(A) Clinical score out of 20 points established according to the most recurrent clinical features presented by patients (the weight assigned to each symptom being based on its recurrence): clinical symptoms are out of 15 points, while the facial appearance is out of 5 points. EV: enlarged ventricules; CCA/H: corpus callosum agenesis or hypoplasia, CA: cerebral atrophy, CeA: cerebellar atrophy (**B)** Clinical scores calculated for individuals carrying pathogenic variants in *DYRK1A* reported here and for whom photographs were available (n=21)(initial cohort, DYRK1A_I, scores 13- 17.5 with a mean of 15.5), the previously published individuals (replication cohort, DYRK1A_R, scores 13.5-18.5, mean=15.3) and the individuals affected with other frequent monogenic forms of ID, associated to variants in *ANKRD11*, *MED13L*, *DDX3X*, *ARID1B*, *SHANK3*, *TCF4* or *KMT2A* (scores 3-12.5, mean=7). The clinical score for the individuals carrying missense or distal frameshift variants are indicated in yellow (test); the threshold of CS_{DYRK1A} >=13 appeared to be discriminant between individuals with LoF variants in *DYRK1A* (all ≥13) and individuals suffering from another form of ID (all<13). A score above this threshold was therefore considered "highly suggestive". We classified individuals with CS_{DYRK1A}<10 as "poorly evokative" and individuals with a CS_{DYRK1A} comprised between 10 and 13 as "intermediate". Brown-Forsythe and Welsh ANOVA tests with Dunnett's T 3 multiple comparisons test were performed. ns: not significant; ** p<0.01; ***< p<0.001, error bars represent SD.

A

Frequent features (% ind. this report - prev. reported)	Points (/20)
Intellectual disability (100% - 100%) *(moderate:1; severe:2)*	2
Impaired language (100% - 100%) *(yes:1; absence or few words:2)*	2
Microcephaly (100% - 94%) *(yes:1; severe<-3SD:2)*	2
Feeding difficulty (neonate or infancy) (94% - 88%)	2
History of seizures (88% - 74%) *(yes:1; febrile seizures :2)*	2
Autistic traits/Anxiety (88% - 89%) *(Anxiety:1; Stereotypies:1; ASD diagnosis:2)*	2
Brain anomaly on MRI (81% - 75%) *(any:0,5; if EV, CCA/H, CA, CeA:1)*	1
Motor delay (82% - 88%)	1
Ataxic walk/hypertonia (64% - 73%)	0.5
Atopic or translucide skin (68% -)	0.5
Dysmorphy:	
Thin hair or erratic hairline	0.5
Upper eyelid edema	1
Deep set eyes	1
Protruding nose or pointed nasal tip	0.5
Dysplastic ears or ear lobe attached	0.5
Thin upper lip	0.5
Widely spaced teeth, protruding upper dental arch	0.5
Retrognathism, smal chin	0.5

B

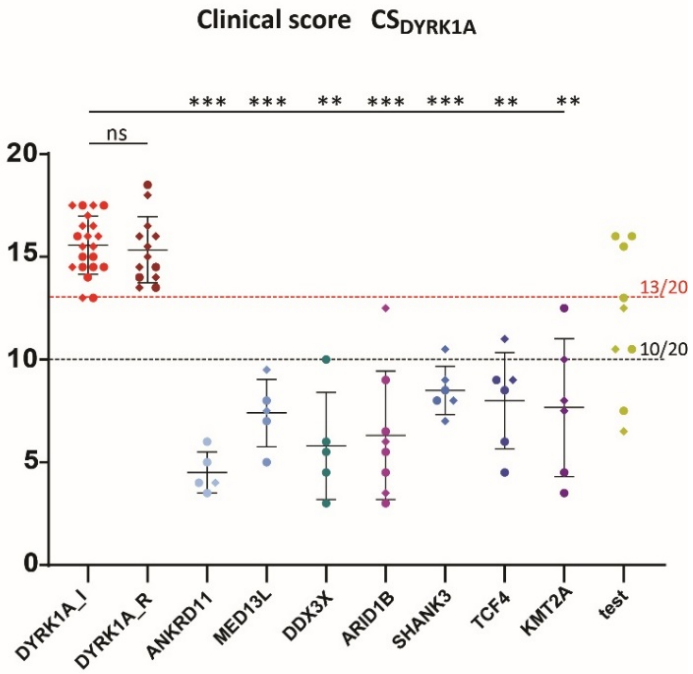

Figure 2. Expression, localization and Tyr321 phosphorylation of DYRK1A mutant proteins

(A) Level of variant DYRK1A proteins expressed in HeLa, HEK293 and COS cells transiently transfected with DYRK1A constructs. Protein levels were normalized on the level of GFP proteins (expressed from a cotransfected pEGFP plasmid). Quantifications were performed on a total of n >=9 series of cells (n>=3 Hela cells, n>= 3 HEK293 and n >= 3 COS cells) using ImageJ software. One-way ANOVA with multiple comparison test was performed to compare the level of variant DYRK1A proteins to the level of wild-type DYRK1A protein (orange dashes), applying Bonferroni's correction: ns: not significant; *p<0.05; **p < 0.01;***p<0.001; error bars represent SEM, standard error of the mean; in green, the variant from gnomAD, in red, a truncating variant and in gold, the variants tested in this study (**B)** DYRK1A's ability to autophosphorylate on Tyr321 was tested in HEK293 cells (n=3) by immunoprecipitations with anti-DYRK1A followed by an immunoblot using anti-phospho-HIPK2 as described in Widowati et al. DYRK1A phospho-Tyr321 levels were normalized with DYRK1A total level (orange dashes). Variant DYRK1A phospho-Tyr321 levels were normalized with total DYRK1A protein levels and expressed as percentage of wild-type level. One-way ANOVA test was performed to compare variants to wild-type DYRK1A levels. ns: not significant; ***p<0.001; error bars represent SEM, standard error of the mean **(C)** Immunofluorescence experiment showing that Ser660fs (alias Ser660Profs*43) variant leads to DYRK1A protein aggregation when overexpressed in HeLa cells, using a FLAG-tagged DYRK1A proteins carrying Ser660Profs43. No aggregation was observed for the Ser660* variant.

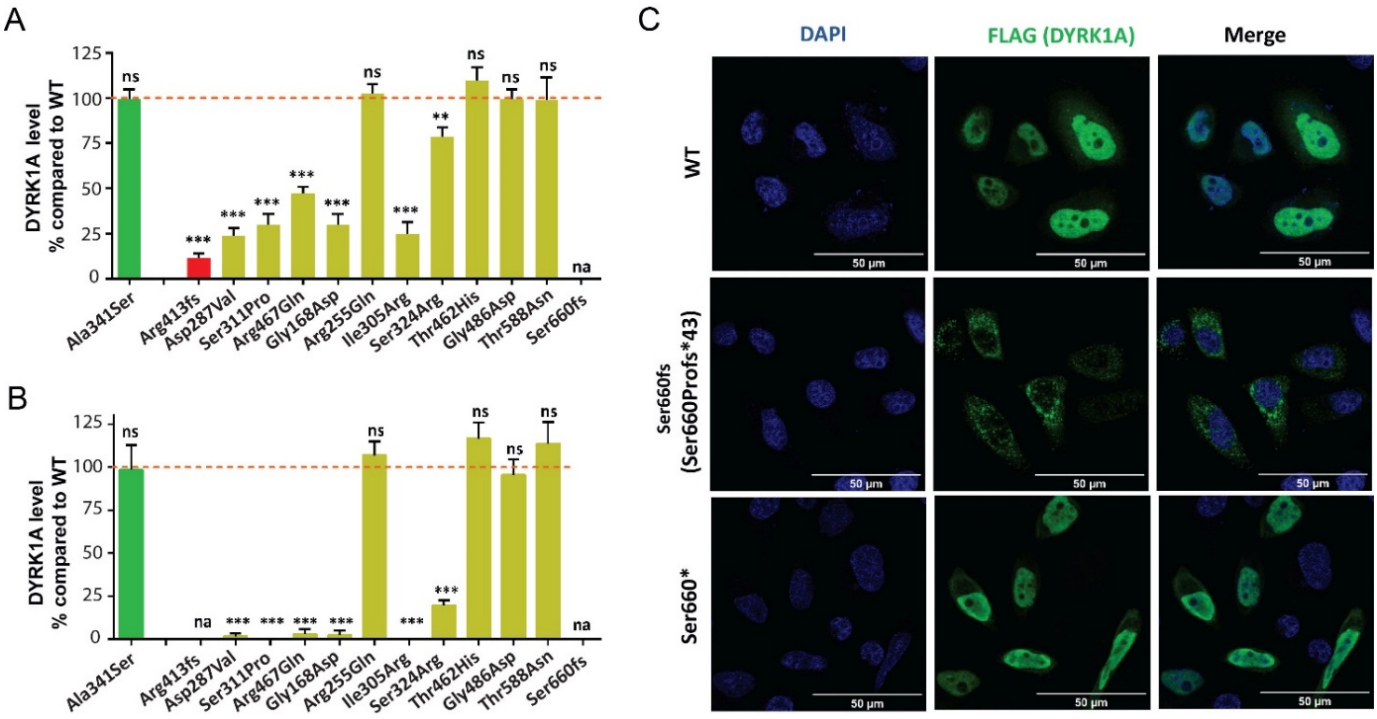

Figure 3. DNA methylation signature of DYRK1A loss-of-function functionally classifies *DYRK1A* VUS.

(A) Heatmap showing the hierarchical clustering of discovery *DYRK1A* LoF cases (n = 10) and age- and sex-matched neurotypical discovery controls (n = 24) used to identify the 402 differentially methylated signature sites shown. Each row corresponds to a CpG site differentially methylated (DM) and the color gradient represents the normalized DNA methylation value from -2.0 (blue) to 2.0 (yellow) at each site. DNA methylation at these sites clearly separate discovery cases (grey) from discovery controls (blue). Euclidian distance metric is used for the clustering dendrogram. **(B)** Principal components analysis (PCA) visualizing the DNAm profiles of the study cohort at the 402 signature sites. Validation of *DYRK1A* LoF cases (not used to define the signature sites; red) cluster with discovery cases, while missense (yellow) and distal LoF (green) variants cluster with either cases or controls. Ind #33 (Gly486Asp) has an opposite DNAm profile to *DYRK1A* LoF cases at these sites, suggesting a GoF. **(C)** Support vector machine (SVM) classification model based on the DNA methylation values in the discovery groups. Each sample is plotted based on its scoring by the model. All samples are clearly positive (>0.5) or negative (<0.5). All *DYRK1A* validation cases from our cohort (n=6) classified positively, all control validation cases (n=94) classified negatively. Missense variants classified clearly positively or negatively (yellow), the distal frameshift variant (Ind #18, c.1978del)(green), analyzed in duplicate, classified positively. Pathogenic *ARID1B* (Coffin-Siris syndrome) and *KMT2A* (Wiedemann Steiner syndrome) also classified negatively.

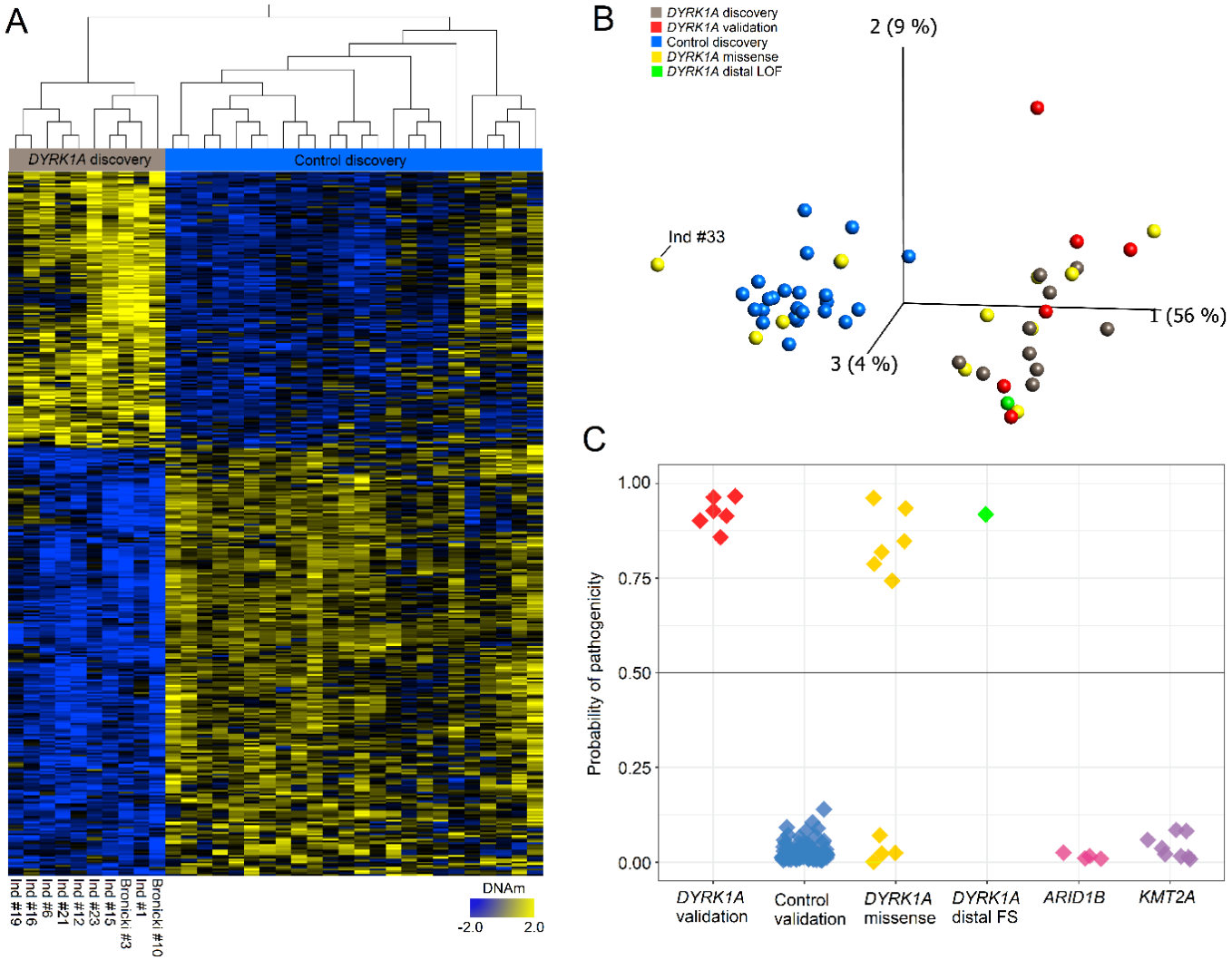

Figure 4. Summary of the analysis performed to reclassify variants in *DYRK1A*

Representation of the DYRK1A protein (the kinase domain is indicated in red and the catalytic domain in dark red) with the positions of the different variants tested with the sample #ID of the individuals indicated inside the circles. Number: number of individuals with ID reported with the variant; gAD: variant reported in individuals from gnomAD; CS_{DYRK1A} poorly (white), intermediate (grey) or highly (black) evocative, or unknown (-); the white star indicates that the individual presents a high CS_{DYRK1A} score but also additional clinical manifestations unusual for *DYRK1A* syndrome; CADD below 25 (white), between 25 and 30 (grey) or above 30 (black); conservation: highly conserved V=100%, M>90%, O>80% (black), moderately V=100%, M>90%, O<80% (grey) or midly V=100% M<90%, O<80% (white); Expression or autophosphorylation being normal (white), intermediate decreased (grey), strongly decreased (black); Localization was normal (white), affected (grey) or not tested (-); DNAmethylation positive (black), negative (white), suggestive of a GoF effect (hashed) or not tested (-). Final classification: Pathogenic (P), Benign/Likely benign (B), Unknown significance (U).

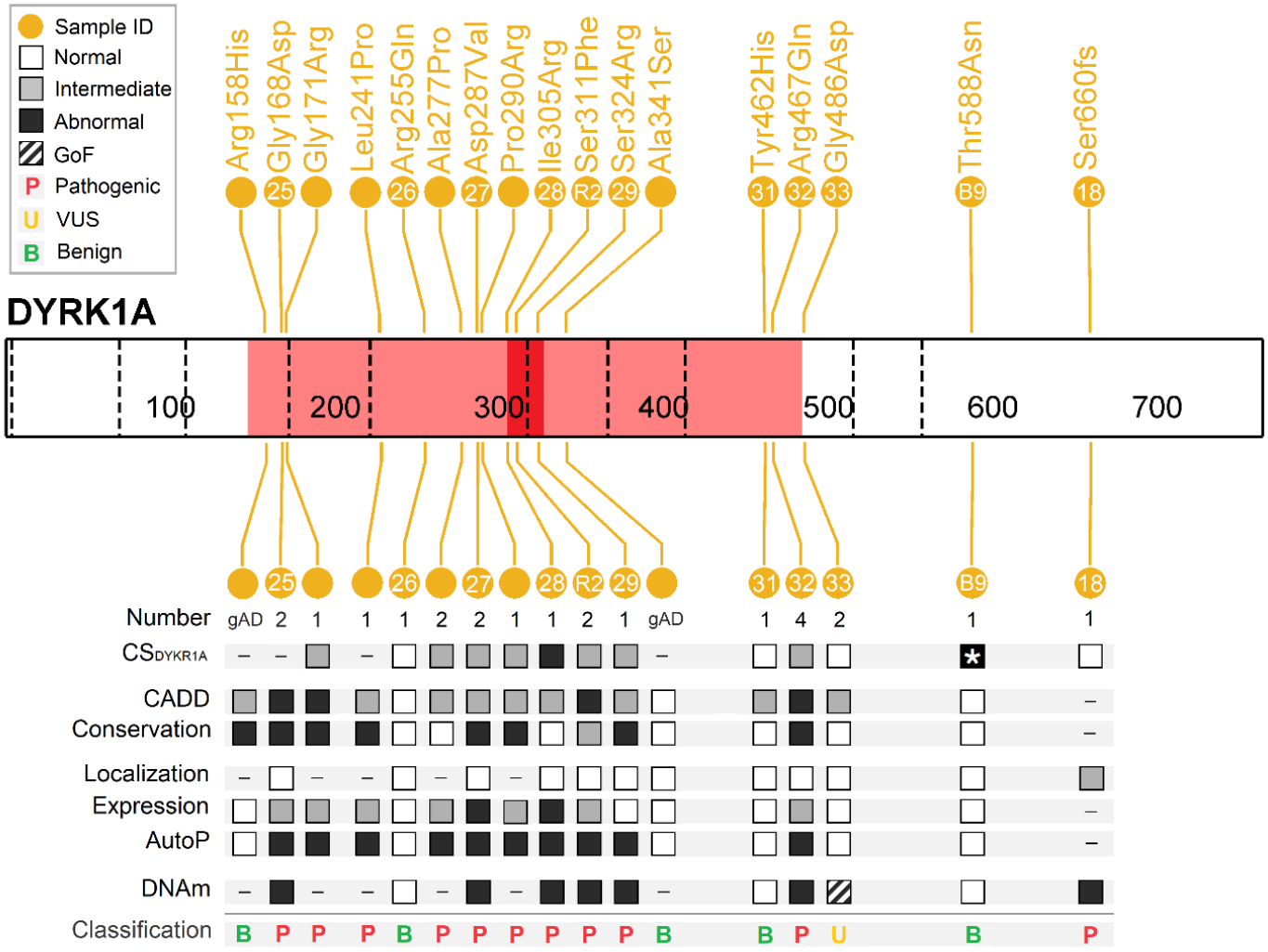

Table 1. List of variants identified in *DYRK1A* in individuals with intellectual disability

This list includes variants identified in the 44 individuals never reported as well as variants previously reported in six individuals [6,7] for whom we collected biological samples and additional clinical information. The truncating variants clearly pathogenic are represented in red; the missense variants and the distal frameshift variant to test are in gold. Variants are reported according to standardized nomenclature defined by the reference human genome GRCh37/hg19 and the *DYRK1A* isoform NM_001396.4; del: deletion of the gene ; Trans.: translocation interrupting the gene ; Ns: nonsense ; Fs: frameshift, Spl: splice ; Ms: missense variants; Infr.: inframe deletion; TES: targeted exome sequencing of ID genes TES[1] : panel of ID genes from Carion et al. [47]; TES[2] : panel of ID gene adapted from Redin et al. [46] ;TES[3] : panel of 44 ID genes; TES[4]: panel of microcephaly genes from Nasser et al. [48] ; CES: clinical exome sequencing, ES: exome sequencing, Sanger: Sanger sequencing, CGH-array: comparative genomic hybridization-array. [a]: the consequences of c.1098G>T is p.Ile318_Glu366del instead of p.Glu366Asp; M : male ; F : female ; DYRK1A_I : initial cohort used to establish DYRK1A clinical score (CS_{DYRK1A}) ; DYRK1A_R : replication cohort used to confirm the relevance of the CS_{DYRK1A} ; Disc : discovery cohort used to establish DNA methylation signature (DNAm) ; Valid: validation cohort used to confirm DNA methylation signature (DNAm); test : variants tested for pathogenicity using DNAm.

Variant					Individual			Reporting		Analyses performed				
GRCh37 (Chr21)	**NM_001396.4**	**NP_001387.2**	**Type**	**Method**	**Ind. number**	**Sex**	**Inheritance**	**this individual**	**Additional ind. (ClinVar)**	**CS_{DYRK1A}**	***In silico***	**mRNA**	***in vitro***	**DNAm**
g:38481804_40190458del (*DYRK1A ; >10 other genes*)	NA	NA	del.	CGH-array	Ind #1	M	de novo	NA	NA	DYRK1A_I	-	yes	-	Disc.
g.38722881_39426450del (*DYRK1A*; *KCNJ2*)	NA	NA	del.	CGH-array	Ind #2	F	de novo	NA	NA	DYRK1A_I	-	-	-	-
g.38302140_40041414del (*DYRK1A ; >5 other genes*)	NA	NA	del.	CGH-array	Ind #40	M	de novo	NA	NA	DYRK1A_I	-	-	-	-
t(9;21)(p12;q22)	between exon 2 & 3	NA	trans.	CGH-array	Ind #3	M	de novo	NA	NA	DYRK1A_I	-	-	-	-
g.38852961C>T	c.349C>T	p.Arg117*	Ns	ES	Ind #4	M	NA	NA	(5x) VCV000373087	DYRK1A_I	-	-	-	-
				ES	Ind #5	F	father mosaic	NA		DYRK1A_I	-	-	-	-
				ES	Ind #6	M	de novo	NA		DYRK1A_I	-	-	-	Disc.
g.38858865C>T	c.613C>T	p.Arg205*	Ns	TES[2]	Bronicki_#2	M	de novo	PMID: 25920557 (ClinVar_SCV000281731= SCV000196058)	(x7) VCV000162153	DYRK1A_R	-	-	-	-
				TES[4]	Ind #44	M	NA	ClinVar_SCV001432338		DYRK1A_I	-	-	-	-
g.38862575C>T	c.763C>T	p.Arg255*	Ns	TES[1]	Ind #7	M	de novo	ClinVar_SCV001712097	(5x) VCV000162152	DYRK1A_I	-	-	-	Valid.
				NA	Ind #43	F	NA	ClinVar_SCV001432353		DYRK1A_I	-	-	-	-
g.38862611C>T	c.799C>T	p.Gln267*	Ns	ES	Ind# 35	M	de novo	Clinvar_SUB9815736	no	DYRK1A_I	-	-	-	-
g.38862748T>A	c.936T>A	p.Cys312*	Ns	CES	Ind #37	F	de novo	Clinvar_SCV001712105	no	DYRK1A_I				
g.38877655C>T	c.1309C>T	p.Arg437*	Ns	TES[4]	Ind #34	F	not in mother	NA	(7x) VCV000162158	DYRK1A_I	-	-	-	-
g.38877745C>T	c.1399C>T	p.Arg467*	Ns	TES[4]	Ind#42	F	de novo	ClinVar_SCV001432351	(3x) VCV000204005	DYRK1A_I	-	-	-	-
g.38850510dup	c.235dup	p.Arg79fs	Fs	TES[4]	Ind #41	F	de novo	ClinVar_SCV001432470	no	DYRK1A_I	-	-	-	-
g.38850565_38850566del	c.290_291 del	p.Ser97fs	Fs	CES	Ind #8	M	de novo	ClinVar_SCV001712106	(2x) VCV000418949	DYRK1A_I	-	-	-	-
g.38850572_38850576del	c.297_301del	p.Leu100fs	Fs	NA	Ind #9	M	de novo	ClinVar_SCV000485020	no	DYRK1A_I	-	-	-	-
g.38853089del	c.477del	p.Tyr159*	Fs	ES	Ind #10	F	de novo	Clinvar_SCV001712094	no	DYRK1A_I	-	-	-	-
g.38862514_38862515del	c.702_703del	p.Cys235fs	Fs	ES	Ind #11	M	de novo	ClinVar _SCV000965742	no	DYRK1A_I	-	yes	-	Valid.
g.38858873_38858876delinsGAA	c.621_624 delinsGAA	p.Glu208fs	Fs	TES[2]	Bronicki_#3	M	de novo	PMID: 25920557 (ClinVar_SCV000281736 = SCV000196059)	no	DYRK1A_R	-	-	-	Disc.
g.38862594del	c.782del	p.Leu261fs	Fs	TES[2]	Ind #12	F	de novo	ClinVar_SCV001437790	no	DYRK1A_I	-	-	-	Disc.
g.38862656dup	c.844dup	p.Ser282fs	Fs	TES[1]	Bronicki_#8	M	de novo	PMID: 25920557 (ClinVar_SCV000196064)	no	DYRK1A_R	-	-	-	-
g.38865371del	c.1004del	p.Gly335fs	Fs	TES[1]	Ind #13	F	not in mother	Clinvar_SCV001712087	no	DYRK1A_I	-	-	-	Valid.
g.38865375dup	c.1008dup	p.Pro337fs	Fs	ES	Ind #14	F	de novo	Decipher_351807	no	DYRK1A_I	-	-	-	-
g.38865400del	c.1033del	p.Trp345fs	Fs	CES	Ind #15	F	de novo	Clinvar_SCV001712108	no	DYRK1A_I	-	-	-	Disc.

g.38868553dup	c.1232dup	p.Arg413fs	Fs	TES[2]	Bronicki_#10	F	de novo	PMID: 25920557 (ClinVar_SCV000196066)	no	DYRK1A_R	-	yes	yes	Disc.
g.38877616del	c.1270del	p.His424fs	Fs	ES	Ind #39	F	de novo	Clinvar_SCV001712090	no	DYRK1A_I	-	-	-	-
g.38877679dup	c.1333dup	p.Thr445fs	Fs	ES	Ind #16	F	de novo	Clinvar_SCV000778256	no	DYRK1A_I	-	-	-	Disc.
g.38877837del	c.1491delC	p.Ala498fs	Fs	ES	Ind #17	F	de novo	Clinvar_SCV000494645	SCV000056592	DYRK1A_I	-	-	-	Valid.
g.38884520del	c.1978del	p.Ser660fs= p.Ser660Profs*43	Fs	TES[1]	Ind #18	F	de novo	Clinvar_SCV001712088	no	test	-	yes	yes	test
g.38852939G>T	c.328-1G>T	p.?	Spl.	TES[2]	Ind #19	F	de novo	Clinvar_SCV001437768	no	DYRK1A_I	-	yes	-	Disc.
g.38862475A>G	c.665-2A>G	p.?	Spl.	Sanger	Ind #20	M	de novo	Clinvar_SCV001712086	SCV000492145	DYRK1A_I	-	-	-	Valid.
g.38862468_38862472del	c.665-9_665-5del	p.?	Spl.	Sanger	Ind #21	M	de novo	Clinvar_SCV001437772	SCV000677027	DYRK1A_I	-	-	-	Disc.
			Spl.	TES[2]	Ind #36	M	de novo			DYRK1A_I	-	-	-	-
g.38862764G>C	951+1G>C	p.?	Spl.	TES[1]	Ind #38	M	de novo	Clinvar_SCV001712091	no	DYRK1A_I	-	-	-	Valid.
g.38862767_38862770del	c.951+4_951+7del	p.?	Spl.	ES	Ind #22	M	de novo	Clinvar_SCV000965731	SCV000709803	DYRK1A_I	-	yes	-	-
g.38877584A>G	c.1240-2A>G	p?	Spl.	ES	Ind #23	M	de novo	Clinvar_SCV000966166	no	DYRK1A_I	-	-	-	Disc.
g.38877585_38877586insTAA	c.1240-1_1240insTAA	p.Glu414*	Spl.	TES[4]	Ind #24	F	de novo	Clinvar_SCV001432455	no	DYRK1A_I	-	yes	-	-
g.38853115G>A	c.503G>A	p.Gly168Asp	Mis.	TES[1]	Ind #25	F	de novo	Clinvar_SCV001712092	SCV000573105	test	yes	-	yes	test
g.38862576G>A	c.764G>A	p.Arg255Gln	Mis.	TES[1]	Ind #26	F	NA	Clinvar_SCV001712093	no	test	yes	-	yes	test
g.38862672A>T	c.860A>T	p.Asp287Val	Mis.	ES	Ind #27	M	de novo	Clinvar_SCV000598121	SCV001446739	test	yes	-	yes	test
g.38862726T>G	c.914T>G	p.Ile305Arg	Mis.	Sanger	Ind #28	F	de novo	Clinvar_SCV001712110	no	test	yes	-	yes	test
g.38862744C>T	c.932C>T	p.Ser311Phe	Mis	NA	Ruaud_#2	M	de novo	PMID: 25641759 (Clinvar_SCV000586742)	SCV000520979	test	yes	-	yes	test
g.38865339T>A	c.972T>A	p.Ser324Arg	Mis.	TES[3]	Ind #29	M	de novo	Clinvar_SCV000902439	no	test	yes	-	yes	test
g.38865465G>T	c.1098G>T[a]	p.Ile318_Glu366del	Infr.	ES	Ind #30	F	de novo	Decipher_434484	no	test	yes	yes	yes	-
g.38877730T>C	c.1384T>C	p.Tyr462His	Mis.	TES[2]	Ind #31	M	de novo	Clinvar_SCV001437769	no	test	yes	-	yes	test
g.38877746G>A	c.1400G>A	p.Arg467Gln	Mis.	TES[2]	Ind #32	F	de novo	Clinvar_SCV001437771	(3x) VCV000209150	test	yes	-	yes	test
g.38877803G>A	c.1457G>A	p.Gly486Asp	Mis.	ES	Ind #33	M	de novo	Clinvar_SCV000747759	no	test	yes	-	yes	test
g.38884305C>A	c.1763C>A	p.Thr588Asn	Mis	ES	Bronicki_#9	F	de novo	PMID: 25920557 (ClinVar_SCV000965705= SCV000196065)	no	test	yes	yes	yes	test

SUPPLEMENTARIES

Supplementary methods - Antibodies

DYRK1A protein quantification (Western Blot)	mouse anti-FLAG antibody (1:1:000; Sigma Aldrich #F1804)
	mouse anti-GFPantibody (in house)
DYRK1A localization (Immunocytochemistry)	mouse anti-FLAG antibody (1:1:000; Sigma Aldrich #F1804)
Immunoprecipitation	rabbit anti-DYRK1A antibody (1:1000; Cohesion Biosciences #CPA1357)
Interaction with DCAF7	anti-WDR68 antibody (1:2500; abcam ab138490)
DYRK1A autophosphorylation	rabbit anti-phospho-HIPK2 antibody (1:1000, Thermofisher #PA5-13045)
	rabbit anti-DYRK1A antibody (1:1000; Cohesion Biosciences #CPA1357)
MAPT phoshorylation	mouse anti-TAU-5 antibody (Thermofisher #MA5-12808)
	rabbit anti-pTAU-T212 antibody (Thermofisher #44-740G)
	mouse anti-FLAG antibody (1:1:000; Sigma Aldrich #F1804)
	Mouse anti-GAPDH (Sigma #MAB374)

Supplementary text

Details on splice and frameshift variants and their consequences on *DYRK1A* mRNA

Deletions encompassing *DYRK1A* and chromosomal rearrangement t(9;21)(p12;q22) interrupting the gene were reported in four individuals (**Ind #1-3, 40**). We identified recurrent nonsense variants p.Arg117*(**Ind #4, #5, #6**), p.Arg205* (**Ind #44**), p.Arg255* (**Ind #7, #43)**, p.Arg437*(**Ind#34) and p.** p.Thr467* **(Ind#42)** as well as novel nonsense variants (**Ind#35, #37**) or small indels (**Ind #8-17, #39, #41**), one of them occurring in the last exon affecting the distal region of the protein: p.Ser660fs (**Ind #18**). Seven of the variants identified are predicted to affect splice sites, half of them previously reported elsewhere (**Ind #19-24, #36, #38**). The remaining individuals (**Ind #25-33**) carry missense variants, three of them already reported: p.Gly168Asp, p.Asp287Val and p.Arg467Gln. We tested the consequences of splice variants identified on *DYRK1A* mRNA (**Figure S2**) when possible (blood or fibroblasts available) by RNA-sequencing (**Ind #19, 22, 24**) or RT-qPCR (**Ind #18**). We found that c.328-1G>T (**Ind #19)** leads to abnormal splicing events between exons 4 and 5 including intron 4 retention and use of alternative cryptic acceptor sites in exon 5 (**Figure S2A**). The c.951+4_951+7 del (**Ind #22)** leads to retention of intron 7 or skipping of exon 7, both resulting in a premature truncation **(Figure S2B)**. RNA sequencing performed on mRNA extracted from **Ind #24** fibroblasts revealed that the TAA insertion at the beginning of exon 10 was included in the transcripts, leading to a stop codon p.Glu414*. *DYRK1A* mRNA levels were only slightly decreased in **Ind #22** and **#24** when compared to individual carrying truncating variant (**Ind #11**), suggesting that the aberrant transcripts escape nonsense mediated mRNA decay (NMD), at least partially (**Figure S2D**). The variant previously reported c.1232dup, p.Arg413fs (**Bronicki #10**)[1] is subjected to NMD as illustrated by the decrease of *DYRK1A* mRNA level in patient's fibroblasts, and the low level of mutant allele in cells, restored by NMD blocking agent (**Figure S2E**). However, it is worth noting that mutant transcripts carrying the distal frameshift c.1978del (**Ind #18)**, located in the last exon of the gene, escape to NMD and therefore result in a truncated protein p.Ser660fs having its entire kinase domain (**Figure S2F**).

Clinical manifestations in individuals with pathogenic variant in *DYRK1A*

All the individuals with clearly loss-of-function variants in *DYRK1A* present with moderate to severe ID except two (**Ind #3, #34)**. Language was affected in all individuals, severely in most (no speech, or only few words or short sentences). Individuals tend to present failure to thrive, even sometimes from the uterine stage (20/32), especially on the weight gain (from -1 to -4SD). The size is less affected comprised between -0.5 to -2SD. Microcephaly is however a constant trait, although not always present from birth. All individuals except two (31/33) had feeding difficulties during the neonatal period (poor sucking, gastrostomy, etc), which can be very severe during infancy and can persist during childhood and even into adulthood (selective, smashed food only, etc). The large majority of individuals present a history of seizures (29/33) mainly including febrile episodes (n=18). Hypotonia was noted in only half of the individuals (16/29), but a majority had motor delay with a walk acquired after 18 months of age (27/33)(mean = 23 months), and the gait could continue to be unstable and ataxic (9). Hypereflexia and hypertonia have been observed in some patients (12). Sleep disorders were reported in some patients (10). Behavioral manifestations observed in patients included anxiety (13) and autistic traits with stereotyped behaviours (24). A diagnosis of autism spectrum disorder (ASD) has been established in only four patients, but few have had the appropriate tests. Other behavioral manifestations such as water fascination (5), absence of fear (5) were noted. MRI revealed ventricular dilation (9), thin corpus callosum (9), as well as cortical or cerebellar atrophy (9). Other manifestations include gastrointestinal manifestations such as constipation (14) or gastroesophageal reflux (10), intestinal anomalies such as inguinal hernia (4) and urogenital anomalies already reported to be frequent[2], including cryptoorchidism (4). No obvious kidney anomalies have been reported but not all the individuals underwent a renal ultrasound. We observed a thin skin in a high frequency of patients (15), often associated with dermatitis or atopic skin after birth or during infancy (11), sometimes very pronounced. After reanalysis of literature, we found that atopic demartitis was also reported in additional individuals. Vision anomalies include myopia (6), hypermetropia (8) and astigmatism (6). An optic nerve hypoplasia was noticed in at least three individuals. A papillary pallor was reported in some individuals (6). Individuals shared common facial appearance including erratic hairline with thin hair, deep set eyes with upper eyelid edema, protruding nose or pointed nasal tip, dysplastic ears, thin upper lip, widely spaced teeth with protruding upper dental arch, retro/micrognathism (**Figure 1, Figure S3**).

Effect of missense variants on DYRK1A subcellular localization

The cellular localization of overexpressed WT and variant DYRK1A proteins in Hela cells, studied by immunostaining, revealed three types of cellular distributions: 1) mainly nuclear (N), 2) nuclear and cytoplasmic (N+C) and 3) mainly cytoplasmic (C) (**Figure S8C**). WT DYRK1A protein is mainly localized in the nucleus (80% N; 20% N+C), and this localization is affected when we mutated, separately or combined, the two nuclear localization signals NLS1 (aa 117-134) and NLS2 (aa 389-395) confirming that each NLS contributes to the nuclear localization of DYRK1A, as previously reported[3]. We observed a significant decrease of nuclear localization for Arg413fs, but none of the missense variants tested seems to affect DYRK1A localization.

Generating and phenotyping analysis of the DYRK1A Thr588Asn Mutant mouse line

The *Dyrk1a*^{T588N} mutant mouse line was established for YH at the Institut Clinique de la Souris-(PHENOMIN-ICS, Illkirch, France; http://www.phenomin.fr) and breed in our animal facility at the PHENOMIN-ICS (Agreement C67-218-40). The targeting vector was constructed as follows. A 3.4 kb fragment encompassing part of intron 11 and corresponding to the 5' homology arm was amplified by PCR on C57BL/6N ES cell genomic DNA and subcloned in an MCI proprietary vector containing two multiple cloning sites, three repeated SV40 polyA sequences as well as a flipped Neomycin resistance cassette surrounded by 2 LoxP sites. The variant (ACC > A**A**C) leading to the threonine to asparagine change at position 588 (T588N) was introduced in a second cloning step by fusion of 2 PCR products. Finally, a 3.6 kb fragment corresponding to the 3' homology was cloned in a third cloning step to obtain the final targeting construct. The linearized construct was electroporated in C57BL/6N mouse embryonic stem (ES) cells (ICS proprietary line S3). After G418 selection, targeted clones were identified by long-range PCR and further confirmed by Southern blot with an internal (Neo) probe and a 3' external probe. Two positive ES clones were validated by karyotype spreading and microinjected into BALB/cN blastocysts. Resulting male chimeras were bred with Flp deleter females showing maternal contribution[4]. Germline transmission with the direct excision of the selection cassette was achieved in the first litter. The mouse line was bred on a pure C57BL/6N genetic background in a specific pathogen free environment at the PHENOMIN-ICS animal mouse, with poplar wood granulate bedding (SAFE, Augis, France) and access to normal diet (D03 and D04; SAFE, Augis, France) and tap water treated with Chlorine dioxide (0,8ppm) ad libitum under a classical 12-12 light dark cycle (dark 7pm to 7am during phenotyping). We found a close to mendelian transmission ratio for the segregration of the variant both in heterozygotes and homozygotes. The female to male ratio was as expected.

The expression of the Thr588Asn allele of *Dyrk1a* in heterozygous was studied by Western blot at 7 weeks of age in 5 wild type and 5 *Dyrk1a*$^{T588N/+}$ animals. Twenty micrograms of proteins per sample were separated by classical electrophoresis and transferred on a membrane (BIO-RAD, Schiltigheim, Fr). Incubation with primary antibody Anti-Dyrk1a (Abnova, 1/1000) was followed with an incubation with a secondary antibody Anti-mouse (Abnova; 1/5000). We used B-Actin as an internal control that was detected with an anti-mouse B-actin-HRP (Sigma, 1/150000). For revelation, we used the Clarity™ Western ECL Substrate (BIO-RAD-#170-5061). No statistically meaningful difference was observed between the genotypes (Student t.test=0.33; **Figure S12B**). We performed a functional characterization of DYRK1A kinase activity following the protocol already published[5], using 13 *Dyrk1a*$^{T588N/+}$ and 17 control littermate brains (**Figure S12B**). No difference in DYRK1A kinase activity was found regarding the sex or genotype. We raised a cohort with mutant and control littermates from both sex (12 wt male, 12 *Dyrk1a*$^{T588N/+}$ male, 12 wt females and 11 *Dyrk1a*$^{T588N/+}$ females) to test the cognition, memory, locomotor activity, and assess the anxiety and autism like stereotypies on these animals. We performed the battery of tests as shown in (**Figure S12D**) following the pipeline and protocols previously described [6–9]. All the animal experiments were done in compliance with the ARRIVE Guidelines [10,11] in accordance with the Directive of the European Parliament: 2010/63/EU, revising/replacing Directive 86/609/EEC and with French Law (Decret n° 2013-118 01 and its supporting annexes entered into legislation 01February 2013) relative to the protection of animals used in scientific experimentation and supervised by the Com'eth our local ethical committee. The tests were administered in the following order: open field, novel object recognition (noted NOR, performed 24h after the open field), Y-maze, repetitive behaviour, sociability 3 chambers test and reciprocal tests. In the open field test we assessed the locomotor activity, exploratory drive and anxiety; and we have taken into account randomization of the animals, blinding of the experimenter during the animal research. With the EthoVision system (Noldus, the Netherlands), we measured the total distance, time spend on each of the three areas centre, periphery and walls. Sex was not affecting any of these

parameters, so the downstream statistical assessments was done pooling all the animals together divided just by genotype and not considering the sex, increasing the sampling size. We found no difference or effect between the control and mutant *Dyrk1a*$^{T588N/+}$ mice in the total distance travelled or time spend on each area. All the animals performed the test and did not show anxiety as they spent quite a high amount of time travelling over all the arena. The novel object recognition test (NOR) was used to study the memory of the animals to discriminate and explore novel objects over familiar ones. We did not identify a deficit in object recognition between the two genotypes (**Figure S12E**). We evaluated the motor activity and the working memory in the Y maze. There was no difference in the percentage of visits done to each arm, no defect in the spontaneous alternation (**Figure S12F**) or delay leaving the initial arm. Repetitive behaviour is one of the 3 main clinical manifestations of autism, together with deficits in social interaction and communication. Thus, we analysed in a 10 min test the number and time spend climbing, digging, and rearing by the mutant animals and control littermates but we did not observe any special stereotypic of repetitive behaviour in the *Dyrk1a*$^{T588N/+}$ mice except a slight increase in climbing frequency (**Figure S12G**). In the three chambers test, we analysed both the time spent in proximity of the empty cage during the presentation, or for the familiar and then the new congener in the discrimination phase. No phenotype was detected in the presentation phase and a significant difference in exploration was observed for the Thr588Asn mutant in the discrimination phase (**Figure S12H**). For the reciprocal sociability test where the social interactions between pairs of mice is analyzed, always using congeners that were not cage mates and in the case of both mutants and control mice in the cohort adding an unknown wild-type animal of the same sex and similar age and size to assess the interactions. We analysed both the time spend in proximity nose to nose or proximity nose to tail but no difference in interaction was observed for *Dyrk1a*$^{T588N/+}$. Although is worthy to mention that the Gardner-Altman effect size plots show a slight tendency on the *Dyrk1a*$^{T588N/+}$ mice to decrease the number of contacts and increase the distance with the congener (**Figure S12I**).

Supplementary acknowledgements

We would like to thank the Centre National de Génotypage for their participation in library preparation and DNA sequencing. We thank all the people from the GenomEast sequencing platform, IGBMC cloning platform for their technical and bioinformatics supports. They thank people for the diagnostic laboratory of Hôpitaux Universitaire de Strasbourg (HUS) for performing follow-up of variants and giving diagnosis to family as well as additional clinicians not included in the author list for their clinical contributions.

Supplementary Figures

Figure S1. Variants identified in DYRK1A in individuals with ID

Schematic representation of DYRK1A protein secondary structure with its different domains: Nuclear localization sequence 1 and 2 (NLS1 and NLS2); DYRK Homology box (DH); catalytic domain; PEST domain (PEST); His rich domain (His) and Serine Threonine (S/T) repeat domain. Variants identified in the cohort are represented with the number of individuals (Ind#) carrying then (**A)** truncating variants (nonsense, frameshift, splice variants) **(B)** missense variants. The variants identified tested in this study are indicated in gold.

Figure S2. Consequences of variants on *DYRK1A* mRNA

Sashimi plot from Integrative Genome Viewer (IGV) showing consequences of the splice variants identified by RNA-Seq in mRNA extracted from (**A) Ind #19** blood, showing that c.328-1G>T generate different abnormal transcripts with a) intron 4 retention, leading to a premature stop codon (p.Tyr111Argfs*6), b) use of an alternative acceptor site 18bps or c) 21pbs downstream the regular one, leading to deletion of few amino acids (p.Val110_Lys115del or p.Val110Lys116del) **(B) Ind #22** fibroblasts, showing that c.951+4_951+7del variant leads to a skipping of exon 7 in half of the mutated transcripts (p.Val222Aspfs*22) and a retention of intron 7 in the other half (p.Ile318fs*10); **(C)** IGV view of RNA-seq obtained from **Ind #24** fibroblasts, showing c.1240-1_1240insTAA causes the insertion of these 3 nucleotides in the mRNA at the beginning of exon 10 leading to a premature stop codon p.(Glu414*) **(D)** Quantitative expression of *DYRK1A* mRNA (normalized by the expression of two reference genes, *GAPDH* and *YWHAZ*) (**E)** Sequencing of *DYRK1A* mRNA in Individual Bronicki#10 cells (c.1232dup, p.(Arg413fs)) treated or not with a NMD blocking agent (emetine)**.** Sequencing of blood *DYRK1A* cDNA in (**F)** Ind #18 showing an equal amount of transcripts carrying the c.1978del variant compared to wild-type allele, suggesting that mutated transcripts escape to NMD, and in **(G)** Ind #30, carrying the variant c.1098G>T, showing the skipping of exon 8 induced by this variant r.952_1098del) leading to the deletion of 49 amino acids p.Ile318_Glu366del instead of one amino acid substitution p.Glu366Asp as first predicted (the probability of using exon 8 donor splice site was decreased by the variant: MaxEnt: -72.7%; NNSPLICE: -54.1%).

Figure S3. Photographs of individuals with variant in *DYRK1A*

Photographs of individuals with variants in *DYRK1A*, showing that they share similar facial features.

Figure S4. Distribution of the clinical scores calculated without photograph (on 15 points)

Clinical scores calculated without photograph for individuals carrying pathogenic variants in *DYRK1A* from the initial cohort (DYRK1A_I), the replication cohort (DYRK1A_R) and the individuals affected with other frequent monogenic forms of ID, associated to pathogenic variants in *ANKRD11, MED13L, DDX3X, ARID1B, SHANK3, TCF4* or *KMT2A*. Brown-Forsythe and Welsh ANOVA tests with Dunnett's T 3 multiple comparisons test were performed. ns: not significant; ** p<0.01; ***< p<0.001, error bars represent SD.

Figure S5. Predictions of effect of missense variants and conservation of DYRK1A protein

(A) Distribution of the CADD score for missense variants a) not presumed to be not disease-causing (negative set, N-set, n=115, see **Methods**), b) presumed to be pathogenic (positive set, P-set, n=16) and c) other missense variants (test set, T-set, n = 41). A CADD score >=20 means that the variant belongs to the top 1% of variants predicted to be the most deleterious, >= 25 that the variant belongs to the top 0.3% of variants predicted the most deleterious>= 30 the variant belongs to the top 0.1% of variants predicted the most deleterious. Brown-Forsythe and Welsh ANOVA tests with Dunnett's T 3 multiple comparisons test were performed. ns: not significant; ** p<0.01; ***< p<0.001, error bars represent SD (**B**) Percentage of variants from the N-set (presumably benign), P-set (presumably pathogenic) and T-set (to test) having a CADD score >=20, >=25

or >=30, or conserved across 100% of Vertebrate species (V=100%), conserved in at least 90% of Metazoan species (M>=90%), and at least 80% of other animals (O>=80%). [a] p.Arg158His variant (V=100% ; M=96% ; O=92%); [b] all variants except p.Ser311Phe variant (100% ; 100% ; 71%), p.Thr588Asn (V= 85%) and p.Ala277Pro (100%; 12%; 27%); variants ; [c] p.Gly171Arg (100%; 100% ; 86%), p.Lys188Arg (100%; 96%; 97%), p.Leu207Pro (100% ; 93% ; 93%), p.Leu241Pro (100% ; 100% ; 97%), p.Leu245Arg (100% ; 100% ; 97%), p.Asp287Tyr (100% ; 100% ; 97%), p.Asp287Asn (100% ; 100% ; 97%), p.Pro290Arg (100%; 100%; 97%), p.Arg328Trp (100%; 100%; 95%), p.Leu347Arg (100% ; 96% ; 84%).

Figure S6. Conservation of DYRK1A proteins across the different taxons

Schematic view of the Multiple Sequence Alignment (MSA) of DYRK1A protein orthologs from Vertebrates, Metazoans, Protists, Fungi and Plants. MSA positions are numbered according to the human protein and colored by a red gradient according to the level of amino acid conservation in each group.

Figure S7. Effect of variants on DYRK1A half-life and interaction with DCAF7

Investigation of variants consequences on DYRK1A protein stability and interaction with its partner DCAF7. (**A)** Stability of DYRK1A proteins in HEK293 transfected with DYRK1A plasmids and treated with cycloheximide 40µg/mL (stopped at 1, 2, 4 and 8 hours after treatment). Constructs was detected by SDS-PAGE by immunoblotting whole cell lyzates using an anti-FLAG antibody and quantification realized with GAPDH (**B**) Co-immunoprecipitation of DYRK1A in HEK293 cells transfected with *DYRK1A* plasmids using an anti-FLAG antibody, without antibody (Empty) or with Mouse against Rabbit antibody (MAR) as negative and species isotype controls. DCAF7 (WDR68) interaction was detected by SDS-page immunoblotting with a specific antibody (1:2500; abcam anti-WDR68 antibody ab138490).

Figure S8. *In vitro* effects of additional variants on DYRK1A proteins and cellular localization of variant proteins

(A-B) Effect of additional variants on DYRK1A level and ability to autophosphorylate: one variant from the N-set (reported twice in gnomAD) but affecting an highly conserved amino acid position, Arg158His, one variant from the P-set but affecting a position poorly conserved after vertebrates, Ala277Pro, and three variants initially reported as VUS in ClinVar (the last one was reclassified as Likely Pathogenic during the course of this study) and affecting highly conserved positions : p.Gly171Arg, p.Leu241Pro and p.Pro290Arg. We also tested the functional effet of two nonsense changes we created for the need of this study : Ser660* and Ser661*. **(A)** Level of variant DYRK1A proteins expressed in HEK293 (n=3 series) cells transiently transfected with DYRK1A constructs. Protein levels were normalized on the level of GFP proteins (expressed from a cotransfected pEGFP plasmid). One-way ANOVA with multiple comparison test was performed to compare the level of variant DYRK1A proteins to the level of wild-type DYRK1A protein (orange dashes), applying Bonferroni's correction: ns: not significant; *p < 0.05; **p < 0.01;***p<0.001; error bars represent SEM, standard error of the mean, (**B)** DYRK1A's ability to autophosphorylate on Tyr321 was tested in HEK293 cells (n=3) by immunoprecipitations with anti-DYRK1A followed by an immunoblot using an anti-phospho-HIPK2 as described in Widowati et al. DYRK1A phospho-Tyr321 levels were normalized with DYRK1A total DYRK1A protein levels (orange dashes), and expressed as percentage of WT level. One-way ANOVA test was performed to compare variants to wild-type DYRK1A levels. ns: not significant;

***p<0.001; error bars represent SEM, standard error of the mean **(C)** Cellular localization of DYRK1A variant proteins observed in HeLa cells after overexpression of FLAG-tagged wild-type and variant DYRK1A constructs (n=3 series of Hela cells; 50 cells minimum counted per series ; scale bars of illustrative images correspond to 10µm). Three types of localization of DYRK1A protein in cells have been observed: DYRK1A located mostly in the nucleus (N), in both nucleus and cytoplasm (N+C), or mostly in the cytoplasm (C). Scale bars: 50µm. WT protein is mainly localized in the nucleus (N/N+C/C: 80/20/0%). The shift into cytoplasmic localization of DYRK1A is stronger when NLS1 is disrupted (0/63/37%) compared to NLS2 (22/71/7%), and even more drastic when both are mutated, with DYRK1A stacked in the cytoplasm in a large majority of cells (0/26/74%). Chi-square test was performed to compare localization of variant DYRK1A proteins to wild-type DYRK1A protein ns: not significant; ***p<0.001; error bars represent SEM, standard error of the mean. (**D**) Immunofluorescence experiment showing that the Ser661* variant does not lead to DYRK1A protein aggregation when overexpressed in HeLa cells.

Figure S9. DNAm profile of all DYRK1A cases DYRK1A DNAm signature sites.

Heatmap showing the hierarchical clustering of discovery *DYRK1A* LoF cases (n = 10; grey) and age- and sex-matched neurotypical discovery controls (n = 24; blue) used to identify the 402 differentially methylated (DM) signature sites shown (each row corresponds to a CpG site). The DNAm values for *DYRK1A* LoF validation cases (n=6, red), missense variants (n=10, yellow) and distal LoF variant (n=1, green) are shown. The colour gradient represents the normalized DNA methylation value from -2.0 (blue) to 2.0 (yellow) at each site. Ind #33 (Gly486Asp) has an opposite DNAm values to other *DYRK1A* cases at these sites, also clustering out from controls. Euclidean distance metric is use for the clustering dendrogram.

Figure S10. Effect of variants on DYRK1A kinase activity regarding MAPT (TAU) Thr212 phosphorylation levels.

MAPT Thr212 phosphorylation assays performed to test variants with particular profiles : Ser324Arg (partial autophosphorylation), Gly486Asp (potential GoF), Thr588Asn (potential phenocopy), Ser660fs (protein aggregates) as well as Ser660* and Ser661*. Immunoblots on total protein extracts from HEK293 cells transfected with DYRK1A and MAPT plasmids using anti-FLAG, anti TAU-5 and anti-pT212-TAU antibodies (**A**) Transfection of different quantities of DYRK1A WT plasmid and 1µg of MAPT plasmid (**B**) Transfection of DYRK1A proteins harboring the distal truncating variant Ser660fs or the two nonsense changes Ser660* and Ser661* and 1µg of MAPT plasmid (**C**) Transfection of other DYRK1A variants : Ser311Phe (known to abolish kinase activity), Ser324Arg, Gly486Asp and Thr588Asn and 1µg of MAPT plasmid.

Figure S11. DNAm profile of Ind #33 with DYRK1A Gly486Asp variant displays an opposite DNAm profile at individual signature CpGs.

DNA methylation values are shown at the 25 most hypermethylated and hypomethylated CpG sites in the signature. Red bars show the average delta beta value at each site in *DYRK1A* LoF discovery cases (n=10), error bar represents the standard error of the mean (SEM). Yellow bars represent the delta beta value Ind #33

at these sites (the beta value of Ind #33 minus the average beta of discovery controls). At most sites, the delta beta for Ind #33 is opposite that of *DYRK1A* cases, indicating DNAm levels in the opposite direction of *DYRK1A* LoF cases relative to controls. Importantly, this is a different phenomenon than Ind #33 having control-like DNAm values, in which case the bars would be near 0.

Figure S12. Generation, characterisation and behavioural analysis of the heterozygous mouse mutant line carrying a Thr588Asn variant in *Dyrk1a.* (A) Generating the Thr588Asn (T588N) allele. The T588N allele phenotyped is named 'T588N with a WT potential allele' and was obtained by homologous recombination in embryonic stem cells using a targeting vector. LoxP and Flp sites are indicated respectively in green and grey **(B)** No difference in western blot quantification of DYRK1A level, normalized to b-actin level, in 5 hippocampal protein extracts isolated from *Dyrk1a*$^{T588N/+}$ individuals and 5 control littermates **(C)** Simarly no changes was observed in the phosphorylation of a specific DYRK1A-phosphorylation peptide (-tyde) using brain extract isolated from the hippocampi of *Dyrk1a*$^{T588N/+}$ and control littermates (respectively n=13 and 17) **(D)** schematic representation of the behavioural pipeline used to study 23 *Dyrk1a*$^{T588N/+}$ and 24 wild-type (wt) littermates from both sexes at the starting age of 10 weeks **(E)** In the novel object recognition, a preference was found in the percentage of time exploring the novel object (NO) compared to the familiar object (FO) in the *Dyrk1a*$^{T588N/+}$ **(F)** Spontaneous alternation in the Y maze was not affected by the variant (one single t test with 50% chance level). **(G)** A significant difference was observed in specific repetitive behaviour climbing, but not in digging or rearing activities analysed during the repetitive behavioral test **(H)** In the three-chamber sociability test, the percentage of time exploring the familiar stranger **(F)** versus the novel stranger (N) was significantly different in the mutant T588N heterozygotes **(I)** During freely moving social interaction we did not detect any anomaly. The statistical significance is noted as followed *adj P.value=< 0.05, ** 0.05 <adj P.value < 0.01, *** adj P.value < 0.001

Table S1. Clinical information and summary of recurrent clinical signs observed in individuals with pathogenic variants in *DYRK1A*

M: male; F: female; IUGR: Intrauterine growth restriction; CMV: research for cytomegalovirus infection; BW: birth weight; BS: birth size; BOFC: birth occipitofrontal head circumference; A/FW: absence/few words; ID: intellectual disability, ASD: Autism spectrum disorder; M/S: moderate/severe; mo; months old; SD: standard deviation; AtSD: atrial septal defect; VSD: ventricular septal defect; GER: Gastroesophageal reflux; MRI: Magnetic resonance imaging; EV: enlarged ventricles, CCA/H: corpus callosum agenesis/hypoplasia, CA: cortical or subcortical atrophy, CeA: cerebellar atrophy; NA: not available; [a] Previously reported: Individuals with truncating variants in *DYRK1A* reported in literature (n=80)[1,2,12–36]

Table S2. Calculation of the clinical score CS_{DYRK1A} in the different cohorts

NA: not available; DYRK1A_I: Initial cohort of individuals with variants disrupting *DYRK1A* (nonsense, frameshift, splice, deletions or translocations) reported in this study, used to set up the clinical score ; DYRK1A_R: Cohort of replication including individuals with variants disrupting *DYRK1A* who were previously described with enough clinical information and photographs available (n=12)[1,12,18] * mild macrocephaly

Table S3. List of *DYRK1A* missense variants reported in databases (gnomAD, ClinVar, Decipher) and literature and identified in this report (N-set, P-set and T-set)

training sets: N-set: variants not presumed to be disease-causing, i.e missense variants annotated as "benign"/"likely benign" in ClinVar as well as variants reported more than once in GnomAD (november 2019 release) (n=115); P-set: missense variants reported as "pathogenic"/"likely pathogenic" in Clinvar (n=16) T-set: missense variants reported here, in literature, or as VUS in Clinvar (n=44); FreqRefV, FreqRefM, FreqRefO, FreqRefP, FreqRefF: frequency of the reference amino acid among Vertebrates, Metazoans, Other protist animals, Plants or Fungi; FreqSubV, FreqSubM, FreqSubO, FreqSubP, FreqSubF : frequency of the novel amino acid among Vertebrates, Metazoans, Other animals, Plants or Fungi;

Table S4. List of CpG sites included in DYRK1A DNAm signature

GoF: gain-of-function. One third of the signature sites (134/402) the β value for p.Gly486Asp was outside the range observed for that of all discovery controls.

Table S5. SVM score associated with the different variants

SVM: Support Vector Machine classification and scores

Table S6. Summary of the analysis performed to reclassify variants in *DYRK1A*

[1]Highly conserved : V=100% M>=90% O>=80% * The consequences of c.1098G>T is p.Ile318_Glu366del instead of p.Glu366Asp ; ** same individual submitted twice *** : this amino acid change is not reported in gnomAD, but Thr588Pro is reported 44 times (including in one homozygote) and Thr588Ala is reported once ; DD: developmental delay, ID: intellectual disability ; clinical information reported in ClinVar and/or in littérature for the individual [a]: "Abnormality of the frontal hairline, abnormality of the skin, cataract, cerebellar atrophy, feeding difficulties in infancy, intrauterine growth retardation, microcephaly, proportionate short stature, single transverse palmar crease, specific learning disability, ventriculomegaly" ; [b]: « Short chin, Truncal obesity » ; [c]: « Developmental regression, intellectual disability, hypotonia, mild ataxia, intention tremor, dysmorphisms, primary microcephaly, failure to thrive, demyelination, sun sensitivity, incontinence and anxiety » ; [d]: « ASD, learning disorder and macrocephaly » ; [e]: « Abnormal facial shape, Down-sloping shoulders, Genu valgum, Global developmental delay, Hypoplastic toenails » in an individual carrying an additional nonssense variant in *DYRK1A* ; [f]: « Decreased facial expression, Global developmental delay, Hypoplastic left heart, Micrognathia, Postnatal microcephaly, Retinal dystrophy » ; [g]: DYRK1A-related » ; [h]: « MR/ID/DD; Seizures; Brain MRI positive, Dysmorphic features, Cardiovascular; Craniofacial; Hematologic (child onset), Gastrointestinal (child onset); Musculoskeletal/Structural; Neurologic (child onset), Ophthalmologic, Renal conditions » ; [i] : « Brachycephaly, Intellectual disability, Seizures, Muscular hypotonia, Global developmental delay » ; dn : *de novo* ; ACMG/AMP Criteria : PS2 : *De novo* confirmed ; PS3 : *in vitro* or *in vivo* functional studies supportive of a damaging effect on the gene or gene product; PM2 :Absent from controls ; in Exome Sequencing Project, 1000 Genomes or ExAC ; PP3 : *in silico* analysis support a deleterious effect on the gene product ; PP4 :Patient's phenotype is highly specific for gene ; BS1: Allele frequency is greater than expected for disorder ; BS3 :Well-established *in vitro* or *in vivo* functional studies shows no damaging effect on protein function or splicing ; BP4 :in silico analysis suggest no impact on gene or gene product.

Table S7. Summary of functional studies previously performed for additional missense variants in *DYRK1A*

[1]Highly conserved : V=100% M>=90% O>=80% * The consequences of c.1098G>T is p.Ile318_Glu366del instead of p.Glu366Asp ; DD: developmental delay, ID: intellectual disability ; Clinical information reported in ClinVar and/or in litterature : [a]: "speech delay, motor delay, moto coordination disorder, seizures and mild physical dysmorphy"; [b]: "mild ID, infantile spasms, speech delay, social interaction and repetitive behaviors, anxiety"; [c]: "Abnormality of the palmar creases, abnormality of the skeletal system, amblyopia, astigmatism, cleft soft palate, constipation, delayed speech and language development, global developmental delay, intrauterine growth retardation, microcephaly"; [d]: "IUGR, DD, microcephaly, ID, severe speech delay"; [e]: "ASD+ID, anxiety, perseveration and additional upsets and aggressive behavior"; [f]: "Severe ID, seizures febrile + generalized tonico-clonic"; [g]: "ID, seizures and microcephaly"; [h]: "Intellectual disability, microcephaly, feeding difficulties; absent or delayed speech development; seizures; deeply set eye"; [i]: "Global developmental delay, Microcephaly, Seizures"; [j]: "Microcephaly, ID, seizures, spasticity, global developmental delay, motor delay, hypertonia, abnormal facial shape, cortical dysplasia, short stature, cortical gyral simplification"; dn : de novo ; ACMG/AMP Criteria : PS2 : De novo confirmed ; PS3 : in vitro or in vivo functional studies supportive of a damaging effect on the gene or gene product; PM2 :Absent from controls ; in Exome Sequencing Project, 1000 Genomes or ExAC ; PP3 : in silico analysis support a deleterious effect on the gene product ; PP4 :Patient's phenotype is highly specific for gene ; BS1: Allele frequency is greater than expected for disorder ; BS3 :Well-established in vitro or in vivo functional studies shows no damaging effect on protein function or splicing ; BP4 :in silico analysis suggest no impact on gene or gene product.

Table S8. Distal frameshift variants (last exon) identified in individuals with NDD

Three distal frameshift variants are reported in Clinvar and in literature[16]. Their clinical interpretation remains ambiguous, especially for c.1726C>T p.Gln576* and c.2040C>A p.Tyr680*, for which inheritance is unknown and clinical manifestations do not really overlap those of *DYRK1A* syndrome. [a]: "Severe psychomotor delay, no walk aquisition and no language, severe amblyopia, self-injurious behavior, ASD, dysmorphic features (frontal bossing, hypertelorism, nystagmus, epicanthal folds, a flat nasal bridge, bilateral low-set ears, down-slanting palpebral fissures, a short philtrum, a high arched palate, downturned mouth and micrognathia). Relative macrocephaly (OFC: 52 cm, +0.6 SD; weight: 14.6 kg, −2.2 SD; height: 103.5 cm, −3.1 SD)" [16]; [b]: "Infantile spasms, west syndrome, ASD, aggression, hyperactivity" (personal communication Aida Telegrafi, Genedx); However, the most distal variant ever reported in *DYRK1A*, c.2213_2218delinsAGAG p.Thr738fs, occurred *de novo* in an individual with clinical features consistent with *DYRK1A* syndrome. [c]: "Autism, microcephaly, seizures, history of failure to thrive and IUGR, mitochondrial complex IV deficiency noted on muscle biopsy" (personal communication Aida Telegrafi, Genedx).

References

1. Widowati EW, Ernst S, Hausmann R, Müller-Newen G, Becker W. Functional characterization of DYRK1A missense variants associated with a syndromic form of intellectual deficiency and autism. *Biol Open*. 2018;7(4). doi:10.1242/bio.032862

2. Quartier A, Courraud J, Thi Ha T, et al. Novel mutations in NLGN3 causing autism spectrum disorder and cognitive impairment. *Hum Mutat*. 2019;40(11):2021-2032. doi:10.1002/humu.23836

3. Mattioli F, Isidor B, Abdul-Rahman O, et al. Clinical and functional characterization of recurrent missense variants implicated in THOC6-related intellectual disability. *Hum Mol Genet*. 2019;28(6):952-960. doi:10.1093/hmg/ddy391

4. Lee K-S, Choi M, Kwon D-W, et al. A novel de novo heterozygous DYRK1A mutation causes complete loss of DYRK1A function and developmental delay. *Sci Rep*. 2020;10(1):9849. doi:10.1038/s41598-020-66750-y

5. Bronicki LM, Redin C, Drunat S, et al. Ten new cases further delineate the syndromic intellectual disability phenotype caused by mutations in DYRK1A. *Eur J Hum Genet*. 2015;23(11):1482-1487. doi:10.1038/ejhg.2015.29

6. Blackburn ATM, Bekheirnia N, Uma VC, et al. DYRK1A-related intellectual disability: a syndrome associated with congenital anomalies of the kidney and urinary tract. *Genet Med*. 2019;21(12):2755-2764. doi:10.1038/s41436-019-0576-0

7. Alvarez M, Estivill X, de la Luna S. DYRK1A accumulates in splicing speckles through a novel targeting signal and induces speckle disassembly. *J Cell Sci*. 2003;116(Pt 15):3099-3107. doi:10.1242/jcs.00618

8. Birling M-C, Dierich A, Jacquot S, Hérault Y, Pavlovic G. Highly-efficient, fluorescent, locus directed cre and FlpO deleter mice on a pure C57BL/6N genetic background. *Genesis*. 2012;50(6):482-489. doi:10.1002/dvg.20826

9. Nguyen TL, Duchon A, Manousopoulou A, et al. Correction of cognitive deficits in mouse models of Down syndrome by a pharmacological inhibitor of DYRK1A. *Dis Model Mech*. 2018;11(9). doi:10.1242/dmm.035634

10. Ung DC, Iacono G, Méziane H, et al. Ptchd1 deficiency induces excitatory synaptic and cognitive dysfunctions in mouse. *Mol Psychiatry*. 2018;23(5):1356-1367. doi:10.1038/mp.2017.39

11. Marechal D, Lopes Pereira P, Duchon A, Herault Y. Dosage of the Abcg1-U2af1 region modifies locomotor and cognitive deficits observed in the Tc1 mouse model of Down syndrome. *PLoS ONE*. 2015;10(2):e0115302. doi:10.1371/journal.pone.0115302

12. Arbogast T, Iacono G, Chevalier C, et al. Mouse models of 17q21.31 microdeletion and microduplication syndromes highlight the importance of Kansl1 for cognition. *PLoS Genet*. 2017;13(7):e1006886. doi:10.1371/journal.pgen.1006886

13. Dubos A, Meziane H, Iacono G, et al. A new mouse model of ARX dup24 recapitulates the patients' behavioral and fine motor alterations. *Hum Mol Genet*. 2018;27(12):2138-2153. doi:10.1093/hmg/ddy122

14. Karp NA, Meehan TF, Morgan H, et al. Applying the ARRIVE Guidelines to an In Vivo Database. *PLoS Biol*. 2015;13(5):e1002151. doi:10.1371/journal.pbio.1002151

15. Kilkenny C, Browne WJ, Cuthill IC, Emerson M, Altman DG. Improving bioscience research reporting: the ARRIVE guidelines for reporting animal research. *PLoS Biol*. 2010;8(6):e1000412. doi:10.1371/journal.pbio.1000412

16. van Bon BWM, Hoischen A, Hehir-Kwa J, et al. Intragenic deletion in DYRK1A leads to mental retardation and primary microcephaly. *Clin Genet*. 2011;79(3):296-299. doi:10.1111/j.1399-0004.2010.01544.x

17. van Bon BWM, Coe BP, Bernier R, et al. Disruptive de novo mutations of DYRK1A lead to a syndromic form of autism and ID. *Mol Psychiatry*. 2016;21(1):126-132. doi:10.1038/mp.2015.5

18. O'Roak BJ, Vives L, Fu W, et al. Multiplex targeted sequencing identifies recurrently mutated genes in autism spectrum disorders. *Science*. 2012;338(6114):1619-1622. doi:10.1126/science.1227764

19. Courcet J-B, Faivre L, Malzac P, et al. The DYRK1A gene is a cause of syndromic intellectual disability with severe microcephaly and epilepsy. *J Med Genet*. 2012;49(12):731-736. doi:10.1136/jmedgenet-2012-101251

20. Okamoto N, Miya F, Tsunoda T, et al. Targeted next-generation sequencing in the diagnosis of neurodevelopmental disorders. *Clin Genet*. 2015;88(3):288-292. doi:10.1111/cge.12492

21. Iglesias A, Anyane-Yeboa K, Wynn J, et al. The usefulness of whole-exome sequencing in routine clinical practice. *Genet Med*. 2014;16(12):922-931. doi:10.1038/gim.2014.58

22. Ruaud L, Mignot C, Guët A, et al. DYRK1A mutations in two unrelated patients. *Eur J Med Genet*. 2015;58(3):168-174. doi:10.1016/j.ejmg.2014.12.014

23. Ji J, Lee H, Argiropoulos B, et al. DYRK1A haploinsufficiency causes a new recognizable syndrome with microcephaly, intellectual disability, speech impairment, and distinct facies. *Eur J Hum Genet*. 2015;23(11):1473-1481. doi:10.1038/ejhg.2015.71

24. Rump P, Jazayeri O, van Dijk-Bos KK, et al. Whole-exome sequencing is a powerful approach for establishing the etiological diagnosis in patients with intellectual disability and microcephaly. *BMC Med Genomics*. 2016;9:7. doi:10.1186/s12920-016-0167-8

25. Luco SM, Pohl D, Sell E, Wagner JD, Dyment DA, Daoud H. Case report of novel DYRK1A mutations in 2 individuals with syndromic intellectual disability and a review of the literature. *BMC Med Genet*. 2016;17:15. doi:10.1186/s12881-016-0276-4

26. Murray CR, Abel SN, McClure MB, et al. Novel Causative Variants in DYRK1A, KARS, and KAT6A Associated with Intellectual Disability and Additional Phenotypic Features. *J Pediatr Genet*. 2017;6(2):77-83. doi:10.1055/s-0037-1598639

27. Evers JMG, Laskowski RA, Bertolli M, et al. Structural analysis of pathogenic mutations in the DYRK1A gene in patients with developmental disorders. *Hum Mol Genet*. 2017;26(3):519-526. doi:10.1093/hmg/ddw409

28. Lee K-S, Choi M, Kwon D-W, et al. A novel de novo heterozygous DYRK1A mutation causes complete loss of DYRK1A function and developmental delay. *Sci Rep*. 2020;10(1):9849. doi:10.1038/s41598-020-66750-y

29. Dang T, Duan WY, Yu B, et al. Autism-associated Dyrk1a truncation mutants impair neuronal dendritic and spine growth and interfere with postnatal cortical development. *Mol Psychiatry*. 2018;23(3):747-758. doi:10.1038/mp.2016.253

30. Qiao F, Shao B, Wang C, et al. A De Novo Mutation in DYRK1A Causes Syndromic Intellectual Disability: A Chinese Case Report. *Front Genet*. 2019;10:1194. doi:10.3389/fgene.2019.01194

31. Ernst J, Alabek ML, Eldib A, et al. Ocular findings of albinism in DYRK1A-related intellectual disability syndrome. *Ophthalmic Genet*. Published online August 24, 2020:1-6. doi:10.1080/13816810.2020.1814349

32. Tran KT, Le VS, Bui HTP, et al. Genetic landscape of autism spectrum disorder in Vietnamese children. *Sci Rep*. 2020;10(1):5034. doi:10.1038/s41598-020-61695-8

33. Møller RS, Kübart S, Hoeltzenbein M, et al. Truncation of the Down syndrome candidate gene DYRK1A in two unrelated patients with microcephaly. *Am J Hum Genet*. 2008;82(5):1165-1170. doi:10.1016/j.ajhg.2008.03.001

34. Fujita H, Torii C, Kosaki R, et al. Microdeletion of the Down syndrome critical region at 21q22. *Am J Med Genet A*. 2010;152A(4):950-953. doi:10.1002/ajmg.a.33228

35. Oegema R, de Klein A, Verkerk AJ, et al. Distinctive Phenotypic Abnormalities Associated with Submicroscopic 21q22 Deletion Including DYRK1A. *Mol Syndromol*. 2010;1(3):113-120. doi:10.1159/000320113

36. Yamamoto T, Shimojima K, Nishizawa T, Matsuo M, Ito M, Imai K. Clinical manifestations of the deletion of Down syndrome critical region including DYRK1A and KCNJ6. *Am J Med Genet A*. 2011;155A(1):113-119. doi:10.1002/ajmg.a.33735

37. Valetto A, Orsini A, Bertini V, et al. Molecular cytogenetic characterization of an interstitial deletion of chromosome 21 (21q22.13q22.3) in a patient with dysmorphic features, intellectual disability and severe generalized epilepsy. *Eur J Med Genet*. 2012;55(5):362-366. doi:10.1016/j.ejmg.2012.03.011

38. Kim O-H, Cho H-J, Han E, et al. Zebrafish knockout of Down syndrome gene, DYRK1A, shows social impairments relevant to autism. *Mol Autism*. 2017;8:50. doi:10.1186/s13229-017-0168-2

39. Meissner LE, Macnamara EF, D'Souza P, et al. DYRK1A pathogenic variants in two patients with syndromic intellectual disability and a review of the literature. *Mol Genet Genomic Med*. Published online November 7, 2020:e1544. doi:10.1002/mgg3.1544

40. Matsumoto N, Ohashi H, Tsukahara M, Kim KC, Soeda E, Niikawa N. Possible narrowed assignment of the loci of monosomy 21-associated microcephaly and intrauterine growth retardation to a 1.2-Mb segment at 21q22.2. *Am J Hum Genet*. 1997;60(4):997-999.

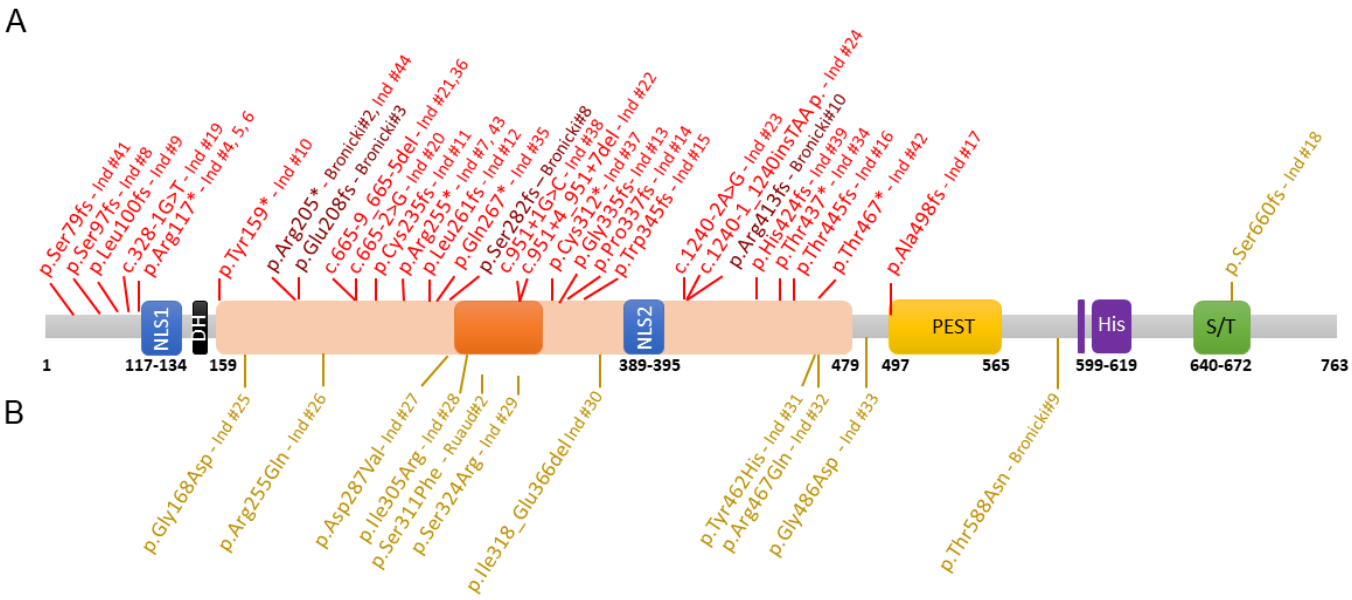

Figure S1

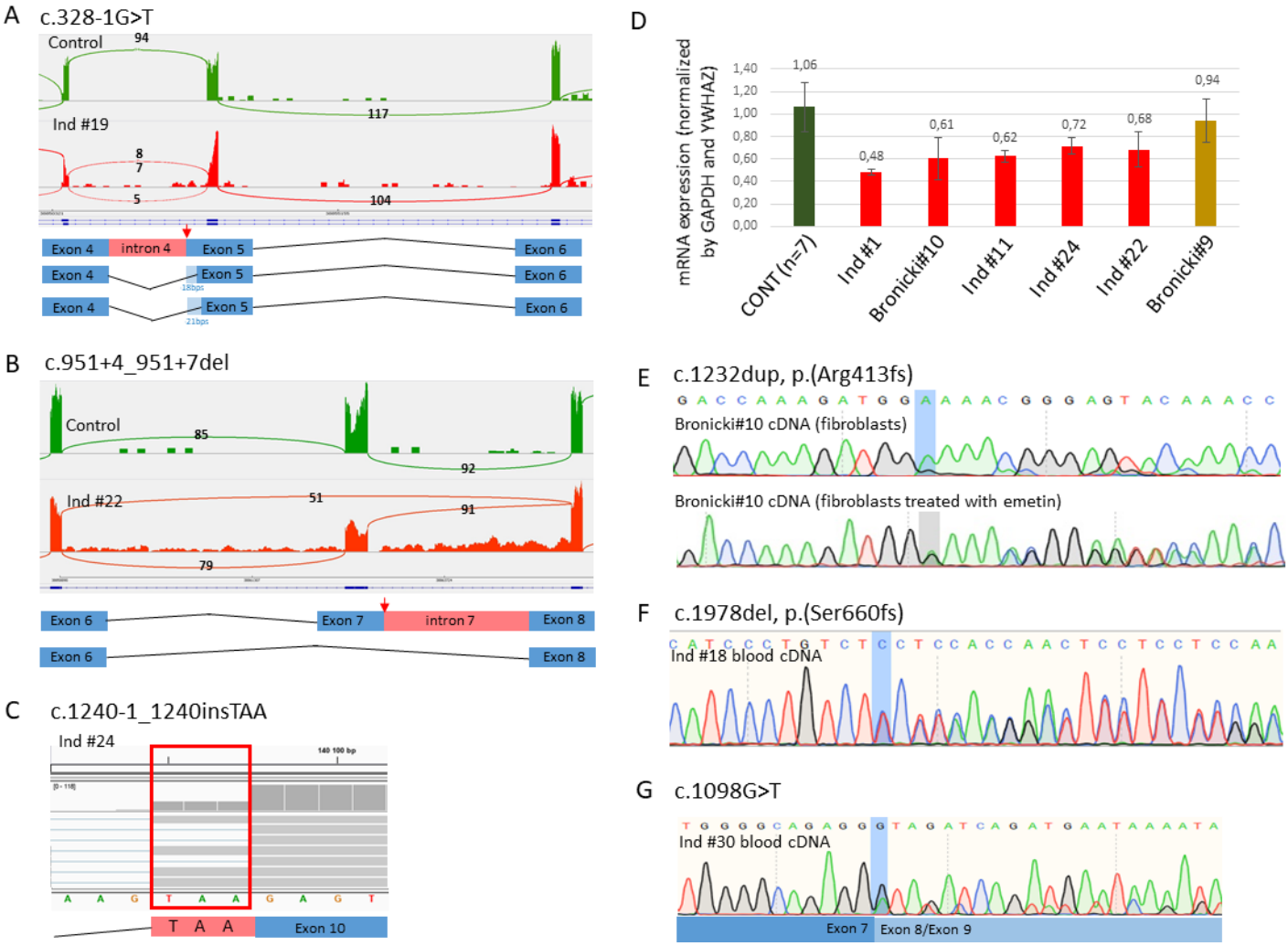

Figure S2

Figure S3

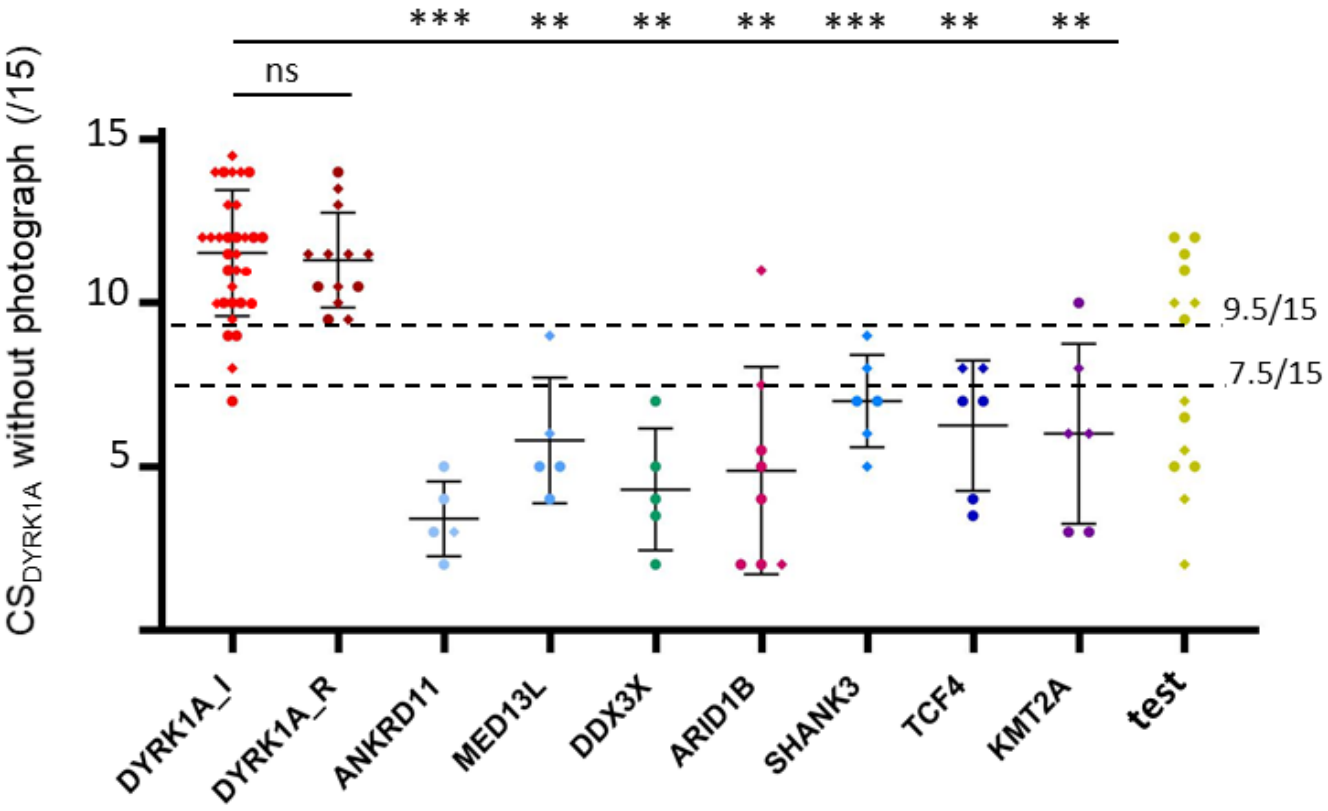

Figure S4

A

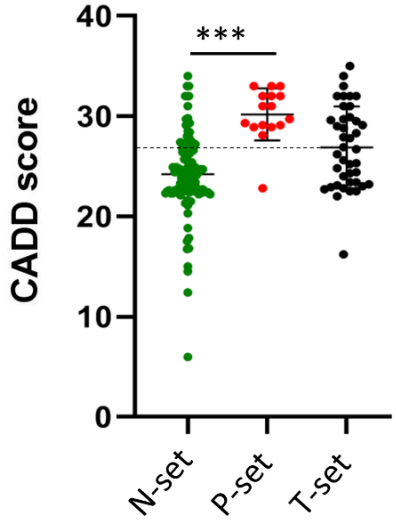

B

	CADD score			Conservation		
	>=20	>=25	>=30	V=100%	V=100% M>=90%	V=100% M>=90% O>=80%
N-set *(n=115)*	92,2% *(106)*	32,2% *(37)*	7% *(8)*	27,8% *(32)*	5% *(6)*	0,9% *(1[a])*
P-set *(n=16)*	100% *(16)*	93,75% *(15)*	50% *(8)*	93,75% *(15)*	87,5% *(14)*	81,25% *(13[b])*
T-set *(n=44)*	97,8% *(43)*	61,4% *(27)*	22,7% *(10)*	70,5% *(31)*	27,3% *(12)*	22,7% *(10[c])*

Figure S5

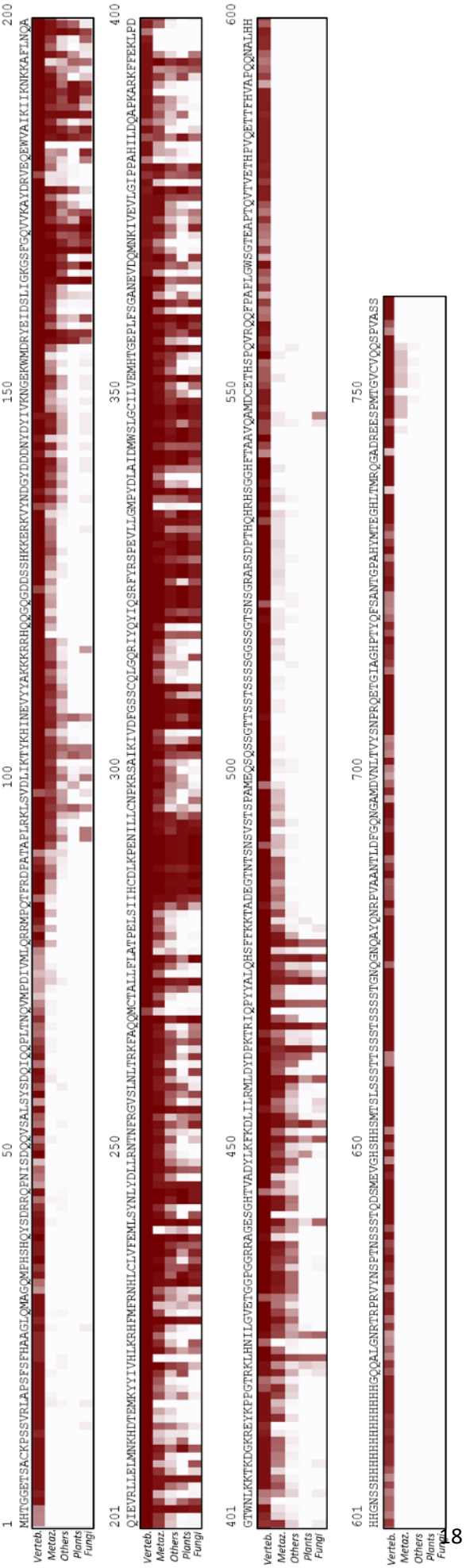

Figure S6

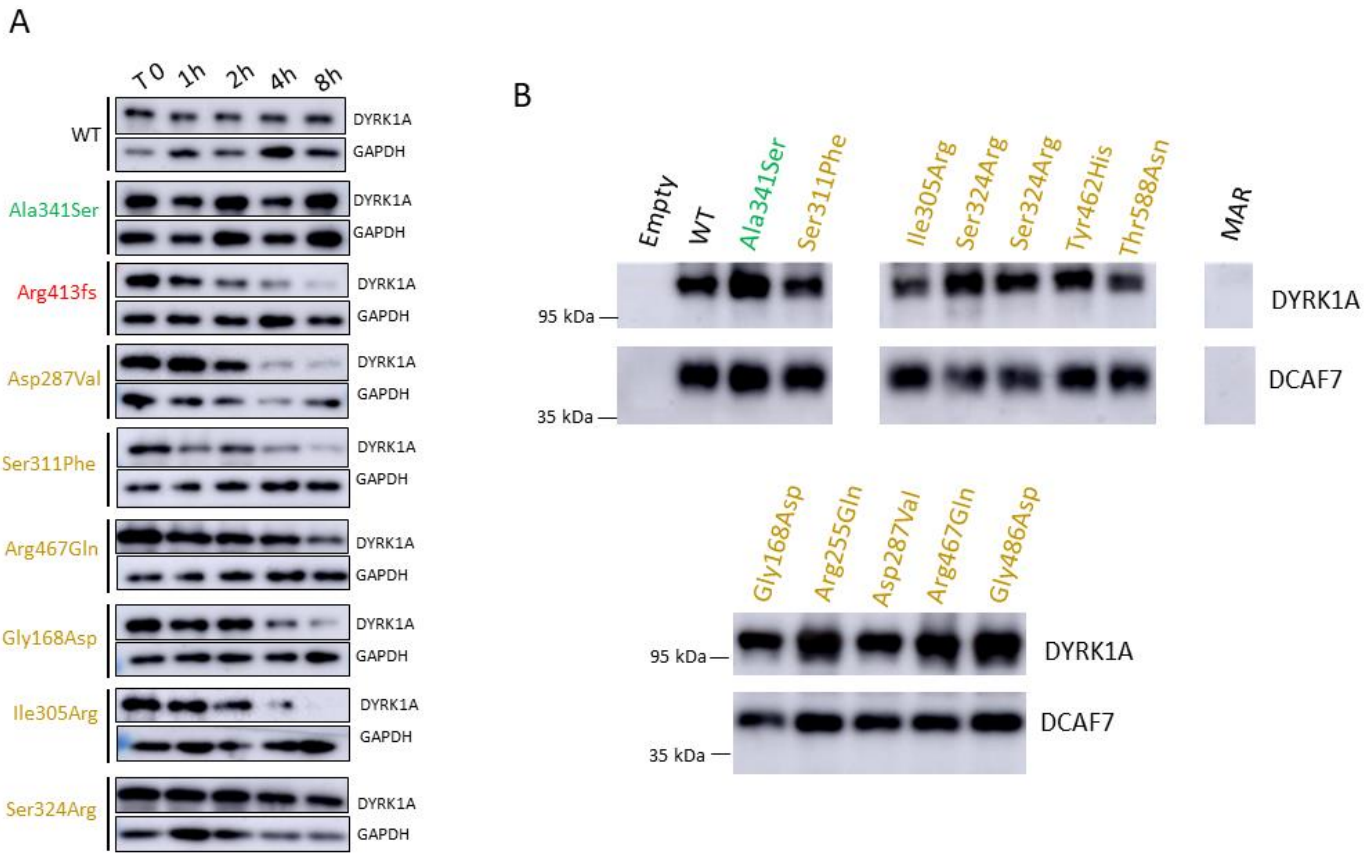

Figure S7

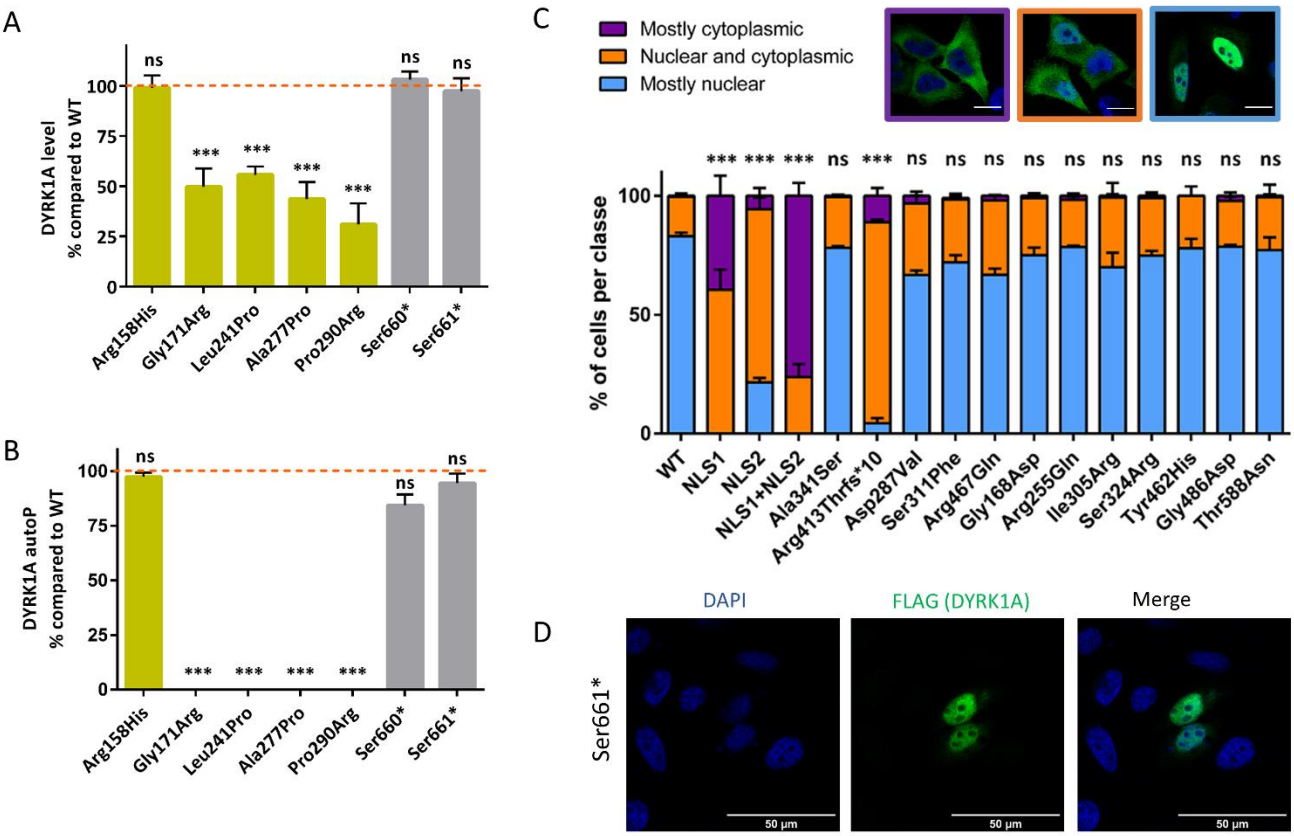

Figure S8

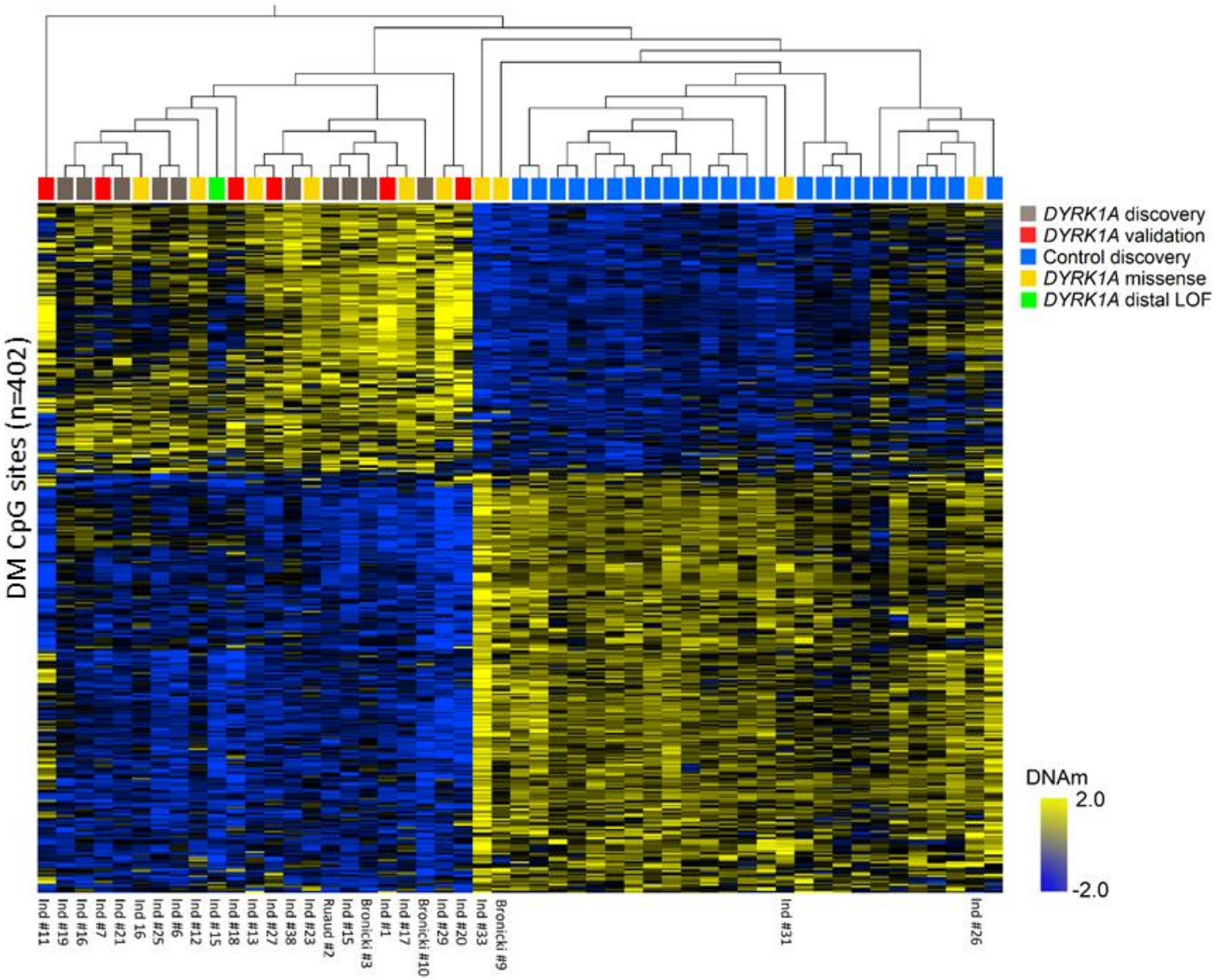

Figure S9

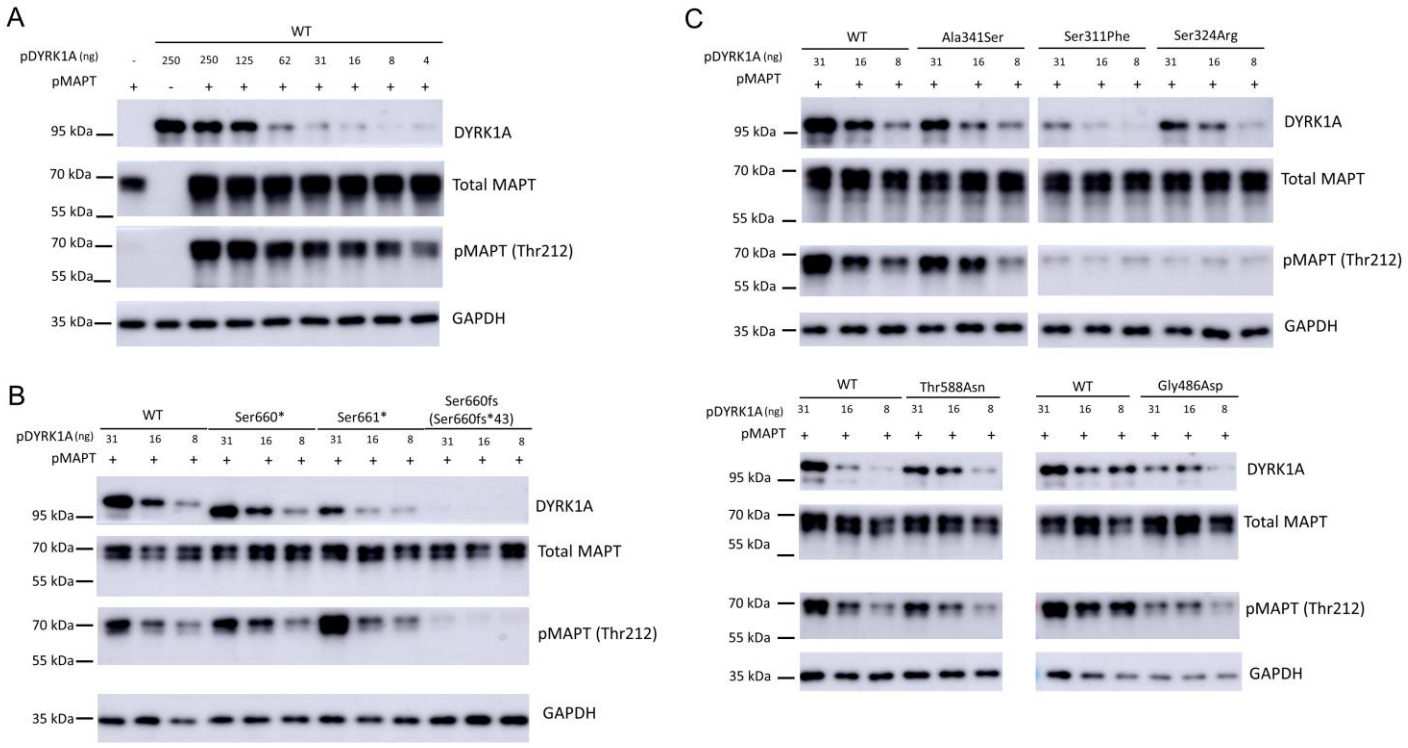

Figure S10

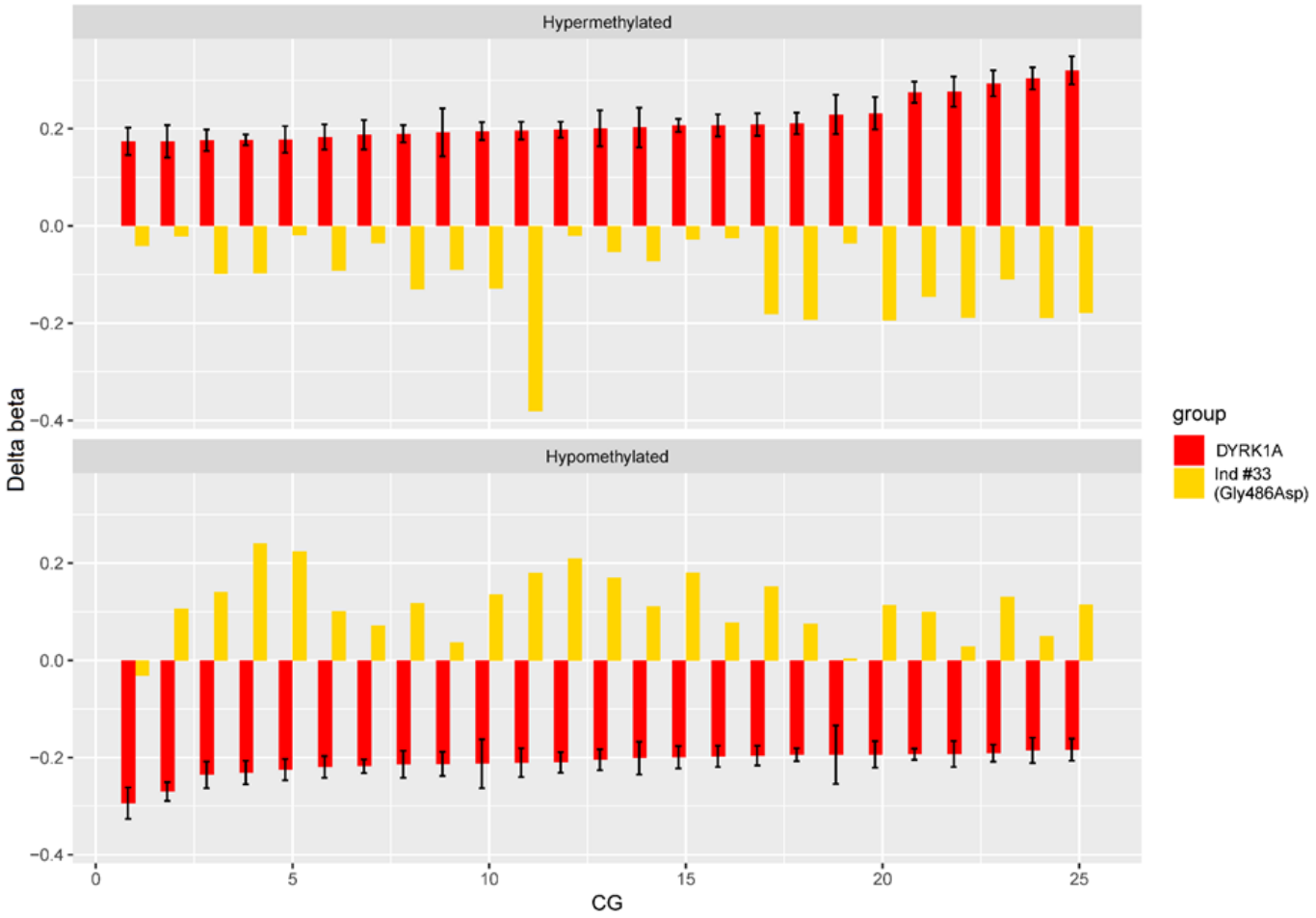

Figure S11

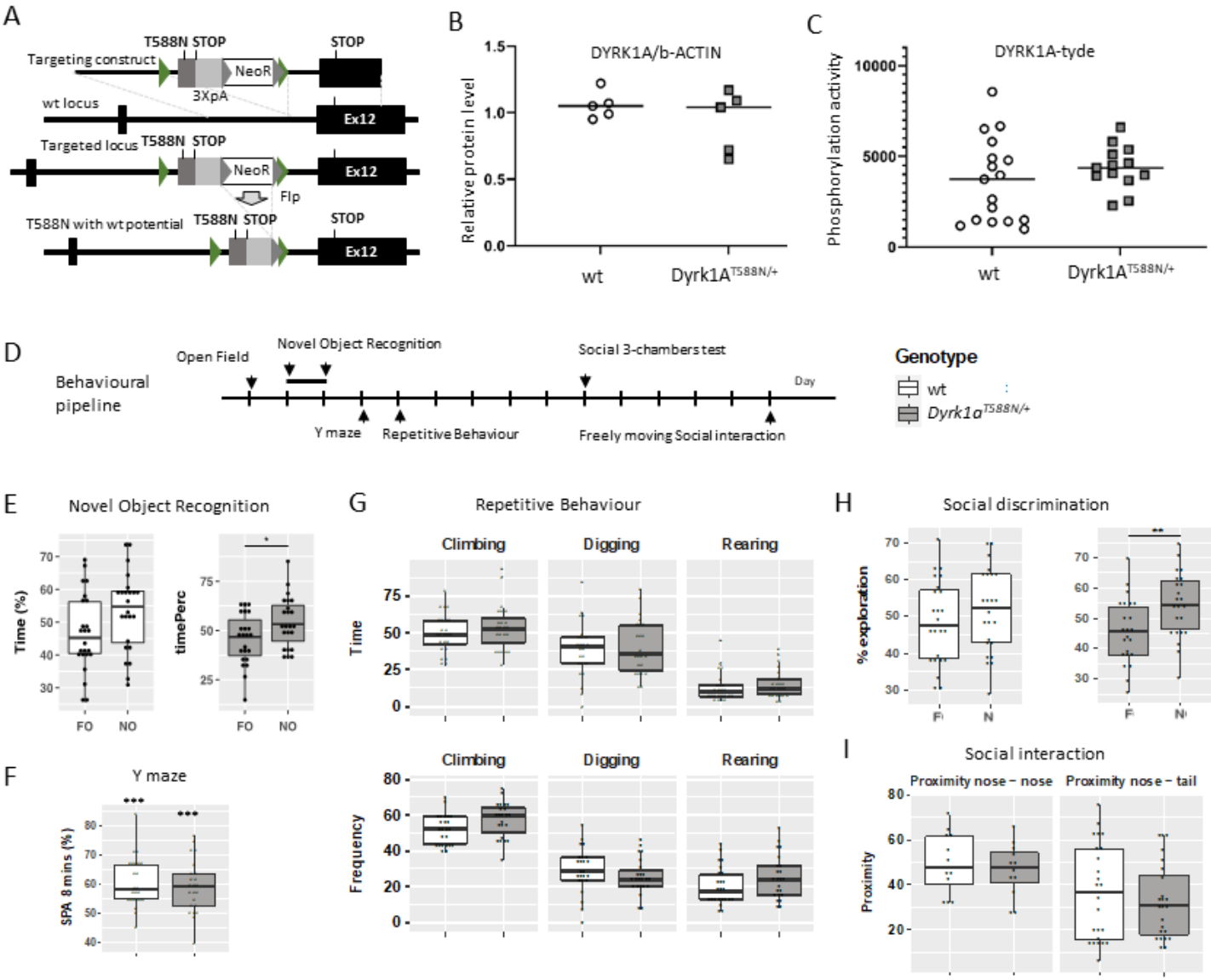

Figure S12

		Ind #1	Ind #2	Ind #3	Ind #4	Ind #5	Ind #6	Ind #7	Ind #8	Ind #9	Ind #10	Ind #11
		M	F	M	M	F	M	M	M	M	F	M
***DYRK1A* variant**	nomenclature (NM_001396.4)	g:38481804_4019	g.38722881_394	t(9;21)(p12;q22	c.349C>T	c.349C>T	c.349C>T	c.763C>T	c.290_291 delCT	c.297_301delCTTGA	c.477del	c.702_703delCT
	nomenclature (NP_001387.2)	-	-	-	p.Arg117*	p.Arg117*	p.Arg117*	p.Arg255*	p.Ser97fs	p.Leu100fs	p.Tyr159*	p.Cys235fs
	variant type	deletion	deletion	translocation?	nonsense	nonsense	nonsense	nonsense	frameshift	frameshift	nonsense	frameshift
	inheritance	de novo	de novo	de novo	NA	mosaic father	de novo	NA	de novo	de novo	de novo	de novo
Pregnancy and birth	IUGR	yes	no	no	NA	NA	no	no	yes	yes	yes	no
	other	NA	NA	NA	antenatal anom	NA	NA	NA	NA	NA	NA	NA
	delivery	42	term	term	35	term	term	term	term	term	term	term
	APGAR	10/10	10/10	NA	low	NA	9/10	9/10	10/10	10/10	NA	10/10
	BW	2710	3430	2400	2060	3060	3150	3780	2290	2220	2710	2780
	BS	47.5	48	45	NA	47,5	45	51	45	43	46	48
	BOFC	32	33	29.5	31.3	NA	30	35	32	31	31	33
Development	**speech**	**absence**	**NA**	**few words**	**few words**	**few sentences**	**few words**	**absence**	**absence**	**absence**	**few sentences**	**few words**
	ID level (estimated)	**moderate**	**NA**	**mild**	**severe**	**severe**	**severe**	**severe**	**moderate**	**severe**	**severe**	**moderate/severe**
	History of seizures	**yes**	**yes**	**yes**	**yes**	**yes**	**yes**	**yes**	**yes**	**no**	**yes**	**yes**
	comment	tonico-clonic	febrile, typical at	febrile, tonico cl	absence, tonico	febrile	NA	NA	febrile, then tonico-c	NA	febrile	absence
	hypotonia	no	yes	no	yes	no	NA	no	yes	yes	no	yes
	motor delay walk acquisition >=1	**yes (19.5 mo)**	**NA**	**no (15 mo)**	**yes (24 mo)**	**yes (18 mo)**	**yes (>36 mo)**	**no (16 mo)**	**yes (30 mo)**	**yes (18 mo)**	**yes (18 mo)**	**no (17 mo)**
	motor manifestations	**hypereflexia**	**no**	**no**	**no**	**hypereflexia, Bab**	**hypereflexia**	**no**	**ataxic walk**	**ataxic walk**	**hypereflexia**	**ataxic walk, dysmet**
	stereotypies/autistic traits/anxie	**anxiety**	**no**	**no**	**stereotypies**	**stereotypies, anx**	**anxiety**	**stereotypies (ASD di**	**stereotypies (ASD di**	**stereotypies**	**stereotypies, anxiet**	**stereotypies**
	other	behavioral proble	no	no	no	behavioral proble	sleep disorder	behavioral problem	sleep disorder, wate	water fascination, be	behavioral problem	no
General exam	age	10	0.5	12	3	NA	13	18	11	11.5	17	9
	weight (kg)	22	7.85	26.8	14.4	NA	23	66	24.5	22.5	49.5	26,3
	weight (SD)	-3.2	NA	NA	N	NA	-2.5	NA	-3.5	<-2	-2	-1
	size (cm)	128	NA	141	99	NA	142	168	129.5	133	148	135,2
	size (SD)	-1	NA	NA	N	NA	-1.5	NA	-1.5	-1.8	-2	N
	OFC (cm)	47	38	47.4	43.5	NA	48	53	47.5	47.5	49.5	46.5
	OFC (SD)	**<-4**	**<-4**	**<-4**	**<-4**	**NA**	**-4,5**	**-2**	**<-4**	**<-4**	**-3,5**	**-3,5**
	skin	**thin skin, dermati**	**NA**	**thin skin, derma**	**no**	**dermatitis**	**thin skin, dermat**	**severe dermatitis**	**thin skin, dermatitis**	**dermatitis at birth**	**no**	**no**
	member anomalies	no	no	no	no	NA	NA	no	yes (syndactyly foot)	no	yes	no
	cardiac anomalies	no	no	no	yes (VSD)	no	no	no	no	no	no	no
	skeletal anomalies	no	no	no	no	mild pectus excav	NA	no	no	no	yes	no
	urogenital anomalies	NA	no	NA	cryptorchidism	no	NA	hypospade	cryptorchidism	no	no	unilateral cryptorchi
	other anomalies	inguinal hernia, py	NA	inguinal hernia	NA	bilateral coxa valg	NA	NA	NA	NA	NA	NA
	vision problems	no	NA	hypermetropia	no	NA	NA	NA	hypermetropia, astig	no	myopia, astigmatism	hypermetropia, astig
	other opthtalmic problems	no	NA	no	no	NA	NA	papillary pallor	no	no	no	no
	feeding problems	**yes**	**yes**	**yes**	**yes**	**yes**	**yes**	**yes**	**yes**	**yes**	**yes**	**yes**
	comments	difficulties in infan	difficult, vomitin	NA	frequent occlusi	NA	important difficul	mastication problem	in infancy, better no	low appetite, highly	sucking difficulty	in infancy
	constipation	no	no	yes	yes	NA	yes	NA	no	yes	no	no
	GER	no	no	yes	NA	NA	NA	yes	no	no	yes	no
MRI	**performed**	done	done	done	done	done	done	NA	done	done	done	done
	comment	**EV, CA**	**EV, CCH, gyratio**	**CA, CCH**	**hypersignal T2, l**	**nothing**	**EV, gyration ano**	**NA**	**EV**	**EV, ECC**	**nothing**	**CA**

DYRK1A_I

Ind #12	Ind #13	Ind #14	Ind #15	Ind #16	Ind #17	Ind #19	Ind #20	Ind #21	Ind #22	Ind #23	Ind #24	Ind #34
F	F	F	F	F	F	F	M	M	M	M	F	F
c.782del	c.1004del	c.1008dup	c.1033del	c.1333dup	c.1491delC	c.328-1G>T	c.665-2A>G	c.665-9_665-5delTT(	c.951+4_951+7delG1	c.1240-2A>G	c.1240-1_1240insTA	c.1309C>T
p.Leu261fs	p.Gly335fs	p.Pro337fs	p.Trp345fs	p.Thr445fs	p.Ala498fs	p.?	p.?	p.?	p.?	p.?	p.Glu414*	p.Arg437*
frameshift	Frameshift	frameshift	frameshift	frameshift	frameshift	splice	splice	splice	splice	splice	nonsense	nonsense
de novo	absent in the mother	de novo	de novo	de novo	de novo	de novo	de novo	de novo	de novo	de novo	de novo	NA
no	yes	no	yes	yes	yes	no	no	no	yes	yes	yes	yes
cerebellar anomaly	NA	NA	CGH-array + CMV + MRI	NA	NA	NA	NA	NA	NA	NA	caesarian	single umbilical arter
term	38	term	term	37	36	term	term	39	NA	term	term	term
10/10	NA	NA	NA	10/10	9	10	NA	10/10	NA	NA	10/10	10/10
3030	2400	3550	1865	1970	1990	3450	3110	3085	2690	3160	2410	2450
46	42	52	42	43,5	43	49	52	50	47	48	45	47
32	30.5	NA	29.5	30	28.5	32	33	34	NA	33	31	31
absence	**few words**	**few words**	**few words/few sentenc**	**few words**	**few sentences**	**few words**	**absence**	**few sentences**	**few words**	**absence**	**few sentences**	**few sentences**
severe	**severe**	**moderate**	**moderate to severe**	**severe**	**severe**	**severe**	**moderate**	**moderate**	**severe**	**severe**	**moderate**	**mild**
yes	**yes**	**yes**	**no**	**yes**	**no**	**yes**	**yes**	**yes**	**yes**	**yes**	**yes**	**yes**
NA	atonic	febrile seizures	NA	febrile, then tonico-c	NA	febrile	febrile	tonico-clonic	febrile	febrile	febrile seizures + oth	febrile
no	no	no	yes	yes	yes	yes	yes	no	NA	no	NA	yes
yes (19 mo)	**yes (>36mo)**	**yes (>36mo)**	**yes (24 mo)**	**yes (28 mo)**	**no (16 mo)**	**yes (36 mo)**	**yes (31 mo)**	**no (16.5 mo)**	**yes (18 mo)**	**yes (18 mo)**	**yes (22 mo)**	**yes (23 mo)**
no	**no**	**ataxic walk**	**hypereflexia**	**hypereflexia**	**NA**	**ataxic walk, hyperef**	**NA**	**ataxic walk, hyperef**	**NA**	**no**	**hypereflexia**	**no**
stereotypies	**stereotypies**	**stereotypies**	**stereotypies**	**stereotypies, anxiet**	**stereotypies**	**stereotypies**	**stereotypies**	**stereotypies (ASD di**	**stereotypies, anxiet**	**stereotypies (ASD di**	**stereotypies**	**stereotypies, anxiet**
sleep disorder, beha	no	no	sleep disorder	behavioral problem	NA	behavioral problem,	water fascination	behavioral problem	no	sleep disorder, anxie	sleep disorder, beha	NA
7.5	27	18.5	2	12.5	3.5	11	1.5	20	NA	7	NA	13
16.5	67	47.3	7.6	30	10.9	28.1	11.6	41	NA	18.1	11	27
-2	NA	-2.7	NA	-2	-2.5	NA	1	-4	NA	-2	-3	-2
118	150	164	76	140	93.5	149	82	172.5	NA	114.5	NA	130
-1	NA	-0.88	NA	-2	-2	NA	0	-0.5	NA	-1.3	-2	-2
46	48.5	50.5	40.5	48	44.5	47.5	45	51	NA	45	43	47
<-4	**-3,5**	**<-3**	**-4**	**<-4**	**-4**	**<-4**	**-3**	**-4**	**-4**	**<-4**	**-5**	**-5**
no	**NA**	**thin skin**	**no**	**thin skin**	**thin skin, dermatitis**	**dermatitis at birth**	**thin skin**	**thin skin, dermatitis**	**no**	**thin skin**	**thin skin**	**thin skin, dermatitis**
no	no	short 5th metatars, s	yes (adductus thumb)	no	NA	no	no	yes. Bilateral postaxi	no	no	NA	no
no	NA	no	no	yes (AtSD)	NA	no	NA	no	no	no	NA	no
no	scoliosis,eqinus feet	abnormalities of the	no	no	NA	no	no	no	no	no	NA	no
NA	anal malposition	no	no	no	NA	NA	NA	no	cryptorchidism	no	NA	grade II vesicoureter
inguinal hernia, vaso	hiatal hernia	Acrocyanosis – hand	NA	NA	NA	NA	NA	NA	inguinal hernia	NA	NA	velopalatine insuffici
astigmatism	NA	myopia	NA	myopia	hypermetropia	no	NA	myopia, astigmatism	myopia	NA	NA	NA
no	NA	no	no	no	NA	papillary pallor	papillary pallor	hypolasia optic nerve	no	no	no	hypolasia optic nerve
yes	**yes**	**yes**	**yes**	**yes**	**yes**	**yes**	**yes**	**no**	**yes**	**yes**	**yes**	**yes**
difficult in infancy	gastrostomy	breast, additional	NA	important feeding di	very difficult betwee	first months	low appetite	NA	highly selective	very selective	NA	very selective
no	no	no	yes	yes	yes	yes	no	no	yes	no	yes	yes
no	yes	NA	NA	no	NA	yes	NA	no	NA	no	NA	yes
done	done	done	done	done	done	done	done	done	not done	done	done	done
CCH, CeA (pre and p	**EV**	**nothing**	**NA**	**CCH, atrophy CSE**	**delayed myelinatior**	**CCH, CA, EV**	**EV, CA**	**EV**	**NA**	**CA, CeA**	**nothing**	**enlarged pericerebr**

										Total (n=34)		Previously reported[a] (n=80)	
Ind#35	Ind#36	Ind #37	Ind #38	Ind#39	Ind #40	Ind #41	Ind #42	Ind #43	Ind #44	Total	%	Total	%
M	M	F	M	F	M	F	F	F	M	17 F/ 17 M			
c.799C>T	c.665-9_665-5delTT(	c.936T>A	951+1G>C	c.1270del	g.38302140_400414	c.235dupA	c.1399C>T	c.763C>T	c.613C>T				
p.Gln267*	p.?	p.Cys312*	p.?	p.His424fs	-	p.Arg79fs	p.Arg467*	p.Arg255*	p.Arg205*				
nonsense	splice	nonsense	splice	frameshift	deletion	frameshift	nonsense	nonsense	nonsense				
de novo	de novo	de novo	de novo	de novo	de novo	de novo	de novo	NA	NA				
no	yes	yes	no	yes	yes	yes	yes	yes	yes	20/32	63%	22/32	69%
NA	NA	NA	NA	NA	NA	NA	NA	NA	kidney asymetry				
term	term	term	term	term	term	term	term	35	term				
NA	10/10	NA	10/10	9/10	10/10	10/10	9/10	NA	NA				
2880	2580	2175	2810	2700	3395	2160	2530	1695	2590				
50	44	43	49	47	46	43.6	43	43.5	44				
34	33	30,2	33	31.5	NA	30	31.5	28.5	32				
few sentences	**absence**	**few words**	**NA**	**few sentences**	**absence**	**NA**	**few words**	**few words**	**absence**	**30/30** (A/FW: 22/31)	**100%** (71%)	**74/74**	**100%**
moderate	**severe**	**NA**	**NA**	**moderate/severe**	**severe**	**NA**	**severe**	**severe**	**severe**	**32/32** (M/S:28/30)	**100%** (93%)	**73/73**	**100%**
yes	**yes**	**yes**	**NA**	**yes**	**yes**	**yes**	**yes**	**yes**	**no**	**29/33** (febrile: 18)	**88%**	**56/76** (febri	**74%**
febrile	febrile + tonicoclonic	febrile	NA	febrile, absence, my	febrile, tonico-clonic	NA	absence, tonico-clon	NA	NA				
yes	yes	yes	yes	no	NA	yes	no	no	NA	16/29	55%		
yes (19 mo)	**yes (21 mo)**	**yes (25 mo)**	**yes (>26 mo)**	**yes (24 mo)**	**yes (28 mo)**	**yes (21 mo)**	**no (17 mo)**	**yes (20 mo)**	**yes (>36 mo)**	**27/33**	**82%**	**59/67**	**88%**
no	**NA**	**digitigrade walk**	**hypereflexia**	**no**	**pyramidal signs**	**pyramidal signs, hyp**	**hypertonia**	**NA**	**NA**	**18/28**	**64%**	**32/44**	**73%**
stereotypies	**stereotypies, anxiet**	**stereotypies**	**NA**	**anxiety**	**stereotypies, anxiet**	**NA**	**anxiety**	**no**	**no**	**28/32**	**88%**	**40/45**	**89%**
sleep disorder	behavioral problem	water fascination, be	NA	NA	sleep disorder, wate	sleep disorders	sleep disorders, wat	absence of fear	no				
23	18	3	NA	13	8.5	5	15	6	4				
63	40,5	12	NA	31.6	19	16.7	36.6	15.8	13.1				
N	NA	-1	NA	-1.3	-2	NA	-2.5	-1.4	-1.7				
173	159,5	87	NA	139	120	102	150.5	113	95				
N	NA	-2	NA	-1.7	-1.5	NA	-2	N	-2				
52.5	52	44	NA	50	45.5	45	49.3	44	44.5				
-3	**-3**	**-3,5**	NA	**-2**	**-6**	**<-3**	**<-3**	**<-4**	**<-4**	**32/32**	**100%**	**72/77**	**94%**
no	**no**	**thin skin**	**NA**	**NA**	**thin skin**	**NA**	**thin skin**	**no**	**NA**	**19/28**	**68%**	**10/?**	
no	no	yes	NA	long fingers, small th	no	NA	no	no	no	7			
no	no	NA	NA	pulmonary valve dys	no	NA	no	no	no	3			
cyphosis	scoliosis	pectus	NA	no	no	NA	no	no	no	7			
testicular ectopia	no	ovarian hernia	NA	no	NA	NA	no	no	micropenis	10/23	43%	13/?	
NA	NA	NA	NA	no	nail dystrophy	NA	no	no	no				
myopia	hypermetropia	no	NA	hypermetropia	NA	NA	hypermetropia	no	hypermetropia, astig	15/21	71%		
no	no	no	strabism	nystagmus	hypolasia optic nerv	NA	no	strabism	no				
no	**yes**	**yes**	**yes**	**yes**	**yes**	NA	**yes**	**yes**	**yes**	**31/33**	**94%**	**50/57**	**88%**
NA	smashed food	NA	NA	first months	poor eating	NA	NA	very selective	NA				
yes	no	no	NA	NA	no	NA	yes	no	yes			12/?	
no	no	yes	yes	yes	no	NA	yes	no	NA			11/?	
not done	done	done	NA	NA	done	done	done	done	done				
NA	**periventricular whit**	**NA**	**NA**	**NA**	**CCH, enlarged cister**	**enlarged pericerebr**	**nothing**	**CA**	**CCH**	**22/27**	**81%**	**39/52**	**75%**

DYRK1A_R (Bronicki et al., 2014)				Individuals with variants to test											
Bronicki_#2	Bronicki_#3	Bronicki_#8	Bronicki_#10	Ind #18	Ind #25	Ind #26	Ruaud #2	Ind #29	Ind #31	Ind #30	Ind #28	Ind #32	Ind #27	Ind #33	Bronicki_#9
M	M	M	F	F	F	F	M	M	M	F	F	F	M	M	F
c.613C>T	c.621_624 delin	c.844dupA	c.1232dup	c.1978del	c.503G>A	c.764G>A	c.932C >T	c.972T>A	c.1384T>C	c.1098G>T	c.914T>G	c.1400G>A	c.860A>T	c.1457G>A	c.1763C>A
p.Arg205*	p.Glu208fs	p.(Ser282Lysfs*(	p.Arg413fs	p.Ser660fs	p.Gly168Asp	p.Arg255Gln	p.Ser311Phe	p.Ser324Arg	p.Tyr462His	p.Ile318_Glu366	p.Ile305Arg	p.Arg467Gln	p.Asp287Val	p.Gly486Asp	p.Thr588Asn
nonsense	frameshift	frameshift	frameshift	frameshift	missense	missense	missense	missense	missense	inframe del	missense	missense	missense	missense	missense
de novo	de novo	de novo	de novo	de novo	de novo	NA	de novo	de novo	de novo	de novo	de novo	de novo	de novo	de novo	de novo
NA	NA	no	yes	yes	NA	no	yes	yes	NA	yes	yes	NA	yes	NA	no
NA	NA	NA	NA	heart ventricula	NA	NA	artery	NA	NA	NA	NA	NA	NA	NA	NA
term	term	term	term	term	NA	term	term	term	term	term	term	NA	prematurity	NA	term
10/10	10/10	8/10/10	10/10	10/10	NA	10/10	NA	NA	7/10	9/10	NA	NA	NA	NA	8/3
2720	3280	3290	2215	2660	NA	3490	3170	2575	3440	2570	2550	NA	2200	NA	3000
47	49	47	46	46	NA	51,5	49	46	50,5	48	47	NA	NA	NA	48
32	33	34	32	31	NA	36	33.5	33	37	31	31.5	NA	NA	NA	32
few words	**few words**	**absence**	**few words**	**few sentences/**	**NA**	**few words**	**few words**	**few sentences**	**normal**	**absence**	**few words**	**NA**	**few words**	**normal**	**absence**
moderate	**moderate**	**moderate/seve**	**moderate/seve**	**moderate**	**NA**	**NA**	**moderate**	**mild**	**mild**	**severe**	**severe**	**NA**	**severe**	**no ID**	**severe**
yes	**absence?**	**yes**	**yes**	**no**	**NA**	**no**	**yes**	**yes**	**yes**	**yes**	**yes**	**no**	**yes**	**no**	**yes**
NA	NA	febrile, tonico-cl	febrile, myoclon	NA	NA	NA	febrile	atonic	febrile	febrile, tonic-clo	febrile	NA	febrile	NA	absence, tonic
NA	NA	yes	NA	no	NA	no	NA	yes	no	yes	NA	NA	no	NA	yes
yes	**yes (23mo)**	**no (16 mo)**	**yes (20 mo)**	**yes (18 mo)**	**NA**	**yes (18 mo)**	**yes**	**yes (22 mo)**	**no (13 mo)**	**yes (36 mo)**	**yes**	**NA**	**yes (20 mo)**	**no**	**yes (>36 mo)**
NA	**hypertonia**	**hypereflexia**	**NA**	**no**	**NA**	**no**	**NA**	**no**	**normal**	**no**	**ataxic walk, hyp**	**NA**	**NA**	**no**	**ataxia**
anxiety	stereotypies	ASD diagnosis	flapping	anxiety	NA	stereotypies	stereotypies	ASD, anxiety	anxiety	sterotypies	sterotypies	sterotypies	stereotypies	ASD	stereotypies
NA	sleep disorders	water fascinatio	NA	NA	NA	behavioral probl	NA	sleep disorder,b	aggresivity	sleep disorder, water fascination, behavioral prob			NA	NA	sleep disorder, w
15	3	NA	NA	12	NA	3	NA	5	22,5	16	NA	NA	6	10	38
43.8	13.5	NA	NA	39	NA	15,7	NA	11,5	89	44	NA	NA	21	39.4	75
NA	-1	NA	-2	N	NA	N	NA	+1.2	NA	-2.3	-1.5	NA	NA	NA	+3.5
167	94	NA	NA	154	NA	NA	NA	101,5	181	162	NA	NA	117	156	170
NA	-1	NA	-0,5	+1.7	NA	NA	NA	-1,5	NA	-1	NA	NA	NA	NA	1
43,8	46	NA	NA	50	NA	NA	NA	52	60,5	47	NA	NA	46.5	58.5	NA
-3	**-4**	**<-3**	**-3.5**	**-2.5**	**NA**	**2**	**<-4**	**+1**	**NA**	**<-3**	**-4**	**NA**	**<-3**	**NA**	**-3**
thin skin	**NA**	**no**	**thin skin**	**no**	**NA**	**no**	**NA**	**no**	**no**	**no**	**NA**	**dermatitis**	**NA**	**+2**	**thin skin**
no	NA	no	NA	no	NA	no	no	clinodactyly 5th	no	long fingers, can	NA		flat feet	NA	no
no	NA	VSD	NA	no	NA	no	no	no	no	NA	NA	NA	NA	NA	NA
pectus excavatu	NA	scoliosis	NA	NA	NA	no	no	no	scoliosis	NA	NA	NA	NA	NA	NA
no	NA	NA	no	no	NA	no	no	no	no	NA	NA	NA	micropenis	NA	no
no	NA	NA	NA	NA	NA	no	no	no	no	NA	NA	NA	NA	NA	NA
hypermetropia	hypermetropia,	hypermyopia	NA	hypermetropia	NA	no	NA	NA	hypermyopia	NA	NA	NA	NA	NA	NA
NA		NA	NA	no	NA	NA	no	NA	no	NA	NA	NA	NA	NA	NA
yes	**yes**	**yes**	**yes**	**no**	**NA**	**no**	**no**	**yes**	**no**	**yes**	**NA**	**yes**	**NA**	**NA**	**yes**
NA	NA	gastrostomy	NA	NA	NA	NA	no	NA	NA	difficulty during	no	NA	NA	NA	mild
NA	yes	yes	NA	no	NA	no	NA	yes	no	yes	NA	NA	yes	NA	yes
NA	NA	yes	NA	no	NA	no	NA	yes	no	no	NA	NA	NA	NA	no
done	done	done	done	done	NA	done	done	done	done	done	done	done	NA	NA	not done
EV, plagiocepha	**EV**	**EV**	**EV, CCA**	**thin optic nerve**	**NA**	**nothing**	**EV**	**nothing**	**EV**	**CA, EV**	**CCH**	**normal**	**NA**	**NA**	**NA**

Cohort	Name	Ind	Sex	Mutation nomenclature		Type	Inheritance	Intellectual disability	Impaired language	Microcephaly	Feeding difficulty	History of seizures	Autistic traits / Anxiety	Brain anomaly on MRI	Motor delay	Ataxic walk/hypertoni	Atopic or transluside s	/15	Dysmorphy	total /20	calculated on clinical data coming from
DYRK1A_I	*this report*	Ind #1	M	g:38481804_40190458del	-	deletion	de novo	1	2	2	2	1	1	1	1	0.5	0.5	12	4	16	this report
		Ind #2	F	g.38722881_39426450del	-	deletion	de novo	NA	NA	2	2	2	0	1	NA	0	NA	7	NA	NA	this report
		Ind #40	M	g.38302140_40041414del	-	deletion	de novo	2	2	2	2	2	1	1	1	0.5	0.5	14	NA	NA	this report
		Ind #3	M	t(9;21)(p12;q22)	-	translocation?	de novo	0	2	2	2	2	0	1	0	0	0.5	9.5	3.5	13	this report
		Ind #4	M	c.349C>T	p.Arg117*	nonsense	NA	2	2	2	2	1	1	1	1	0	0	12	NA	NA	this report
		Ind #5	F	c.349C>T	p.Arg117*	nonsense	mosaic father	2	1	NA	2	2	1	0	1	0.5	0.5	10	NA	NA	this report
		Ind #6	M	c.349C>T	p.Arg117*	nonsense	de novo	2	2	2	2	1	1	1	1	0.5	0.5	13	NA	NA	this report
		Ind #10	F	c.477del	p.Tyr159*	nonsense	de novo	2	1	2	2	2	1	0	1	0.5	0	11.5	3.5	15	this report
		Ind #44	M	c.613C>T	p.Arg205*	nonsense	NA	2	2	2	2	0	0	1	1	NA	NA	10	NA	NA	this report
		Ind #7	M	c.763C>T	p.Arg255*	nonsense	NA	2	2	1	2	1	2	NA	0	0	0.5	10.5	4	14.5	this report
		Ind #43	F	c.763C>T	p.Arg255*	nonsense	NA	2	2	2	2	1	0	1	1	NA	0	11	NA	NA	this report
		Ind #35	M	c.799C>T	p.Gln267*	nonsense	de novo	1	1	2	0	2	1	NA	1	0	0	8	NA	NA	this report
		Ind #37	F	c.936T>A	p.Cys312*	nonsense	de novo	1	2	2	2	2	1	NA	1	0.5	0.5	12	3	15	this report
		Ind #34	F	c.1309C>T	p.Arg437*	nonsense	NA	0	1	2	2	2	1	0.5	1	0	0.5	10	NA	NA	this report
		Ind #42	F	c.1372C>T	p.Arg467*	nonsense	de novo	2	2	2	1	1	1	0	0	0.5	0.5	10	4	14	this report
		Ind #41	F	c.235dupA	p.Arg79fs	frameshift	de novo	NA	NA	2	NA	1	NA	0.5	1	0.5	NA	NA	NA	NA	this report
		Ind #8	M	c.290_291 delCT	p.Ser97fs	frameshift	de novo	1	2	2	2	2	2	1	1	0.5	0.5	14	3.5	17.5	this report
		Ind #9	M	c.297_301delCTTGA	p.Leu100fs	frameshift	de novo	2	2	2	2	0	1	1	1	0.5	0.5	12	4.5	16.5	this report
		Ind #11	M	c.702_703delCT	p.Cys235fs	frameshift	de novo	2	2	2	2	1	1	1	0	0.5	NA	11.5	4	15.5	this report
		Ind #12	F	c.782del	p.Leu261fs	frameshift	de novo	2	2	2	2	1	1	1	1	0	NA	12	4	16	this report
		Ind #13	F	c.1004del	p.Gly335fs	frameshift	NA	2	2	2	2	1	1	1	1	0	NA	12	2.5	14.5	this report
		Ind #14	F	c.1008dup	p.Pro337fs	frameshift	de novo	1	2	2	2	2	1	0	1	0.5	0.5	12	2.5	14.5	this report
		Ind #15	F	c.1033del	p.Trp345fs	frameshift	de novo	2	1	2	2	0	1	0.5	1	0.5	0	10	3	13	this report
		Ind #39	F	c.1270del	p.His424fs	frameshift	de novo	2	1	1	1	2	1	NA	1	0	0	9	NA	NA	this report
		Ind #16	F	c.1333dup	p.Thr445fs	frameshift	de novo	2	2	2	2	2	1	1	1	0.5	0.5	14	3.5	17.5	this report
		Ind #17	F	c.1491del	p.Ala498fs	frameshift	de novo	2	1	2	2	0	1	0.5	0	NA	0.5	9	NA	NA	this report
		Ind #19	F	c.328-1G>T	p.?	splice	de novo	2	2	2	2	2	1	1	1	0.5	0.5	14	3.5	17.5	this report
		Ind #20	M	c.665-2A>G	p.?	splice	de novo	1	2	2	2	2	1	1	1	0.5	0.5	13	4	17	this report
		Ind #21	M	c.665-9_665-5delTTCTC	p.?	splice	de novo	1	1	2	2	1	2	1	0	0.5	0.5	11	4.5	15.5	this report
		Ind #36	M	c.665-9_665-5delTTCTC	p.?	splice	de novo	2	2	2	2	2	2	1	1	NA	NA	14	2	16	this report
		Ind #38	M	c.951+1G>C	p.?	splice	de novo	NA	NA	NA	2	NA	NA	NA	1	NA	NA	NA	NA	NA	this report
		Ind #22	M	c.951+4_951+7delGTAA	p.?	splice	de novo	2	2	2	2	2	1	0	1	NA	0	12	4.5	16.5	this report
		Ind #23	M	c.1240-2A>G	p.?	splice	de novo	2	2	2	2	2	2	1	1	0	0.5	14.5	3	17.5	this report
		Ind #24	F	c.1240-1_1240insTAA	p.?	splice	de novo	1	1	2	2	2	1	0	1	0.5	0.5	11	3.5	14.5	this report
DYRK1A_R	Bronicki et al. 2014	Bronicki_#2	M	c.613C>T	p.Arg205*	nonsense	de novo	1	2	2	2	0	1	0	1	NA	0.5	9.5	5	14.5	this report
		Bronicki_#3	M	c.621_624 delinsGAA	p.Glu208fs	frameshift	de novo	1	2	2	2	1	1	1	1	0.5	NA	11.5	3.5	15	this report
		Bronicki_#8	M	c.844dupA	p.Ser282fs	frameshift	de novo	2	2	2	2	2	2	1	0	0.5	0	13.5	3	16.5	this report
		Bronicki_#10	F	c.1232dup	p.Arg413fs	frameshift	de novo	2	2	2	2	2	1	1	1	0.5	0.5	14	4.5	18.5	this report
	Ruaud et al., 2015	Ruaud_#1	M	c.613C>T	p.Arg205*	nonsense	de novo	1	1	1	2	2	2	1	1	0.5	NA	11.5	4.5	16	literature
	Van Bon et al. 2016	VanBon_SSC138	F	c.1098 +1G>A	p.?	splice	de novo	2	2	1	2	0	2	0	NA	0.5	NA	9.5	4.5	14	literature
		VanBon_SSC120	M	c.143_144 del	p.Ile48fs	frameshift	de novo	1	2	2	2	2	2	NA	NA	0.5	NA	11.5	4	15.5	literature
		VanBon_SSC135	M	c.1491del	p.Ala498fs	frameshift	de novo	1	1	2	2	2	2	0	NA	NA	NA	10	3.5	13.5	literature
		VanBon_UMCN 1	F	c.799C>T	p.Gln267*	nonsense	NA	2	2	2	2	2	NA	NA	NA	0.5	NA	10.5	3	13.5	literature
		VanBon_UMCN 2	M	c.1240-2 A>G	p.?	splice	de novo	1	2	2	2	0	2	0	1	0.5	NA	10.5	3.5	14	literature
		VanBon_Troina 1	M	c.516 +2 T>C	p.?	splice	de novo	2	2	2	2	2	1	1	NA	0.5	0.5	13	5	18	literature
		VanBon_GF2852	M	c.367C>T	p.Gln123*	nonsense	de novo	1	2	2	2	2	2	0	0	0.5	NA	11.5	4.5	16	literature
		VanBon_Leuven3	F	c.665-9_665-5delTTCTC	p.?	splice	de novo	1	2	2	2	0	2	0	1	0.5	NA	10.5	4	14.5	literature
test	*this report*	Ind #18	F	c.1978del	p.Ser660fs	frameshift	de novo	1	0.5	1	0	0	1	0.5	1	0	0	5	2.5	7.5	this report
		Ind #25	F	c.503G>A	p.Gly168Asp	missense	de novo	NA	NA	NA	NA	NA	NA	NA	NA	NA	NA	NA	NA	NA	this report
		Ind #26	F	c.764G>A	p.Arg255Gln	missense	NA	1	2	0	0	0	1	0	1	0	0	5	NA	NA	this report
		Ind #27	M	c.860A>T	p.Asp287Val	missense	de novo	2	2	2	NA	2	1	NA	1	NA	NA	10	NA	NA	this report
		Ind #28	F	c.914T>G	p.Ile305Arg	missense	de novo	2	2	2	0	2	1	1	1	0.5	NA	11.5	4.5	16	this report
		Ind #29	M	c.972T>A	p.Ser324Arg	missense	de novo	0	1	0	2	1	2	0	1	0	0	7	3.5	10.5	this report
		Ind #30	F	c.1098G>T	p.Ile318_Glu366del	inframe	de novo	2	2	2	1	2	1	1	1	0	0	12	4	16	this report
		Ind #31	M	c.1384T>C	p.Tyr462His	missense	de novo	0	0	0*	0	2	1	1	0	0	0	4	2.5	6.5	this report
		Ind #32	F	c.1400G>A	p.Arg467Gln	missense	de novo	1	2	2	0	0	1	NA	0	NA	0.5	6.5	4	10.5	this report
		Ind #33	M	c.1457G>A	p.Gly486Asp	missense	de novo	0	0	0*	NA	0	2	NA	0	NA	NA	2	NA	NA	this report
	Bronicki et al. 2014	Bronicki_#9	F	c.1763C>A	p.Thr588Asn	missense	de novo	2	2	2	1	1	1	NA	1	0.5	0.5	11	4.5	15.5	this report
	Ruaud et al., 2015	Ruaud_#2	M	c.932C >T	p.Ser311Phe	missense	de novo	1	2	2	0	2	1	1	NA	NA	NA	10	2.5	12.5	this report
	Ji et al ., 2015	Ji_#P7	F	c.563A>T	p.Lys188Ile	missense	de novo	1	2	1	2	0	1	1	1	0.5	NA	9.5	3.5	13	literature
		Ji_#P8	F	c.734T>G	p.Leu245Arg	missense	de novo	2	2	2	2	1	1	0.5	1	0.5	NA	12	NA	NA	literature
		Ji_#P9	M	c.883C>T	p.Leu295Phe	missense	de novo	0	2	2	0	0	1	NA	NA	0.5	NA	5.5	NA	NA	literature
other monogenic forms	ANKRD11	ANKRD11_1	F	pathogenic variant			de novo	0	0	0	1	0	1	0	0	0	NA	2	1.5	3.5	this report
		ANKRD11_2	F	pathogenic variant			inherited moth	1	1	0	2	0	0	0	1	0	0	5	1	6	this report
		ANKRD11_3	M	pathogenic variant			de novo	1	1	0	0	NA	1	0	0	0	0	3	1	4	this report
		ANKRD11_4	F	pathogenic variant			de novo	1	0	0	2	0	1	0	0	0	0	4	1	5	this report
		ANKRD11_5	F	pathogenic variant			de novo	1	0	0	2	0	0	0	0	0	0	3	1	4	this report
	MED13L	MED13L_1	M	pathogenic variant			de novo	1	1	0	0	2	1	0	1	0	NA	6	1.5	7.5	this report
		MED13L_2	M	pathogenic variant			de novo	1	2	1	2	0	1	1	1	0	0	9	0.5	9.5	this report
		MED13L_3	F	pathogenic variant			de novo	2	2	0	0	0	0	0	1	0	0	5	3	8	this report
		MED13L_4	F	pathogenic variant			de novo	1	1	1	0	0	1	0	1	0	0	5	2	7	this report
		MED13L_5	F	pathogenic variant			de novo	1	1	0	0	0	1	0	1	0	0	4	1	5	this report
	DDX3X	DDX3X_1	F	pathogenic variant			de novo	1	1	1	2	1	0	0	1	0	0	7	3	10	this report
		DDX3X_2	F	pathogenic variant			de novo	1	0	0	2	0	1	NA	1	0	NA	5	1	6	this report
		DDX3X_3	F	pathogenic variant			de novo	1	0	0	0	0	0	0	1	0	0	2	1	3	this report
		DDX3X_4	F	pathogenic variant			de novo	1	1	0	0	0	0	0	1	0.5	0	3.5	2	5.5	this report
		DDX3X_5	F	pathogenic variant			de novo	1	1	0	0	0	0	1	1	0	0	4	0.5	4.5	this report
	ARID1B	ARID1B_1	F	pathogenic variant			de novo	0	1	0	0	1	2	NA	0	0	NA	4	1.5	5.5	this report
		ARID1B_2	M	pathogenic variant			de novo	1	1	0	0	0	0	0	0	0	0	2	1.5	3.5	this report
		ARID1B_3	F	pathogenic variant			de novo	2	1	0	0	0	1	0	1	0	0	5	1.5	6.5	this report
		ARID1B_4	F	pathogenic variant			de novo	1	1	0	0	0	0	0	0	0	0	2	2.5	4.5	this report
		ARID1B_5	F	pathogenic variant			de novo	1	1	0	0	0	0	0	0	0	0	2	1	3	this report
		ARID1B_6	M	pathogenic variant			de novo	2	2	0	2	2	1	0	1	0.5	0.5	11	1.5	12.5	this report
		ARID1B_7	M	pathogenic variant			de novo	2	1	0	0	0	0	1	1	0.5	0	5.5	0.5	6	this report
		ARID1B_8	F	pathogenic variant			de novo	2	1	0	2	0	1	0	1	0	0.5	7.5	1.5	9	this report
	SHANK3	SHANK3_1	F	pathogenic variant			de novo	2	2	0	0	1	2	NA	0	0	NA	7	1	8	this report
		SHANK3_2	M	pathogenic variant			de novo	2	2	1	0	2	0	0.5	1	0.5	0	9	1.5	10.5	this report
		SHANK3_3	M	pathogenic variant			de novo	1	2	0	2	0	1	0	0	0	0	6	1	7	this report
		SHANK3_4	M	pathogenic variant			de novo	2	1	0	0	1	1	0	0	0	0	5	3	8	this report
		SHANK3_5	F	pathogenic variant			de novo	2	2	0	0	1	1	0	1	0	0	7	1.5	8.5	this report
		SHANK3_6	M	pathogenic variant			de novo	2	2	0	0	1	2	NA	1	0	0	8	1	9	this report
	TCF4	TCF4_1	M	pathogenic variant			de novo	2	2	0	0	1	1	0.5	1	0.5	0	8	3	11	this report
		TCF4_2	M	pathogenic variant			de novo	2	2	0	0	1	1	0.5	1	0.5	0	8	1	9	this report
		TCF4_3	F	pathogenic variant			de novo	1	2	0	0	0	0	0	1	0	0	4	2	6	this report
		TCF4_4	F	pathogenic variant			de novo	2	2	0	0	0	1	0.5	1	0.5	0	7	1.5	8.5	this report
		TCF4_5	F	pathogenic variant			de novo	1	1	0	0	0	0	0	1	0.5	0	3.5	1	4.5	this report
		TCF4_6	F	pathogenic variant			de novo	2	2	0	0	1	1	0	1	0	0	7	2	9	this report
	KMT2A	KMT2A_1	M	pathogenic variant			de novo	1	2	1	1	0	0	0.5	0	0.5	0	6	1.5	7.5	this report
		KMT2A_2	F	pathogenic variant			de novo	1	0	1	0	1	0	0	0	0	0	3	0.5	3.5	this report
		KMT2A_3	M	pathogenic variant			de novo	1	2	2	2	0	0	0	1	0	0	8	2	10	this report
		KMT2A_4	F	pathogenic variant			de novo	1	0	0	2	0	0	0	0	0	0	3	1.5	4.5	this report
		KMT2A_5	M	pathogenic variant			de novo	1	1	0	2	0	1	0	1	0	0	6	2	8	this report
		KMT2A_6	F	pathogenic variant			de novo	2	2	2	2	0	1	0	1	0	0	10	2.5	12.5	this report

													Freq Allele Reference					Freq Allele Variant					
training set	source	gnomAD allele	chr	pos	id	ref	alt	c.	p.	kinase domain	CADD	Freq RefV	Freq RefM	Freq RefO	Freq RefP	Freq RefF	Freq SubV	Freq SubM	Freq SubO	Freq SubP	Freq SubF	
N-set	gnomad>=2	2	21	38 845 018	rs7802	G	A	c.43G>A	p.Val15Ile	no	26.6	94	0	0	-1	0	0	0	0	-1	0	
N-set	gnomad>=2	4	21	38 845 018	rs7802	G	T	c.43G>T	p.Val15Phe	no	28.5	94	0	0	-1	0	0	0	0	-1	0	
T-test	clinvar_VUS	0	21	38 845 022		G	A	c.47G>A	p.Arg16Gln	no	23.2	94	0	0	-1	0	0	0	7	-1	0	
N-set	gnomad>=2	2	21	38 845 030	rs7765	C	T	c.55C>T	p.Pro19Ser	no	27.5	94	0	0	-1	0	0	0	0	-1	0	
T-test	clinvar_VUS	0	21	38 845 078		C	T	c.103C>T	p.Pro35Ser	no	22.5	78	-1	-1	-1	-1	21	-1	-1	-1	-1	
N-set	gnomad>=2	4	21	38 845 097	rs7541	G	A	c.122G>A	p.Ser41Asn	no	26.8	95	4	0	-1	-1	4	0	0	-1	-1	
N-set	gnomad>=2	2	21	38 845 097	rs7541	G	C	c.122G>C	p.Ser41Thr	no	26.4	95	4	0	-1	-1	0	0	0	-1	-1	
N-set	gnomad>=2	8	21	38 845 102	rs3675	C	T	c.127C>T	p.Arg43Cys	no	24	82	0	3	-1	-1	17	0	0	-1	-1	
T-test	clinvar_VUS	1	21	38 845 103		G	A	c.128G>A	p.Arg43His	no	25.6	82	0	3	-1	-1	0	0	0	-1	-1	
N-set	gnomad>=2	3	21	38 845 105	rs7585	C	T	c.130C>T	p.Arg44Cys	no	26.5	56	4	3	-1	-1	0	0	0	-1	-1	
N-set	gnomad>=2	2	21	38 845 106	rs7802	G	A	c.131G>A	p.Arg44His	no	22.5	56	4	3	-1	-1	43	0	0	-1	-1	
T-test	clinvar_VUS	0	21	38 845 114		A	G	c.139A>G	p.Asn47Asp	no	22.9	52	-1	-1	-1	-1	0	-1	-1	-1	-1	
N-set	gnomad>=2	10	21	38 845 144	rs1045	T	C	c.169T>C	p.Ser57Pro	no	5.976	39	0	0	-1	-1	52	0	1	-1	-1	
N-set	gnomad>=2	2	21	38 850 498	rs8883	G	A	c.223G>A	p.Val75Ile	no	22.3	39	4	0	-1	-1	0	0	0	-1	-1	
N-set	gnomad>=2	3	21	38 850 514	rs1442	G	A	c.239G>A	p.Arg80Gln	no	24.5	73	29	0	-1	-1	0	0	1	-1	-1	
T-test	clinvar_VUS	1	21	38 850 514		G	T	c.239G>T	p.Arg80Leu	no	24.3	73	29	0	-1	-1	0	0	0	-1	-1	
T-test	clinvar_VUS	0	21	38 850 529		T	G	c.254T>G	p.Phe85Cys	no	29.9	100	29	0	-1	-1	0	0	0	-1	-1	
N-set	gnomad>=2	5	21	38 850 543	rs7674	A	G	c.268A>G	p.Thr90Ala	no	21.1	47	19	15	-1	0	4	5	6	-1	0	
N-set	gnomad>=2	2	21	38 850 552	rs1388	C	G	c.277C>G	p.Leu93Val	no	23.4	100	76	24	0	53	0	8	18	58	0	
T-test	Dang et al., 2018	0	21	38852967		C	T	c.355C>T	p.His119Tyr	no	22.8	100	-1	-1	-1	-1	0	-1	-1	-1	-1	
T-test	Dang et al., 2018	0	21	38852988		G	T	c.376G>T	p.Asp126Tyr	no	31	100	41	0	-1	0	0	0	0	-1	0	
T-test	clinvar_VUS	0	21	38 853 002		G	C	c.390G>C	p.Lys130Asn	no	25.3	100	71	9	-1	0	0	0	6	-1	7	
T-test	Dang et al., 2018	0	21	38853010		G	A	c.398G>A	p.Arg133Gln	no	25.2	100	55	0	-1	7	0	0	0	-1	0	
N-set	gnomad>=2	4	21	38 853 019	rs7501	A	G	c.407A>G	p.Tyr136Cys	no	25.6	73	52	11	-1	0	0	0	0	-1	0	
T-test	clinvar_VUS	0	21	38 853 043		A	G	c.431A>G	p.Asn144Ser	no	25.2	100	86	23	-1	7	0	0	0	-1	0	
N-set	gnomad>=2	2	21	38 853 085	rs7566	G	A	c.473G>A	p.Arg158His	no	29.8	100	96	92	86	52	0	0	0	0	0	
N-set	gnomad>=2	3	21	38 853 112	rs1456	A	G	c.500A>G	p.Lys167Arg	yes	29.1	100	100	64	0	9	0	0	4	0	0	
P-set	clinvar_likpatho, this report	0	21	38 853 115		G	A	c.503G>A	p.Gly168Asp	yes	31	100	100	86	69	100	0	0	0	0	0	
T-test	clinvar VUS	0	21	38 853 123		G	A	c.511G>A	p.Gly171Arg	yes	32	100	100	86	66	80	0	0	0	0	0	
P-set	clinvar_likpatho	0	21	38 858 785		A	G	c.533A>G	p.Asp178Gly	yes	32	100	93	86	60	15	0	0	0	0	5	
N-set	gnomad>=2	3	21	38 858 795	rs7545	G	T	c.543G>T	p.Glu181Asp	yes	12.42	100	57	8	3	0	0	11	3	3	0	
P-set	clinvar_likpatho	0	21	38 858 815		A	T	c.563A>T	p.Lys188Ile	yes	31	100	96	97	95	92	0	0	0	0	0	
T-test	NA	0	21	38 858 815		A	G	c.563A>G	p.Lys188Arg	yes	27.9	100	96	97	95	92	0	0	0	0	0	
T-test	Dang et al., 2018	0	21	38 858 835		G	A	c.583G>A	p.Ala195Thr	yes	23.4	100	14	26	61	56	0	3	0	0	0	
N-set	gnomad>=2	2	21	38 858 866	rs7577	G	A	c.614G>A	p.Arg205Gln	yes	25.6	100	30	8	0	4	0	4	3	0	0	
T-test	DDD, 2015	0	21	38 858 872		T	C	c.620T>C	p.Leu207Pro	yes	29.5	100	93	93	92	92	0	0	0	0	0	
T-test	clinvar_VUS	0	21	38 862 480		A	G	c.668A>G	p.His223Arg	yes	22	100	0	3	0	0	0	35	59	93	63	
N-set	gnomad>=2	2	21	38 862 488	rs1462	C	T	c.676C>T	p.Arg226Cys	yes	32	100	59	5	0	0	0	0	3	0	0	
N-set	gnomad>=2	3	21	38 862 489	rs7587	G	A	c.677G>A	p.Arg226His	yes	25.7	100	59	5	0	0	0	0	9	0	5	
T-test	clinvar_VUS	0	21	38 862 534		T	C	c.722T>C	p.Leu241Pro	yes	29.7	100	100	97	100	92	0	0	0	0	0	
T-test	Ji, 2015	0	21	38 862 546		T	G	c.734T>G	p.Leu245Arg	yes	29	100	100	97	100	92	0	0	0	0	0	
T-test	this report	0	21	38 862 576		G	A	c.764G>A	p.Arg255Gln	yes	24	100	75	23	46	57	0	0	5	0	5	
T-test	Dang et al., 2018; DDD, 2015	0	21	38 862 589		G	T	c.777G>T	p.Leu259Phe	yes	24.8	100	89	84	67	9	0	3	0	0	0	
N-set	gnomad>=2	3	21	38 862 619	rs7672	G	A	c.807G>A	p.Met269Ile	yes	22.4	73	16	0	2	5	0	5	43	58	34	
N-set	gnomad>=2	2	21	38 862 626	rs1385	G	T	c.814G>T	p.Ala272Ser	yes	24.7	100	90	57	65	22	0	5	1	0	22	
P-set	clinvar_likpatho	0	21	38 862 641		G	C	c.829G>C	p.Ala277Pro	yes	28.9	100	12	27	0	3	0	0	0	0	0	
N-set	gnomad>=2	14	21	38 862 657	rs7588	G	A	c.845G>A	p.Ser282Asn	yes	22.6	100	42	16	4	0	0	36	17	7	0	
N-set	gnomad>=2	2	21	38 862 659	rs7803	A	G	c.847A>G	p.Ile283Val	yes	22.4	100	89	53	79	31	0	10	32	6	5	
T-test	Zhang et al., 2015	0	21	38 862 671		G	T	c.859G>T	p.Asp287Tyr	yes	32	100	100	97	95	100	0	0	0	0	0	
T-test	Widowati	0	21	38 862 671		G	A	c.859G>A	p.Asp287Asn	yes	32	100	100	97	95	100	0	0	0	0	0	
P-set	clinvar_patho, this report	0	21	38 862 672		A	T	c.860A>T	p.Asp287Val	yes	28.9	100	100	97	95	100	0	0	0	0	0	
T-test	clinvar_VUS	0	21	38 862 681		C	G	c.869C>G	p.Pro290Arg	yes	28.3	100	100	97	95	100	0	0	0	0	0	
P-set	clinvar_patho	0	21	38 862 695	rs7970	C	T	c.883C>T	p.Leu295Phe	yes	29.1	100	96	87	51	72	0	3	0	0	0	
N-set	gnomad>=2	2	21	38 862 719	rs7778	A	G	c.907A>G	p.Ile303Val	yes	24	100	100	74	67	65	0	0	12	28	19	
T-test	this report	0	21	38 862 726		T	G	c.914T>G	p.Ile305Arg	yes	26.4	100	80	25	26	73	0	0	0	0	0	
P-set	clinvar_likpatho	0	21	38 862 734		T	G	c.922T>G	p.Phe308Val	yes	29.1	100	100	89	65	94	0	0	0	0	0	
P-set	clinvar_likpatho	0	21	38 862 735		T	C	c.923T>C	p.Phe308Ser	yes	32	100	100	89	65	94	0	0	0	0	0	
P-set	clinvar_patho	0	21	38 862 744		C	T	c.932C>T	p.Ser311Phe	yes	33	100	100	71	30	27	0	0	0	0	0	
N-set	gnomad>=2	2	21	38 862 751	rs7708	G	T	c.939G>T	p.Gln313His	yes	14.51	100	71	9	0	0	0	11	12	0	4	
P-set	clinvar_likpatho = this report	0	21	38 865 339		T	A	c.972T>A	p.Ser324Arg	yes	28.1	100	100	95	100	92	0	0	0	0	0	
P-set	clinvar_likpatho	0	21	38 865 341		G	A	c.974G>A	p.Arg325His	yes	33	100	100	95	100	92	0	0	0	0	0	
P-set	clinvar_likpatho	0	21	38 865 347		A	G	c.980A>G	p.Tyr327Cys	yes	29.3	100	100	95	100	92	0	0	0	0	0	
T-test	clinvar_VUS, Stessman et al., 2017	0	21	38 865 349		C	T	c.982C>T	p.Arg328Trp	yes	34	100	100	95	100	92	0	0	0	0	0	
N-set	gnomad>=2	89	21	38 865 388	rs2005	G	T	c.1021G>T	p.Ala341Ser	yes	24.9	100	82	53	49	48	0	0	16	12	38	
N-set	gnomad>=2	4	21	38 865 398	rs7465	T	C	c.1031T>C	p.Met344Thr	yes	26.9	100	84	64	66	68	0	0	2	0	0	
P-set	clinvar_likpatho	0	21	38 865 403		T	C	c.1036T>C	p.Ser346Pro	yes	29.7	100	100	92	100	92	0	0	0	0	0	
P-set	clinvar_likpatho	0	21	38 865 404		C	T	c.1037C>T	p.Ser346Phe	yes	32	100	100	92	100	92	0	0	0	0	0	
T-test	Trujillano et al., 2017	0	21	38 865 407		T	G	c.1040T>G	p.Leu347Arg	yes	31	100	96	84	47	83	0	0	0	0	0	
N-set	gnomad>=2; clinvar_benign	573	21	38 865 433	rs1458	A	G	c.1066A>G	p.Thr356Ala	yes	26.3	100	88	77	27	8	0	0	0	0	0	
N-set	gnomad>=2	2	21	38 865 461	rs7563	A	G	c.1094A>G	p.Asn365Ser	yes	22.5	100	89	22	0	0	0	3	25	84	71	
N-set	gnomad>=2	2	21	38 865 461	rs7563	A	T	c.1094A>T	p.Asn365Ile	yes	27.3	100	89	22	0	0	0	0	0	0	0	
T-test	this report	0	21	38 865 465		G	T	c.1098G>T	p.Glu366Asp	yes	35	100	100	55	65	68	0	0	3	0	0	=p.Ile318_Glu366del
N-set	gnomad>=2	2	21	38 868 453	rs7584	G	A	c.1132G>A	p.Gly378Ser	yes	25.4	89	100	88	100	79	4	0	0	0	13	
N-set	gnomad>=2	2	21	38 868 454	rs1384	G	A	c.1133G>A	p.Gly378Asp	yes	28.4	89	100	88	100	79	0	0	4	0	0	
T-test	clinvar_VUS	0	21	38 868 466		C	T	c.1145C>T	p.Ala382Val	yes	22.7	53	3	9	0	0	4	10	17	0	8	
N-set	gnomad>=2	2	21	38 868 469	rs7546	A	G	c.1148A>G	p.His383Arg	yes	22.8	94	34	29	7	0	0	0	0	2	0	
N-set	gnomad>=2; clinvar_benign	27	21	38 868 526	rs7772	C	G	c.1205C>G	p.Thr402Ser	yes	17.86	85	18	6	-1	0	8	42	3	-1	0	
N-set	gnomad>=2	2	21	38 868 546	rs1411	A	G	c.1225A>G	p.Lys409Glu	yes	23.4	94	49	3	-1	7	0	0	3	-1	0	
T-test	clinvar_VUS	0	21	38 868 553		G	A	c.1232G>A	p.Gly411Glu	yes	23.4	94	60	3	-1	0	0	0	0	-1	0	
N-set	gnomad>=2	2	21	38 868 559	rs7704	G	A	c.1238G>A	p.Arg413Gln	yes	27.4	89	8	3	-1	0	0	0	0	-1	0	
T-test	clinvar_VUS	0	21	38 877 588		G	C	c.1242G>C	p.Glu414Asp	yes	16.22	83	-1	-1	-1	-1	0	-1	-1	-1	-1	
N-set	gnomad>=2	4	21	38 877 602	rs9786	G	C	c.1256G>C	p.Gly419Ala	yes	16.82	67	85	19	-1	-1	26	0	0	-1	-1	
N-set	gnomad>=2	2	21	38 877 607	rs7783	C	T	c.1261C>T	p.Arg421Cys	yes	34	94	86	31	3	11	0	0	0	0	0	
N-set	gnomad>=2	5	21	38 877 613	rs2026	C	T	c.1267C>T	p.Leu423Phe	yes	28	100	92	70	65	64	0	0	0	0	0	
N-set	gnomad>=2	21	21	38 877 614	rs5750	C	T	c.1268T>C	p.Leu423Pro	yes	32	100	92	70	65	64	0	0	0	0	0	
N-set	gnomad>=2	3	21	38 877 620	rs7770	A	C	c.1274A>C	p.Asn425Thr	yes	22.7	60	0	6	0	0	4	4	0	5	0	
N-set	gnomad>=2	2	21	38 877 632	rs7702	T	C	c.1286T>C	p.Val429Ala	yes	24.8	100	74	38	0	0	0	13	6	7	0	
N-set	gnomad>=2	3	21	38 877 637	rs1459	A	G	c.1291A>G	p.Thr431Ala	yes	22.3	65	55	35	0	0	26	0	0	3	3	
T-test	Wang et al., 2016	1	21	38 877 659		G	A	c.1313G>A	p.Arg438His	yes	33	100	92	61	0	0	0	0	0	0	0	
N-set	gnomad>=2	2	21	38 877 680	rs7595	C	T	c.1334C>T	p.Thr445Met	yes	27.9	56	29	12	-1	-1	0	0	0	-1	-1	
N-set	gnomad; clinvar_benign	2	21	38 877 712	rs1266	A	G	c.1366A>G	p.Ile456Val	yes	22.2	91	64	22	0	11	8	23	43	23	49	
T-test	Dang et al., 2018	0	21	38 877 719		G	T	c.1373G>T	p.Arg458Met	yes	32	100	89	27	0	2	0	0	3	0	0	
T-test	clinvar_VUS (=this report)	0	21	38 877 730		T	C	c.1384T>C	p.Tyr462His	yes	29.6	100	68	57	0	0	0	0	0	0	0	
T-test	Lelieved et al.	0	21	38877731		A	G	c.1385A>G	p.Tyr462Cys	yes	28.9	100	68	57	0	0	0	0	0	0	0	
P-set	clinvar_patho, this report	0	21	38 877 746		G	A	c.1400G>A	p.Arg467Gln	yes	33	100	96	92	91	76	0	0	0	0	0	
T-test	clinvar_VUS	0	21	38 877 776		G	C	c.1430G>C	p.Ser477Thr	yes	22.5	100	19	9	0	0	0	5	0	0	0	
T-test	clinvar_VUS (=this report); Dang et	0	21	38 877 803		G	A	c.1457G>A	p.Gly486Asp	no	29.1	100	34	0	-1	-1	0	0	0	-1	-1	
T-test	clinvar_VUS	0	21	38 877 817		A	C	c.1471A>C	p.Asn491His	no	23	65	29	3	-1	-1	0	4	0	-1	-1	
N-set	gnomad>=2	2	21	38 877 823	rs1395	G	A	c.1477G>A	p.Val493Ile	no	20.3	100	3	0	-1	-1	0	10	0	-1	-1	
N-set	gnomad>=2	2	21	38 877 883	rs1447	T	A	c.1537T>A	p.Ser513Thr	no	22.7	100	6	0	-1	-1	0	0	0	-1	-1	
N-set	gnomad>=2	6	21	38 878 411	rs5564	C	T	c.1556C>T	p.Ser519Leu	no	26.8	100	1	0	-1	-1	0	0	0	-1	-1	
N-set	gnomad>=2	2	21	38 878 420	rs1180	G	A	c.1565G>A	p.Ser522Asn	no	24.3	100	8	0	-1	-1	0	5	0	-1	-1	
N-set	gnomad>=2	2	21	38 878 423	rs7650	A	T	c.1568A>T	p.Asn523Ile	no	22.6	65	0	5	-1	-1	0	0	0	-1	-1	
N-set	gnomad>=2	3	21	38 878 426	rs7500	G	C	c.1571G>C	p.Ser524Thr	no	24.2	100	6	4	-1	-1	0	5	0	-1	-1	
N-set	gnomad>=2	6	21	38 878 435	rs1444	C	G	c.1580C>G	p.Ala527Gly	no	24.9	100	15	0	-1	-1	0	0	0	-1	-1	
N-set	gnomad>=2	4	21	38 878 437	rs1448	C	T	c.1582C>T	p.Arg528Trp	no	24	100	11	0	-1	-1	0	0	0	-1	-1	
N-set	gnomad>=2	3	21	38 878 438	rs1465	G	A	c.1583G>A	p.Arg528Gln	no	24.4	100	11	0	-1	-1	0	5	0	-1	-1	
N-set	gnomad>=2	7	21	38 878 446	rs7576	C	T	c.1591C>T	p.Pro531Ser	no	23.1	100	16	0	-1	-1	0	5	0	-1	-1	
T-test	clinvar_VUS	0	21	38 878 446		C	T	c.1591C>T	p.Pro531Ser	no	23.1	100	16	0	-1	-1	0	5	0	-1	-1	
N-set	gnomad>=2	37	21	38 878 450	rs1487	C	T	c.1595C>T	p.Thr532Met	no	31	100	11	0	-1	-1	0	3	0	-1	-1	
T-test	clinvar_VUS	0	21	38 878 450		C	T	c.1595C>T	p.Thr532Met	no	31	100	11	0	-1	-1	0	3	0	-1	-1	
N-set	gnomad>=2	5	21	38 878 461	rs7804	C	T	c.1606C>T	p.Arg536Trp	no	33	91	0	0	-1	-1	0	0	0	-1	-1	
N-set	gnomad>=2	8	21	38 878 470	rs3694	G	A	c.1615G>A	p.Gly539Ser	no	22.5	91	0	0	-1	-1	8	4	0	-1	-1	
T-test	clinvar_VUS	0	21	38 878 476		C	T	c.1621C>T	p.His541Tyr	no	22.8	100	9	0	-1	-1	0	0	0	-1	-1	
N-set	gnomad>=2	2	21	38 878 489	rs1882	C	T	c.1634C>T	p.Ala545Val	no	23.8	100	0	0	-1	-1	0	0	0	-1	-1	
N-set	gnomad>=2	3	21	38 878 491	rs7625	G	A	c.1636G>A	p.Val546Met	no	22.7	73	0	0	-1	-1	26	0	0	-1	-1	
N-set	gnomad>=2	20	21	38 878 512	rs7591	A	G	c.1657A>G	p.Thr553Ala	no	22.8	65	9	0	-1	0	0	0	0	-1	18	
N-set	gnomad>=2	5	21	38 878 521	rs7577	C	T	c.1666C>T	p.Pro556Ser	no	24.4	100	6	0	-1	-1	0	8	0	-1	-1	
T-test	clinvar_VUS	1	21	38 878 524		C	G	c.1669C>G	p.Gln557Glu	no	26.2	82	1	7	-1	-1	0	0	0	-1	-1	
N-set	gnomad>=2	14	21	38 884 217	rs7572	C	T	c.1675C>T	p.Arg559Cys	no	23.3	91	-1	-1	-1	-1	0	-1	-1	-1	-1	

N-set	gnomad>=2	32	21	38 884 218	rs1441	G	A	c.1676G>A	p.Arg559His	no	22.7	91	-1	-1	-1	-1	0	-1	-1	-1	-1
N-set	gnomad>=2	2	21	38 884 227	rs7457	T	A	c.1685T>A	p.Phe562Tyr	no	16.75	53	-1	-1	-1	-1	40	-1	-1	-1	-1
N-set	gnomad>=2	4	21	38 884 253	rs7797	A	G	c.1711A>G	p.Thr571Ala	no	18.84	44	-1	-1	-1	-1	0	-1	-1	-1	-1
N-set	gnomad>=2	10	21	38 884 254	rs7466	C	G	c.1712C>G	p.Thr571Ser	no	15.02	44	-1	-1	-1	-1	13	-1	-1	-1	-1
N-set	gnomad>=2	4	21	38 884 262	rs7682	C	G	c.1720C>G	p.Pro574Ala	no	24.7	80	-1	-1	-1	-1	0	-1	-1	-1	-1
N-set	gnomad>=2	4	21	38 884 271	rs7713	G	C	c.1729G>C	p.Val577Leu	no	24.6	89	-1	-1	-1	-1	0	-1	-1	-1	-1
N-set	gnomad>=2	8	21	38 884 274	rs7746	A	G	c.1732A>G	p.Thr578Ala	no	21.6	89	-1	-1	-1	-1	0	-1	-1	-1	-1
T-test	clinvar_VUS	0	21	38 884 281		A	G	c.1739A>G	p.Glu580Gly	no	26.7	89	-1	-1	-1	-1	0	-1	-1	-1	-1
N-set	gnomad>=2	2	21	38 884 286	rs1293	C	T	c.1744C>T	p.His582Tyr	no	24.8	89	-1	-1	-1	-1	0	-1	-1	-1	-1
N-set	gnomad>=2	2	21	38 884 287	rs7595	A	C	c.1745A>C	p.His582Pro	no	24.9	89	-1	-1	-1	-1	0	-1	-1	-1	-1
N-set	gnomad>=2	3	21	38 884 289	rs7678	C	A	c.1747C>A	p.Pro583Thr	no	27.2	89	-1	-1	-1	-1	0	-1	-1	-1	-1
N-set	gnomad>=2	3	21	38 884 301	rs3681	A	G	c.1759A>G	p.Thr587Ala	no	26.5	89	-1	-1	-1	-1	0	-1	-1	-1	-1
N-set	gnomad>=2	44	21	38 884 304	rs1495	A	C	c.1762A>C	p.Thr588Pro	no	23.4	85	-1	-1	-1	-1	0	-1	-1	-1	-1
P-set	clinvar_likpatho	0	21	38 884 305		C	A	c.1763C>A	p.Thr588Asn	no	22.8	85	-1	-1	-1	-1	0	-1	-1	-1	-1
N-set	gnomad>=2	8	21	38 884 331	rs2008	G	A	c.1789G>A	p.Ala597Thr	no	22.1	84	-1	-1	-1	-1	0	-1	-1	-1	-1
N-set	gnomad>=2	3	21	38 884 347	rs7583	A	T	c.1805A>T	p.His602Leu	no	22.8	51	-1	-1	-1	-1	0	-1	-1	-1	-1
N-set	gnomad>=2	2	21	38 884 352	rs1466	A	G	c.1810A>G	p.Asn604Asp	no	22.7	61	-1	-1	-1	-1	0	-1	-1	-1	-1
N-set	gnomad>=2	2	21	38 884 359	rs3675	C	A	c.1817C>A	p.Ser606Tyr	no	24.2	72	-1	-1	-1	-1	0	-1	-1	-1	-1
N-set	gnomad>=2	4	21	38 884 388	rs7605	C	G	c.1846C>G	p.His616Asp	no	26.6	88	-1	-1	-1	-1	0	-1	-1	-1	-1
N-set	gnomad>=2	2	21	38 884 398	rs7540	A	G	c.1856A>G	p.His619Arg	no	23.2	88	-1	-1	-1	-1	0	-1	-1	-1	-1
N-set	gnomad>=2	3	21	38 884 412	rs7504	T	G	c.1870T>G	p.Leu624Val	no	22.3	62	-1	-1	-1	-1	0	-1	-1	-1	-1
N-set	gnomad>=2	8	21	38 884 421	rs7583	C	T	c.1879C>T	p.Arg627Trp	no	32	80	-1	-1	-1	-1	0	-1	-1	-1	-1
N-set	gnomad>=2	5	21	38 884 422	rs7614	G	A	c.1880G>A	p.Arg627Gln	no	22.5	80	-1	-1	-1	-1	0	-1	-1	-1	-1
N-set	gnomad>=2	9	21	38 884 440	rs1476	A	T	c.1898A>T	p.Tyr633Phe	no	24.7	85	-1	-1	-1	-1	0	-1	-1	-1	-1
N-set	gnomad>=2	12	21	38 884 443	rs3700	A	G	c.1901A>G	p.Asn634Ser	no	22.6	77	-1	-1	-1	-1	8	-1	-1	-1	-1
N-set	gnomad>=2	6	21	38 884 452	rs1421	C	T	c.1910C>T	p.Thr637Met	no	23.4	81	-1	-1	-1	-1	0	-1	-1	-1	-1
N-set	gnomad>=2	6	21	38 884 455	rs7755	A	G	c.1913A>G	p.Asn638Ser	no	21.5	72	-1	-1	-1	-1	0	-1	-1	-1	-1
N-set	gnomad>=2	4	21	38 884 484	rs2014	G	A	c.1942G>A	p.Val648Ile	no	26.8	94	-1	-1	-1	-1	0	-1	-1	-1	-1
N-set	gnomad>=2	2	21	38 884 505	rs7654	A	G	c.1963A>G	p.Met655Val	no	22.5	94	-1	-1	-1	-1	0	-1	-1	-1	-1
N-set	gnomad>=2	4	21	38 884 527	rs7515	C	T	c.1985C>T	p.Thr662Met	no	24.9	51	-1	-1	-1	-1	0	-1	-1	-1	-1
N-set	gnomad>=2	2	21	38 884 556	rs7487	A	G	c.2014A>G	p.Thr672Ala	no	24.4	94	-1	-1	-1	-1	0	-1	-1	-1	-1
N-set	gnomad>=2	9	21	38 884 567	rs7567	A	C	c.2025A>C	p.Gln675His	no	22.3	60	-1	-1	-1	-1	34	-1	-1	-1	-1
N-set	gnomad>=2	5	21	38 884 572	rs5438	A	G	c.2030A>G	p.Asn677Ser	no	23.2	94	-1	-1	-1	-1	0	-1	-1	-1	-1
N-set	gnomad>=2; clinvar_benign	388	21	38 884 577	rs5572	G	C	c.2035G>C	p.Ala679Pro	no	25.2	94	-1	-1	-1	-1	0	-1	-1	-1	-1
N-set	gnomad>=2; clinvar_benign	8	21	38 884 589	rs2015	C	T	c.2047C>T	p.Arg683Cys	no	24.3	94	-1	-1	-1	-1	0	-1	-1	-1	-1
N-set	gnomad>=2	57	21	38 884 640	rs5405	G	A	c.2098G>A	p.Val700Ile	no	22.5	38	-1	-1	-1	-1	0	-1	-1	-1	-1
N-set	gnomad>=2	23	21	38 884 652	rs2005	G	A	c.2110G>A	p.Val704Ile	no	24.5	55	-1	-1	-1	-1	0	-1	-1	-1	-1
N-set	gnomad>=2	5	21	38 884 653	rs7637	T	C	c.2111T>C	p.Val704Ala	no	22.4	55	-1	-1	-1	-1	38	-1	-1	-1	-1
N-set	gnomad>=2	9	21	38 884 662	rs1513	A	G	c.2120A>G	p.Asn707Ser	no	24.1	94	-1	-1	-1	-1	0	-1	-1	-1	-1
N-set	gnomad>=2	2	21	38 884 667	rs7816	C	T	c.2125C>T	p.Arg709Cys	no	33	94	-1	-1	-1	-1	0	-1	-1	-1	-1
N-set	gnomad>=2	4	21	38 884 668	rs3747	G	A	c.2126G>A	p.Arg709His	no	23.7	94	-1	-1	-1	-1	0	-1	-1	-1	-1
N-set	gnomad>=2	6	21	38 884 682	rs5546	A	G	c.2140A>G	p.Ile714Val	no	22.2	55	-1	-1	-1	-1	8	-1	-1	-1	-1
N-set	gnomad>=2	3	21	38 884 697	rs7744	A	G	c.2155A>G	p.Thr719Ala	no	17.54	68	-1	-1	-1	-1	21	-1	-1	-1	-1
N-set	gnomad>=2	23	21	38 884 713	rs1434	C	G	c.2171C>G	p.Ala724Gly	no	24.6	51	-1	-1	-1	-1	0	-1	-1	-1	-1
N-set	gnomad>=2	2	21	38 884 715	rs1401	A	C	c.2173A>C	p.Asn725His	no	26.5	90	-1	-1	-1	-1	0	-1	-1	-1	-1
T-test	clinvar_VUS	1	21	38 884 719		C	G	c.2177C>G	p.Thr726Arg	no	24.4	94	-1	-1	-1	-1	0	-1	-1	-1	-1
N-set	gnomad>=2	12	21	38 884 722	rs7605	G	T	c.2180G>T	p.Gly727Val	no	24.6	85	-1	-1	-1	-1	8	-1	-1	-1	-1
N-set	gnomad>=2; clinvar_benign	10	21	38 884 757	rs2015	A	G	c.2215A>G	p.Met739Val	no	21.5	94	-1	-1	-1	-1	0	-1	-1	-1	-1
N-set	gnomad>=2	23	21	38 884 757	rs2015	A	T	c.2215A>T	p.Met739Leu	no	21.3	94	-1	-1	-1	-1	0	-1	-1	-1	-1
N-set	gnomad>=2	3	21	38 884 767	rs7498	G	A	c.2225G>A	p.Gly742Glu	no	26.8	94	-1	-1	-1	-1	0	-1	-1	-1	-1
T-test	clinvar_VUS	0	21	38 884 785		C	T	c.2243C>T	p.Ser748Phe	no	28.8	94	25	0	-1	-1	0	0	0	-1	-1
N-set	clinvar_benign	0	21	38 884 788	rs7532	C	T	c.2246C>T	p.Pro749Leu	no	29.3	94	25	0	-1	-1	0	0	0	-1	-1
N-set	gnomad>=2	22	21	38 884 793	rs1475	A	T	c.2251A>T	p.Thr751Ser	no	22.7	77	0	0	-1	-1	0	0	0	-1	-1
N-set	gnomad>=2	2	21	38 884 830	rs7711	C	G	c.2288C>G	p.Ser763Trp	no	32	94	-1	-1	-1	-1	0	-1	-1	-1	-1
N-set	gnomad>=2	4	21	38 884 830	rs7711	C	T	c.2288C>T	p.Ser763Leu	no	29.7	94	-1	-1	-1	-1	0	-1	-1	-1	-1

CpG	limma p raw	limma p adj	delta beta	SVM	chr	pos	strand	Islands Name	Relation to	UCSC RefGene Name	UCSC RefGene Accession	UCSC RefGene Group	GOF site
cg27264462	1,23E-05	0,0153	0,1386		chr1	2106365	-		OpenSea	PRKCZ;PRKCZ;PRKCZ	NM 001033581;NM 001033582;NM	Body;Body;Body	Yes
cg23648809	7.18E-05	0.0335	0.1190	Included	chr1	2106400	+		OpenSea	PRKCZ:PRKCZ:PRKCZ	NM 001033581:NM 001033582:NM	Body:Body:Body	
ce02067531	1.29E-05	0.0156	0.1314	Included	chr1	16714027	-		OpenSea	SZRD1:SZRD1:SZRD1:SZRD1:SZRD1:SZRD	NR 073503:NR 073502:NR 073501:	Body:Body:Body:Body:Body:Body	
cg14076729	7,70E-07	0,0042	-0,1156	Included	chr1	38126628	+		OpenSea				
cg24375409	5,33E-05	0,0296	-0,1490	Included	chr1	38200920	+	chr1:38200919-38201200	Island	EPHA10	NM 001099439	Body	
cg07865091	8,54E-07	0,0044	-0,1255	Included	chr1	43814306	-	chr1:43814305-43815277	Island	MPL	NM 005373	Body	
ce11839415	5.04E-07	0.0034	-0.1249		chr1	43814764	-	chr1:43814305-43815277	Island	MPL	NM 005373	Bodv	Yes
ce08706567	3.91E-06	0.0094	-0.1622		chr1	43814983	+	chr1:43814305-43815277	Island	MPL	NM 005373	Bodv	Yes
cg13393721	1,11E-06	0,0050	-0,1763		chr1	43815035	-	chr1:43814305-43815277	Island	MPL	NM 005373	Body	Yes
cg06496648	1,36E-05	0,0160	-0,1020	Included	chr1	47488961	+	chr1:47489226-47489633	N Shore	CYP4X1	NM 178033	TSS1500	
cg08871545	8,48E-07	0,0044	0,1316	Included	chr1	48559803	+		OpenSea				
ce09313918	7.16E-06	0.0119	0.1694	Included	chr1	54232631	-		OpenSea	NDC1:NDC1:NDC1	NM 001168551:NM 018087:NR 033	3'UTR:3'UTR:Bodv	Yes
ce24803390	1.15E-07	0.0020	0.2879		chr1	56097923	+		OpenSea				
cg21093945	8,04E-06	0,0126	0,2211	Included	chr1	56107046	-		OpenSea				
cg04574764	1,63E-05	0,0172	-0,1193	Included	chr1	56184657	+		OpenSea				
cg24496745	0,0001	0,0400	-0,1191	Included	chr1	57285156	+		OpenSea	C1orf168;C1orf168	NM 001004303;NM 001004303	1stExon;5'UTR	Yes
ce24690588	8.73E-06	0.0129	-0.1222		chr1	57285399	-		OpenSea	C1orf168	NM 001004303	TSS200	
ce05374238	1.94E-06	0.0068	-0.1424		chr1	57285466	+		OpenSea	C1orf168	NM 001004303	TSS200	
cg09467404	2,41E-06	0,0074	-0,1105	Included	chr1	57424327	-		OpenSea	C8B;C8B;C8B	NM 001278544;NM 001278543;NM	Body;Body;Body	Yes
ce17461600	0,0001	0,0390	-0,1076	Included	chr1	57983368	-		OpenSea	DAB1	NM 021080	5'UTR	
ce00026909	2.93E-07	0.0025	-0.1254	Included	chr1	58089001	+		OpenSea	DAB1	NM 021080	5'UTR	
ce20292791	1.70E-05	0.0177	-0.1124	Included	chr1	58089357	+		OpenSea	DAB1	NM 021080	5'UTR	
ce18163452	4.94E-06	0.0103	-0.1020	Included	chr1	63466707	-		OpenSea				Yes
cg00320094	4,08E-05	0,0261	-0,1025	Included	chr1	68695183	+	chr1:68696639-68697628	N Shore	GPR177;GPR177	NM 001002292;NM 024911	Body;Body	Yes
cg02553170	5,45E-05	0,0297	0,1696	Included	chr1	84556762	+		OpenSea	PRKACB;PRKACB	NM 207578;NM 002731	Body;Body	
ce26256793	0.0001	0.0424	-0.1291		chr1	103574469	-		OpenSea	COL11A1:COL11A1:COL11A1:COL11A1	NM 001168249:NM 080629:NM 08	TSS1500:TSS1500:TSS1500:TSS1500	
ce03520644	1.51E-05	0.0166	-0.1486		chr1	103574523	+		OpenSea	COL11A1:COL11A1:COL11A1:COL11A1	NM 001168249:NM 080629:NM 08	TSS1500:TSS1500:TSS1500:TSS1500	Yes
ce06381931	3.74E-05	0.0251	-0.1661		chr1	103574597	+		OpenSea	COL11A1:COL11A1:COL11A1:COL11A1	NM 001190709:NM 080629:NM 00	TSS1500:TSS1500:TSS1500:TSS1500	
ce16968885	6,33E-06	0,0113	-0,1918		chr1	103574619	-		OpenSea	COL11A1;COL11A1;COL11A1;COL11A1	NM 001168249;NM 080629;NM 08	TSS1500;TSS1500;TSS1500;TSS1500	
ce10691490	2,57E-07	0,0025	-0,1242	Included	chr1	103716210	-		OpenSea				Yes
ce00583780	7.75E-05	0.0347	-0.1067	Included	chr1	105031120	+		OpenSea				
ce11452679	1.48E-07	0.0022	-0.1307	Included	chr1	105214890	-		OpenSea				Yes
ce26004771	1.42E-05	0.0163	0.1047	Included	chr1	178456093	-	chr1:178455799-178456286	Island				Yes
cg23898184	2,98E-06	0,0082	0,1183	Included	chr1	192921219	-		OpenSea				
ce10382206	7,97E-05	0,0349	-0,1101	Included	chr1	209373448	-		OpenSea				
ce18086868	5.86E-06	0.0109	-0.1011	Included	chr1	220463627	+		OpenSea				
ce04095097	3.06E-05	0.0229	-0.1100	Included	chr10	15515112	+		OpenSea				
ce06379027	4.19E-06	0.0097	-0.1334	Included	chr10	21179133	+		OpenSea	NEBL:NEBL:NEBL	NM 006393:NM 213569:NM 00117	Bodv:Bodv:Bodv	Yes
cg07541020	0,0001	0,0399	0,1082	Included	chr10	44068714	+	chr10:44069359-44070179	N Shore	ZNF239;ZNF239;ZNF239	NM 001099284;NM 001099282;NM	5'UTR;5'UTR;5'UTR	
ce18768136	5,04E-05	0,0289	0,1198	Included	chr10	52096068	+		OpenSea	SGMS1	NM 147156	Body	
ce12848457	0.0002	0.0481	-0.1152	Included	chr10	52566320	+		OpenSea				Yes
ce00332393	7.01E-05	0.0331	-0.1294	Included	chr10	54277038	-		OpenSea				
ce24059708	1.60E-05	0.0172	-0.1677	Included	chr10	57170612	+		OpenSea				Yes
cg02281493	5,18E-05	0,0292	-0,1209	Included	chr10	67086005	-		OpenSea				Yes
cg09355528	8,53E-06	0,0129	-0,1086	Included	chr10	71712830	+		OpenSea	COL13A1;COL13A1;COL13A1;COL13A1;C	NM 080798;NM 080809;NM 08080	Body;Body;Body;Body;Body;Body;Body;B	Yes
ce21324555	2.44E-05	0.0207	0.1158	Included	chr10	72648679	-	chr10:72647738-72648317	S Shore	PCBD1:PCBD1	NM 001289797:NM 000281	TSS1500:TSS200	
ce10592592	1.47E-11	5.6754E-06	-0.1228		chr10	74034663	-	chr10:74033167-74034698	Island	DDIT4	NM 019058	Bodv	Yes
cg20897136	2,09E-08	0,0008	-0,1187	Included	chr10	74034667	-	chr10:74033167-74034698	Island	DDIT4	NM 019058	Body	Yes
cg04858631	7,09E-06	0,0119	-0,1243	Included	chr10	74035570	-	chr10:74033167-74034698	S Shore	DDIT4	NM 019058	3'UTR	
ce14812036	0,0001	0,0434	0,1196	Included	chr10	82895774	+		OpenSea				
ce19683655	9.28E-06	0.0133	0.1149	Included	chr10	85440299	-		OpenSea				
ce21859615	1.35E-06	0.0056	0.1065	Included	chr10	86708533	-		OpenSea				
cg13463988	6,99E-05	0,0330	-0,1082	Included	chr10	87676204	+		OpenSea	GRID1	NM 017551	Bodv	
cg01102638	2,28E-07	0,0024	0,1829	Included	chr10	87679282	+		OpenSea	GRID1	NM 017551	Bodv	
cg09919819	5,76E-07	0,0036	-0,1029		chr10	100134713	-		OpenSea				
ce19316579	4.26E-05	0.0265	-0.1361	Included	chr10	100843963	-		OpenSea	HPSE2:HPSE2:HPSE2:HPSE2	NM 001166244:NM 001166245:NM	Bodv:Bodv:Bodv:Bodv	Yes
ce02860671	7.88E-06	0.0125	0.1321	Included	chr10	103469861	-		OpenSea				
cg09796529	2,96E-05	0,0226	0,1131	Included	chr10	128771081	+		OpenSea	DOCK1;DOCK1	NM 001290223;NM 001380	Body;Body	
cg14939821	0,0002	0,0471	0,1177	Included	chr10	128947230	+		OpenSea	DOCK1;FAM196A	NM 001380;NM 001039762	Body;Body	
ce19966745	0,0001	0,0445	-0,1106	Included	chr10	134965215	-		OpenSea				
ce00423364	1.03E-05	0.0139	-0.1089	Included	chr11	850952	-	chr11:849087-850982	Island	TSPAN4:TSPAN4:TSPAN4:TSPAN4:TSPAN	NM 001025239:NM 001025237:NM	5'UTR:Bodv:Bodv:Bodv:Bodv:Bodv	Yes
ce12856550	8.12E-08	0.0017	-0.1166	Included	chr11	6348423	+		OpenSea				Yes
cg09535011	3,09E-05	0,0230	0,1121	Included	chr11	18601039	-		OpenSea	UEVLD;UEVLD;UEVLD;UEVLD;UEVLD;UEV	NM 001261385;NM 001261385;NM	5'UTR;1stExon;Body;Body;Body;Body;Bod	
cg03465399	5,98E-05	0,0312	0,1233	Included	chr11	40422876	+		OpenSea	LRRC4C;LRRC4C	NM 001258419;NM 020929	5'UTR;5'UTR	Yes
cg25598685	2,73E-06	0,0079	-0,2075	Included	chr11	42617544	+		OpenSea				Yes
ce15119262	0.0002	0.0465	0.1047	Included	chr11	70827457	-		OpenSea	SHANK2	NM 012309	Bodv	
ce10832886	2.07E-05	0.0190	0.1294	Included	chr11	76058702	+		OpenSea				
cg09407810	2,91E-05	0,0226	0,1069	Included	chr11	81498753	-		OpenSea				
cg07236114	5,99E-07	0,0037	-0,1843		chr11	84254533	-		OpenSea	DLG2;DLG2	NM 001142699;NM 001364	Body;Body	Yes
cg19981409	8,32E-05	0,0357	-0,1147	Included	chr11	89225042	-	chr11:89224416-89224718	S Shore	NOX4;NOX4;NOX4;NOX4	NM 001143836;NM 016931;NM 00	TSS1500;TSS1500;5'UTR;TSS1500	Yes
ce14384230	1.33E-05	0.0158	-0.1705	Included	chr11	90471056	+		OpenSea	DISC1FP1	NR 104190	Bodv	Yes
ce02719051	5.90E-05	0.0310	0.1154	Included	chr11	122735061	-		OpenSea	CRTAM:CRTAM	NM 001304782:NM 019604	Bodv:Bodv	
cg07085632	3,85E-06	0,0094	-0,1058	Included	chr11	125974404	-		OpenSea				
cg12787465	3,13E-09	0,0002	-0,1045	Included	chr12	6876717	-	chr12:6875481-6876923	Island	PTMS	NM 002824	Bodv	
cg16116203	2,61E-12	2,0184E-06	-0,2345		chr12	6876922	+	chr12:6875481-6876923	Island	PTMS	NM 002824	Bodv	Yes
ce18732361	5.29E-10	4.5532E-05	-0.2418	Included	chr12	6877080	-	chr12:6875481-6876923	S Shore	PTMS	NM 002824	Bodv	
ce12403132	2.57E-05	0.0212	0.1297	Included	chr12	17551396	-		OpenSea				
cg25600766	2,99E-06	0,0082	0,1035	Included	chr12	22486484	+	chr12:22486835-22488666	N Shore	ST8SIA1	NM 003034	Body	
cg15026637	1,63E-05	0,0172	0,1022	Included	chr12	43295760	+		OpenSea				
ce12253175	7.23E-07	0.0041	-0.1791		chr12	58132093	+	chr12:58132478-58132734	N Shore	AGAP2:AGAP2	NM 001122772:NM 014770	TSS200:Bodv	
cg09596958	5.70E-06	0.0108	-0.1451		chr12	58132105	+	chr12:58132478-58132734	N Shore	AGAP2:AGAP2	NM 001122772:NM 014770	TSS200:Bodv	
ce17921464	7.95E-06	0.0125	-0.1475		chr12	58132114	+	chr12:58129828-58130361	S Shore	AGAP2:AGAP2	NM 001122772:NM 014770	TSS200:Bodv	
cg08425810	4,02E-06	0,0096	-0,2773		chr12	58132558	-	chr12:58132478-58132734	Island	AGAP2;AGAP2	NM 001122772;NM 014770	TSS1500;Body	
cg01353646	7,54E-05	0,0342	-0,1024	Included	chr12	58132733	+	chr12:58132478-58132734	Island	AGAP2;AGAP2	NM 001122772;NM 014770	TSS1500;Body	
ce07170300	0.0001	0.0444	-0.1352	Included	chr12	59434386	+		OpenSea				
ce17000939	8.73E-08	0.0018	-0.1328		chr12	75688237	+		OpenSea	CAPS2:CAPS2:CAPS2:CAPS2	NM 001286547:NM 032606:NM 00	Bodv:Bodv:Bodv:5'UTR	Yes
ce09884851	4.61E-06	0.0099	0.1022	Included	chr12	79809356	-		OpenSea	SYT1:SYT1:SYT1	NM 005639:NM 001135805:NM 00	Bodv:Bodv:Bodv	Yes
cg15051463	6,76E-08	0,0017	0,1209	Included	chr12	81602112	+		OpenSea	ACSS3	NM 024560	Body	
cg07272474	3,31E-05	0,0236	0,1097	Included	chr12	82386333	+		OpenSea	LOC101928449	NR 110089	Body	Yes
ce10866060	1.46E-05	0.0165	-0.1207	Included	chr12	83592588	-		OpenSea				Yes
ce16717793	1.17E-05	0.0149	-0.1431	Included	chr12	87730921	+		OpenSea				Yes
ce23615096	4.23E-05	0.0265	0.1648	Included	chr12	109548846	-	chr12:109548899-109549174	N Shore				
cg16797699	8,98E-07	0,0044	-0,1086	Included	chr12	109569084	+		OpenSea				
cg10659908	0,0001	0,0434	0,1716	Included	chr12	109796147	-		OpenSea	LINC01486	NR 120462	Body	
ce04562491	1.10E-07	0.0020	0.1241	Included	chr12	113495386	+	chr12:113494389-113495534	Island	DTX1	NM 004416	TSS1500	Yes
ce01660863	5.16E-05	0.0292	0.2297	Included	chr12	129399528	+		OpenSea	GLT1D1	NM 144669	Bodv	
ce25230907	6.27E-05	0.0318	0.1160		chr13	20624124	+		OpenSea	ZMYM2:ZMYM2:ZMYM2:ZMYM2	NM 001190964:NM 001190965:NM	Bodv:Bodv:Bodv:Bodv	
cg09203312	0,000178218	0,0485	-0,1009	Included	chr13	20805196	+	chr13:20806016-20806867	N Shore	GJB6;GJB6;GJB6;GJB6;GJB6	NM 001110220;NM 001110219;NM	5'UTR;5'UTR;5'UTR;5'UTR;1stExon	
cg24350296	1,77E-05	0,0180	-0,1091	Included	chr13	24144486	+		OpenSea	TNFRSF19	NM 148957	TSS1500	
ce24498885	8.21E-05	0.0355	0.1062	Included	chr13	45770307	+		OpenSea	KCTD4:GTF2F2	NM 198404:NM 004128	5'UTR:Bodv	
ce18321943	0.000126198	0.0422	-0.1178	Included	chr13	61990113	-		OpenSea	PCDH20	NM 022843	TSS1500	
ce19868495	1.11E-07	0.0020	-0.1496		chr13	61995249	+		OpenSea				Yes
cg00158092	6,67E-05	0,0324	0,1065	Included	chr13	64210567	+		OpenSea				Yes
cg19935923	7,81E-06	0,0125	-0,1193	Included	chr13	80145898	+		OpenSea				
ce09995544	4.00E-05	0.0259	0.1183	Included	chr13	114015757	+	chr13:114017866-114018463	N Shelf	GRTP1-AS1:GRTP1-	NR 120385:NR 046541:NM 0012867	Bodv:Bodv:Bodv:Bodv	
ce27565337	8.47E-05	0.0360	0.1143	Included	chr13	114856062	+	chr13:114849000-114852746	S Shelf	RASA3	NM 007368	Bodv	
cg02257791	3,51E-05	0,0243	-0,1015	Included	chr14	22217085	+		OpenSea				
cg06351481	3,18E-10	3,0767E-05	-0,1670		chr14	24642219	+	chr14:24641053-24642220	Island	REC8;REC8	NM 001048205;NM 005132	Body;Body	
cg16094352	1,41E-08	0,0006	-0,1410	Included	chr14	24642317	-	chr14:24641053-24642220	S Shore	REC8;REC8	NM 001048205;NM 005132	Body;Body	
ce04188756	3,25E-05	0,0234	0,1507	Included	chr14	33162448	-		OpenSea	AKAP6	NM 004274	Bodv	
ce13954320	6.87E-05	0.0328	0.1054		chr14	33162558	+		OpenSea	AKAP6	NM 004274	Bodv	
cg09856074	4,54E-06	0,0099	-0,1810	Included	chr14	51853814	-		OpenSea				
cg19512582	8,27E-06	0,0127	-0,1067	Included	chr14	61083516	+		OpenSea				Yes
cg02275035	5,36E-06	0,0106	-0,1017	Included	chr14	70327025	-		OpenSea				
ce23830794	5.62E-05	0.0301	0.1398	Included	chr14	94476186	-		OpenSea	LINC00521	NR 024183	Bodv	
ce21878356	4.34E-06	0.0098	-0.1143	Included	chr14	95759068	+		OpenSea	CLMN	NM 024734	Bodv	
cg03242507	3,94E-05	0,0257	0,1070	Included	chr15	36649226	+		OpenSea				
cg06871560	3,34E-08	0,0011	-0,1928	Included	chr15	52944233	+		OpenSea	KIAA1370	NM 019600	Body	Yes
cg17766654	1,54E-10	2,3794E-05	-0,2942		chr15	52944269	+		OpenSea	FAM214A;FAM214A;FAM214A	NM 001286495;NR 104457;NM 019	TSS200;Body;Body	Yes
cg07491514	2,93E-10	3,0767E-05	-0,2043		chr15	52944329	-		OpenSea	FAM214A:FAM214A:FAM214A	NM 001286495:NR 104457:NM 019	TSS200:Bodv:Bodv	Yes
ce06977984	1.45E-10	2.3794E-05	-0.2057		chr15	52944386	-		OpenSea	FAM214A:FAM214A:FAM214A	NM 001286495:NR 104457:NM 019	TSS200:Bodv:Bodv	Yes
cg04710700	0,00018446$	0,0493	0,1570	Included	chr15	84559114	+		OpenSea	ADAMTSL3;ADAMTSL3	NM 207517;NM 001301110	Body;Body	
ce06476519	5,87E-05	0,0309	-0,1119	Included	chr15	84723616	+		OpenSea				Yes
cg08951051	5,49E-06	0,0107	-0,1410	Included	chr16	4993543	-		OpenSea				Yes
cg12564453	6,23E-05	0,0317	0,1087	Included	chr16	56995840	+		OpenSea	CETP:CETP	NM 000078:NM 000078	5'UTR:1stExon	Yes
ce16660091	0.000191667	0.0500	0.1085		chr16	56995856	+		OpenSea	CETP:CETP	NM 000078:NM 000078	5'UTR:1stExon	Yes
cg01838114	2,98E-05	0,0226	-0,1021		chr16	71547733	-		OpenSea				Yes
cg04252928	1,07E-05	0,0142	0,1695	Included	chr16	89168599	-	chr16:89167116-89167482	S Shore	ACSF3;ACSF3;ACSF3	NM 174917;NR 023316;NM 001127	Body;Body;Body	
cg04069539	1,73E-05	0,0178	0,1115	Included	chr16	89168963	-	chr16:89167116-89167482	S Shore	ACSF3;ACSF3;ACSF3	NM 174917;NR 023316;NM 001127	Body;Body;Body	
ce06663305	0.00016539	0.0471	0.1055	Included	chr17	8095813	-	chr17:8092418-8093706	S Shelf				
ce03382923	1.85E-06	0.0067	0.1127	Included	chr17	17929854	+		OpenSea	ATPAF2	NM 145691	Bodv	
cg23008871	0,00014268$	0,0441	0,1087	Included	chr17	45949743	-	chr17:45949676-45949885	Island				
cg06602723	2,58E-05	0,0212	-0,1000	Included	chr17	46693336	-	chr17:46695325-46695553	N Shore	HOXB8	NM 024016	TSS1500	
cg13308964	4,02E-05	0,0259	-0,1501	Included	chr17	69029659	+		OpenSea				
ce17291648	6.37E-06	0.0113	-0.1655		chr17	69029804	+		OpenSea				
ce06459104	8.86E-05	0.0368	0.1149	Included	chr18	5456880	+		OpenSea	EPB41L3	NM 012307	Bodv	
ce16862127	7,55E-05	0,0342	-0,1289		chr18	6219348	+		OpenSea	L3MBTL4	NM 173464	Body	
cg06794977	4,54E-05	0,0274	-0,1235	Included	chr18	6401565	+		OpenSea	L3MBTL4	NM 173464	5'UTR	
cg03513978	7,90E-06	0,0125	-0,1211	Included	chr18	25616805	-		OpenSea	CDH2:CDH2	NM 001308176:NM 001792	TSS1500:Bodv	
cg07018856	1,72E-07	0,0022	0,1124		chr18	25619216	-		OpenSea	CDH2	NM 001792	Body	
cg23244545	6.30E-07	0.0037	0.1058	Included	chr18	25621544	+		OpenSea	CDH2	NM 001792	Bodv	
cg22332722	3,45E-08	0,0011	-0,2289		chr18	25754857	-	chr18:25755414-25758175	N Shore	CDH2	NM 001792	Body	
cg23074481	5,52E-07	0,0036	-0,1239	Included	chr18	25867090	+		OpenSea				Yes
cg22650569	1,51E-09	0,0001	-0,1555	Included	chr18	26121656	+		OpenSea				Yes
ce11145269	2.22E-06	0.0073	-0.1327	Included	chr18	30192761	-		OpenSea				Yes
ce10157663	2.27E-05	0.0200	0.1794	Included	chr18	30696472	-		OpenSea	CCDC178:CCDC178:CCDC178	NM 001308126:NM 001105528:NM	Bodv:Bodv:Bodv	
cg26944958	4,67E-05	0,0278	0,1270	Included	chr18	41659760	-		OpenSea				
cg26156699	4,52E-07	0,0033	-0,1141	Included	chr18	57417334	-		OpenSea				Yes
cg03503934	0,000185746	0,0494	0,1039	Included	chr18	57814763	-		OpenSea				
ce26286826	0.00018824	0.0496	0.1292	Included	chr18	65085608	-		OpenSea				
ce00603097	0.000160867	0.0465	-0.1407	Included	chr18	72125359	-	chr18:72123606-72124717	S Shore	FAM69C	NM 001044369	TSS1500	
cg13218688	4,51E-05	0,0273	-0,1200		chr18	72125544	-	chr18:72123606-72124717	S Shore	FAM69C	NM 001044369	TSS1500	
cg22395733	7,09E-05	0,0332	-0,1207	Included	chr18	73971202	+		OpenSea				
ce06511149	4.19E-06	0.0097	0.1280	Included	chr19	30469222	+		OpenSea	URI1:URI1:URI1	NM 001252641:NR 045557:NM 003	Bodv:Bodv:Bodv	
ce16307919	8.11E-08	0.0017	0.1042	Included	chr19	44112112	+		OpenSea	ZNF428	NM 182498	Bodv	
ce09612768	7.34E-06	0.0120	0.1169		chr19	46946599	+		OpenSea				
cg24485927	7,72E-06	0,0125	-0,1044	Included	chr2	795989	+		OpenSea				
cg18152887	1,44E-05	0,0164	-0,1305	Included	chr2	920593	+		OpenSea				
cg03290846	1.86E-05	0.0184	-0.1073	Included	chr2	6327032	+		OpenSea				
ce25547830	0.000173444	0.0480	-0.1185	Included	chr2	35402075	+		OpenSea				Yes
ce13711653	4.55E-05	0.0274	-0.1088	Included	chr2	79840412	-		OpenSea	CTNNA2:CTNNA2:CTNNA2:CTNNA2	NM 001164883:NM 004389:NM 00	5'UTR:5'UTR:5'UTR:Bodv	
ce14170358	4,20E-06	0,0097	-0,1038	Included	chr2	88527345	+		OpenSea				
cg08916461	0,000110989	0,0403	-0,1113	Included	chr2	105031896	+		OpenSea				
ce03983336	9.87E-05	0.0384	-0.1051	Included	chr2	108602542	+	chr2:108602824-108603467	N Shore	SLC5A7	NM 021815	TSS1500	
ce08317907	4.65E-06	0.0099	-0.1033	Included	chr2	156490617	+		OpenSea				Yes
ce13776884	6.12E-07	0.0037	-0.1242	Included	chr2	176608868	+		OpenSea				Yes
cg04351607	5,87E-05	0,0309	-0,2023	Included	chr2	181276670	+		OpenSea				Yes
cg13659405	2,86E-06	0,0081	-0,1113	Included	chr2	189890245	-		OpenSea				Yes
ce25225763	0.000102794	0.0390	-0.1322	Included	chr2	190075588	+		OpenSea				
ce20115418	7.77E-05	0.0347	0.1475	Included	chr2	198702850	+		OpenSea	PLCL1	NM 006226	Bodv	
cg27474897	0,000112266	0,0405	0,1136	Included	chr2	199480893	-		OpenSea				
cg08475042	2,99E-06	0,0082	-0,1309	Included	chr2	210682860	-		OpenSea	UNC80;UNC80	NM 032504;NM 182587	Body;Body	
cg00724989	6,26E-06	0,0113	-0,1010	Included	chr2	214616504	+		OpenSea	SPAG16;SPAG16;SPAG16	NR 047660;NR 047659;NM 024532	Body;Body;Body	

cg08401872	5,30E-07	0,0035	-0,1135	Included	chr2	218487226	-		OpenSea	DIRC3	NR 026597	Body	
cg20225999	4,60E-05	0,0276	-0,1299		chr2	218843435	+	chr2:218843460-218843742	N Shore				
cg07616871	3,31E-05	0,0236	-0,1361		chr2	218843504	+	chr2:218843460-218843742	Island				
cg05783384	7,81E-05	0,0348	-0,1326	Included	chr2	218843735	-	chr2:218843460-218843742	Island				
cg18951332	5,19E-05	0,0292	-0,1204	Included	chr2	220777552	-		OpenSea				
cg15595588	3,51E-05	0,0243	-0,1017	Included	chr2	223185738	-	chr2:223183013-223185468	S Shore				Yes
cg07554758	0,000104799	0,0393	0,1657	Included	chr2	223904541	+		OpenSea				
cg25614265	6,49E-05	0,0322	0,2045		chr2	223924453	-		OpenSea				
cg12233487	4,70E-05	0,0278	-0,1037	Included	chr20	2517085	-		OpenSea	TMC2	NM 080751	TSS200	
cg20846768	0,000141885	0,0441	0,1235	Included	chr20	6145814	+		OpenSea				Yes
cg24933489	9,72E-06	0,0137	-0,1101	Included	chr20	11550004	-		OpenSea				
cg19628072	2,21E-05	0,0196	-0,1084		chr20	22446131	-		OpenSea				
cg20659967	1,79E-05	0,0180	-0,1384		chr20	22588572	+		OpenSea	LINC01384	NR 109883	TSS1500	
cg11092487	6,14E-05	0,0316	-0,1115		chr20	33585188	-	chr20:33585039-33585450	Island	MYH7B	NM 020884	Body	
cg02209770	1,36E-05	0,0160	0,1331		chr20	35062903	-	chr20:35064516-35064810	N Shore	DLGAP4	NM 014902	Body	
cg11479256	1,58E-05	0,0170	-0,1027		chr20	44872915	-	chr20:44875253-44875454	N Shelf	CDH22	NM 021248	Body	
cg09204484	4,30E-05	0,0266	-0,1221		chr20	60475464	-		OpenSea	CDH4;CDH4;CDH4	NM 001794;NM 001252338;NM 00	Body;Body;Body	
cg09184271	4,69E-05	0,0278	0,1029		chr21	14917769	+		OpenSea	LOC102724188	NR 110544	TSS1500	
cg05713399	6,76E-05	0,0326	0,1442		chr21	17675215	-		OpenSea	MIR99AHG:MIR99AHG:MIR99AHG:MIR9	NR 027790:NR 111005:NR 111004:	Body:Body:Body:Body	
cg00285225	0,000141548	0,0441	-0,1194		chr21	24757350	-		OpenSea	D21S2088E	NR 040254	TSS200	Yes
cg05156137	7,42E-05	0,0341	0,1437		chr21	35898975	-		OpenSea	RCAN1;RCAN1;RCAN1	NM 203417;NM 004414;NM 20341	5'UTR;Body;1stExon	
ce13528349	0,000102678	0,0390	0,1161		chr21	35899082	-		OpenSea	RCAN1:RCAN1:RCAN1:RCAN1:RCAN1:RC	NM 001285392:NM 001285391:NM	TSS1500:TSS1500:1stExon:5'UTR:Body:Bo	
ce12020137	0,000148724	0,0446	0,1422		chr21	39083071	-		OpenSea	KCNJ6	NM 002240	Body	
ce02725398	1,94E-06	0,0068	-0,1245	Included	chr3	9988144	-	chr3:9987895-9989619	Island	PRRT3	NM 207351	Body	
cg24084693	1,84E-07	0,0022	-0,1036	Included	chr3	28013305	-		OpenSea				
cg08043536	1,67E-05	0,0175	-0,1322	Included	chr3	28071539	-		OpenSea				Yes
ce12982775	1,22E-05	0,0152	0,1049	Included	chr3	36668218	-		OpenSea				
ce25959131	5,85E-05	0,0309	-0,1130	Included	chr3	50855436	-		OpenSea	DOCK3	NM 004947	Body	
ce08731961	5,38E-05	0,0297	0,1642		chr3	50988282	-		OpenSea	DOCK3	NM 004947	Body	
cg23759448	2,51E-05	0,0210	0,1336		chr3	57432353	-		OpenSea	DNAH12	NM 001291661	Body	
cg09473396	6,78E-06	0,0116	-0,1099	Included	chr3	65131979	-		OpenSea				
ce06789445	1,19E-06	0,0053	-0,1349	Included	chr3	69942668	+		OpenSea	MITF:MITF:MITF:MITF	NM 198177:NM 198159:NM 00672	Body:Body:Body:Body	Yes
ce02076100	5,64E-06	0,0108	0,1571	Included	chr3	77369657	-		OpenSea	ROBO2:ROBO2:ROBO2:ROBO2:ROBO2	NM 001290065:NM 002942:NM 00	5'UTR:Body:Body:Body:Body	
ce21090457	5,28E-05	0,0295	-0,1750	Included	chr3	77573709	+		OpenSea	ROBO2:ROBO2	NM 001128929:NM 002942	Body:Body	Yes
ce15823315	1,88E-07	0,0022	-0,1906	Included	chr3	85130923	+		OpenSea	CADM2;CADM2	NM 001167675;NM 001167674	Body;Body	Yes
ce17754500	9,93E-07	0,0047	0,3220	Included	chr3	99224966	+		OpenSea				Yes
ce19229209	2,63E-06	0,0078	-0,1478	Included	chr3	99440401	+		OpenSea	COL8A1:COL8A1:MIR548G	NM 001850:NM 020351:NR 031662	5'UTR:5'UTR:Body	
ce15788038	2,53E-07	0,0025	0,1265	Included	chr3	100610093	-		OpenSea	ABI3BP	NM 015429	Body	
ce12182020	4,43E-05	0,0271	0,1471	Included	chr3	103687842	-		OpenSea				Yes
ci15941063	5,19E-05	0,0292	0,1428	Included	chr3	106233545	-		OpenSea				
ce13358761	1,92E-05	0,0185	0,1073	Included	chr3	109056802	-		OpenSea	DPPA4	NM 018189	TSS1500	
ce08755525	2,15E-05	0,0194	-0,1083	Included	chr3	110344467	-		OpenSea				
ce12974379	0,000127739	0,0424	-0,1122	Included	chr3	110788738	+	chr3:110790149-110791401	N Shore	PVRL3-AS1	NR 045114	Body	Yes
ce25779782	5,41E-05	0,0297	0,1128	Included	chr3	124840638	-		OpenSea	SLC12A8:SLC12A8	NM 001195483:NM 024628	Body:Body	
ce26014782	1,28E-05	0,0156	0,1225		chr3	124840721	+		OpenSea	SLC12A8;SLC12A8	NM 001195483;NM 024628	Body;Body	
ce13084360	0,000167076	0,0473	0,1164	Included	chr3	134496358	+		OpenSea				
ce02785222	4,88E-07	0,0034	0,2956	Included	chr3	138892919	-		OpenSea				Yes
ce15901796	0,000128274	0,0424	-0,1029	Included	chr3	146521668	+		OpenSea				
cg01849284	5,44E-05	0,0297	0,1809	Included	chr3	178336190	-		OpenSea	KCNMB2;KCNMB2;KCNMB2-	NM 001278911;NM 005832;NR 126	5'UTR;5'UTR;Body;Body;5'UTR	Yes
cg05892994	2,00E-05	0,0188	-0,1029	Included	chr3	180522985	+		OpenSea	LOC101928882	NR 109986	Body	Yes
ce20060398	3,42E-05	0,0239	-0,1637		chr3	181473901	+		OpenSea				
ce27657132	2,77E-05	0,0221	-0,1266	Included	chr3	181898731	+		OpenSea				
ce23651889	3,70E-07	0,0028	0,1159	Included	chr3	188115336	-		OpenSea	LPP:LPP:LPP	NM 001167672:NM 001167671:NM	5'UTR:5'UTR:5'UTR	
cg07228359	3,30E-07	0,0027	0,1022	Included	chr3	190419123	+		OpenSea				
cg17430979	6,28E-05	0,0319	0,1184	Included	chr4	6034828	-		OpenSea	JAKMIP1	NM 001099433	Body	
ce20793532	0,000152484	0,0452	0,1111	Included	chr4	6344361	-		OpenSea	PPP2R2C;PPP2R2C	NM 181876;NM 020416	Body;Body	
ce07545526	0,00012565	0,0422	0,1175	Included	chr4	13478708	-		OpenSea	RAB28:RAB28:RAB28	NM 001017979:NM 004249:NM 00	Body:Body:Body	Yes
ce12850605	1,90E-05	0,0185	0,1092	Included	chr4	16272758	+		OpenSea				
cg22055989	4,18E-06	0,0097	0,1112	Included	chr4	26060275	-		OpenSea				
cg18825766	0,000185285	0,0494	-0,1003	Included	chr4	27362758	-		OpenSea				Yes
cg21675464	1,50E-05	0,0166	0,1483	Included	chr4	33717878	+		OpenSea				Yes
ce26839512	0,00010971	0,0401	0,1056	Included	chr4	52918489	-	chr4:52917388-52918280	S Shore	SPATA18	NM 145263	Body	
ce13692860	0,000131783	0,0429	-0,1231	Included	chr4	58035366	+		OpenSea				Yes
ci12695778	2,90E-06	0,0082	0,1793	Included	chr4	60684636	-		OpenSea				
ce17185888	1,41E-05	0,0162	0,1124	Included	chr4	66657683	+		OpenSea				
cg24310434	0,000115022	0,0407	-0,1077	Included	chr4	82964312	+	chr4:82965415-82965896	N Shore				Yes
ce24060890	1,87E-05	0,0184	-0,1142	Included	chr4	93229269	-	chr4:93226348-93227007	S Shelf	GRID2	NM 001510	Body	
ce18516067	0,000136446	0,0434	-0,2082	Included	chr4	98239185	+		OpenSea				Yes
ci10179984	1,46E-07	0,0022	-0,1108	Included	chr4	113820081	+		OpenSea	ANK2	NM 001127493	5'UTR	
ci16931969	5,41E-06	0,0106	-0,1495	Included	chr4	113985495	+		OpenSea	ANK2;ANK2;ANK2	NM 001148;NM 001127493;NM 02	Body;Body;Body	Yes
ce18378811	6,66E-05	0,0324	-0,1154	Included	chr4	114900050	+	chr4:114900355-114900810	N Shore	ARSJ;ARSJ	NM 024590;NM 024590	1stExon;5'UTR	
ce01397050	6,34E-08	0,0016	-0,1451		chr4	116894979	+		OpenSea				Yes
ce11755558	2,65E-06	0,0078	0,1390	Included	chr4	122103800	-		OpenSea	TNIP3:TNIP3	NM 001128843:NM 001244764	Body:Body	
cg22819413	2,37E-06	0,0074	-0,1379	Included	chr4	122670640	-		OpenSea				Yes
ci11290351	1,03E-05	0,0139	-0,1134	Included	chr4	122919312	-		OpenSea				
cg01634388	5,38E-05	0,0297	0,1748	Included	chr4	129405035	-		OpenSea				
ce04524417	6,44E-05	0,0321	-0,1372	Included	chr4	129605243	+		OpenSea				
ce17743555	1,90E-05	0,0185	-0,1346	Included	chr4	130467434	-		OpenSea				
cg06099975	4,87E-07	0,0034	-0,1608	Included	chr4	134018369	-		OpenSea	LOC101927359	NR 125885	Body	Yes
cg03147713	2,59E-05	0,0213	-0,1037	Included	chr4	138950261	-		OpenSea				
ce03639671	3,40E-05	0,0239	-0,1104	Included	chr4	145430689	+		OpenSea				Yes
ce23357404	0,000160609	0,0464	0,1116	Included	chr4	145483534	-		OpenSea				Yes
ce06905720	1,49E-05	0,0166	0,2055		chr4	145512579	-		OpenSea				Yes
cg07318204	1,36E-05	0,0160	-0,2273		chr4	145566441	-	chr4:145566242-145567413	Island	HHIP	NM 022475	TSS1500	
cg02524475	1,93E-05	0,0185	-0,1430		chr4	145566595	+	chr4:145566242-145567413	Island	HHIP	NM 022475	TSS1500	Yes
ce13749822	1,29E-05	0,0156	-0,1270	Included	chr4	145566663	-	chr4:145566242-145567413	Island	HHIP	NM 022475	TSS1500	
ce03408024	4,00E-06	0,0096	-0,1055	Included	chr4	147075042	-		OpenSea				
ce25989755	8,33E-06	0,0128	0,1536	Included	chr4	151134483	+		OpenSea	DCLK2:DCLK2:DCLK2	NR 036614:NM 001040261:NM 001	Body:Body:Body	
ci15490177	1,55E-05	0,0169	0,1215	Included	chr4	151540382	+		OpenSea	LRBA;LRBA	NM 006726;NM 001199282	Body;Body	
cg03065175	2,16E-06	0,0072	-0,1658		chr4	155661758	-	chr4:155661678-155661984	Island				
ce00135497	3,68E-05	0,0250	-0,1889		chr4	155661849	-	chr4:155661678-155661984	Island				
ce16610306	2,38E-05	0,0205	0,1116	Included	chr4	157219121	-		OpenSea				
ce17107239	1,83E-05	0,0183	0,1155	Included	chr4	159526798	-		OpenSea	RXFP1:RXFP1:RXFP1:RXFP1:RXFP1:RXFP1	NM 001253730:NM 001253732:NM	Body:5'UTR:5'UTR:Body:Body:Body:Body:	
cg05493407	9,02E-05	0,0369	0,1931	Included	chr4	164816619	+		OpenSea	01-mars	NM 001166373	5'UTR	
cg24308312	3,24E-05	0,0234	-0,1537	Included	chr4	164910272	+		OpenSea	01-mars	NM 001166373	5'UTR	
ce27376282	7,53E-06	0,0122	0,2595	Included	chr4	167893358	+		OpenSea	SPOCK3:SPOCK3:SPOCK3:SPOCK3:SPOCK	NM 001204353:NM 001204354:NM	5'UTR:Body:Body:Body:Body:Body:Body:B	Yes
ce02300027	8,00E-07	0,0043	0,1426	Included	chr4	177711356	+	chr4:177713243-177714457	N Shore	VEGFC	NM 005429	Body	
ce24597353	1,27E-06	0,0054	-0,2207		chr4	177714618	-	chr4:177713243-177714457	S Shore	VEGFC	NM 005429	TSS1500	Yes
cg20791945	7,06E-09	0,0003	-0,1834	Included	chr4	177731880	-		OpenSea				
ci16039660	4,16E-06	0,0097	0,1013	Included	chr4	184686701	+		OpenSea				
ce09120873	1,92E-05	0,0185	0,1087		chr4	184686773	-		OpenSea				
ce22472945	6,68E-05	0,0324	0,1037	Included	chr4	185936478	-	chr4:185937242-185937750	N Shore				
cg19397599	8,63E-06	0,0129	-0,1609	Included	chr5	19768250	-		OpenSea	CDH18:CDH18:CDH18:CDH18	NM 004934:NM 001291956:NM 00	Body:Body:Body:Body	Yes
cg13417066	4,78E-05	0,0281	0,1402	Included	chr5	23012826	+		OpenSea				Yes
cg08160496	4,43E-06	0,0099	0,2153	Included	chr5	33632020	-		OpenSea	ADAMTS12	NM 030955	Body	
ce20576539	0,000100805	0,0387	0,2312	Included	chr5	33642550	-		OpenSea	ADAMTS12	NM 030955	Body	
ce27468328	0,000144483	0,0443	-0,1207		chr5	40909657	-		OpenSea	C7:C7	NM 000587:NM 000587	5'UTR:1stExon	Yes
cg01351601	1,45E-05	0,0164	-0,1288	Included	chr5	42547402	+		OpenSea	GHR;GHR;GHR;GHR;GHR;GHR	NM 001242402;NM 001242403;NM	TSS1500;TSS1500;5'UTR;5'UTR;Body;5'UT	
cg24520368	9,65E-06	0,0136	-0,1197	Included	chr5	50522392	+		OpenSea				Yes
ci12683218	2,52E-05	0,0210	0,1077	Included	chr5	51850304	-		OpenSea				
ce18773977	3,09E-07	0,0026	0,1078	Included	chr5	59678808	-		OpenSea	PDE4D	NM 001165899	5'UTR	
ce05622003	3,17E-07	0,0026	-0,1111		chr5	71234940	+		OpenSea				Yes
cg06335515	9,82E-05	0,0383	0,1073	Included	chr5	71800351	-		OpenSea	ZNF366	NM 152625	5'UTR	
cg05192452	1,67E-05	0,0175	0,1490	Included	chr5	71852759	-		OpenSea				
cg19487738	9,85E-06	0,0138	-0,1006	Included	chr5	87785433	-		OpenSea				
ce16903445	1,48E-05	0,0166	-0,1215	Included	chr5	92371011	+		OpenSea				Yes
ce18766383	0,000113291	0,0406	-0,1110	Included	chr5	92832939	-		OpenSea	FLJ42709:FLJ42709	NR 021491:NR 015369	Body:Body	Yes
cg12977942	1,41E-05	0,0162	-0,1173	Included	chr5	92839308	-		OpenSea	FLJ42709;FLJ42709	NR 021491;NR 015369	Body;Body	Yes
cg01094495	5,07E-05	0,0290	-0,1151	Included	chr5	96633033	-		OpenSea				
ci11780768	9,53E-06	0,0135	-0,1191	Included	chr5	97655532	-		OpenSea				
ce21949355	1,21E-06	0,0053	-0,1017	Included	chr5	107032139	+		OpenSea				
ce11205636	4,34E-05	0,0268	-0,1070	Included	chr5	107108407	+		OpenSea				
cg19152802	9,19E-05	0,0371	0,1295	Included	chr5	109849887	-		OpenSea	MIR548F3;TMEM232	NR 031644;NM 001039763	TSS1500;Body	Yes
cg04017102	3,64E-07	0,0028	-0,1375	Included	chr5	111405936	-		OpenSea				
ci16541222	7,20E-06	0,0119	-0,1499	Included	chr5	111541635	-		OpenSea	EPB41L4A	NM 022140	Body	Yes
ce21321148	3,39E-07	0,0027	-0,1120	Included	chr5	111669022	+		OpenSea	EPB41L4A	NM 022140	Body	Yes
ce00479110	2,85E-11	0,0000	-0,1642		chr5	111963959	-		OpenSea	LOC102467214	NR 104672	TSS200	Yes
cg21760006	2,17E-05	0,0195	-0,1255	Included	chr5	119214672	+		OpenSea				Yes
cg19442021	0,000164416	0,0470	0,1928	Included	chr5	119432237	+		OpenSea				
cg08796299	2,01E-05	0,0188	-0,1555	Included	chr5	119847801	+		OpenSea	PRR16;PRR16;PRR16	NM 001300783;NM 001308087;NM	Body;5'UTR;Body	
ce05006813	5,68E-06	0,0108	-0,1377	Included	chr5	120069936	-		OpenSea				
ce06905511	0,000126696	0,0423	-0,1454	Included	chr5	139062493	+	chr5:139060555-139060934	S Shore	CXXC5	NM 016463	3'UTR	
cg26103104	0,000155056	0,0456	-0,1571	Included	chr5	139490895	+	chr5:139492723-139492966	N Shore				Yes
cg06707825	2,68E-06	0,0078	0,1115	Included	chr5	156559075	-		OpenSea				
ci10392263	8,72E-07	0,0044	0,1016	Included	chr5	177036887	-	chr5:177035351-177035660	S Shore	B4GALT7	NM 007255	3'UTR	Yes
ce00213822	7,08E-05	0,0332	0,1415	Included	chr6	10210316	-		OpenSea				
ce27507960	1,82E-07	0,0022	-0,1579	Included	chr6	26225246	-	chr6:26225386-26225790	N Shore	HIST1H3E	NM 003532	TSS200	Yes
cg26092675	8,92E-08	0,0018	-0,2110		chr6	26225258	-	chr6:26225386-26225790	N Shore	HIST1H3E	NM 003532	TSS200	Yes
cg13836098	1,19E-07	0,0020	-0,1806		chr6	26225268	-	chr6:26225386-26225790	N Shore	HIST1H3E	NM 003532	TSS200	Yes
ce26149875	2,74E-07	0,0025	-0,1999		chr6	26225282	-	chr6:26225386-26225790	N Shore	HIST1H3E	NM 003532	TSS200	Yes
ce12681972	4,64E-08	0,0013	-0,2406		chr6	26225299	-	chr6:26225386-26225790	N Shore	HIST1H3E	NM 003532	TSS200	Yes
cg07922606	2,55E-06	0,0076	-0,1614		chr6	26225389	-	chr6:26225386-26225790	Island	HIST1H3E	NM 003532	1stExon	Yes
cg05037640	1,85E-07	0,0022	-0,1802		chr6	26225407	-	chr6:26225386-26225790	Island	HIST1H3E	NM 003532	1stExon	Yes
cg01603291	1,96E-05	0,0186	-0,1004	Included	chr6	51618661	+		OpenSea	PKHD1;PKHD1	NM 138694;NM 170724	Body;Body	
ce16337165	3,52E-07	0,0028	-0,1641	Included	chr6	53915782	-		OpenSea	MLIP:MLIP	NM 001281746:NM 138569	Body:Body	
ce27535148	1,68E-05	0,0175	0,2158		chr6	70768321	-		OpenSea	COL19A1	NM 001858	Body	Yes
ce02211885	1,23E-05	0,0153	0,1612	Included	chr6	70768372	-		OpenSea	COL19A1	NM 001858	Body	Yes
cg11212463	8,10E-06	0,0126	-0,1255	Included	chr6	76027389	-		OpenSea	FILIP1;FILIP1;FILIP1	NM 001300866;NM 015687;NM 00	Body;Body;Body	
cg20884524	5,37E-06	0,0106	-0,1465	Included	chr6	76108836	-		OpenSea	FILIP1;FILIP1;FILIP1;LOC101928540	NM 001300866;NM 015687;NM 00	Body;Body;Body;Body	Yes
ce27072277	1,47E-06	0,0058	-0,1311	Included	chr6	76141290	+		OpenSea	FILIP1:LOC101928540:FILIP1:FILIP1	NM 001289987:NR 125859:NM 015	Body:Body:5'UTR:5'UTR	Yes
ce19636666	8,96E-07	0,0044	-0,1221	Included	chr6	76234306	+		OpenSea				Yes
ce04504695	2,26E-06	0,0073	-0,1076	Included	chr6	82795545	-		OpenSea				Yes
ci16701167	3,19E-06	0,0084	-0,1252	Included	chr6	84141234	-	chr6:84140412-84140998	S Shore	ME1	NM 002395	TSS1500	
cg21288889	1,72E-06	0,0064	-0,1296	Included	chr6	89792677	+	chr6:89790137-89791781	S Shore	PNRC1	NM 006813	Body	
ce24790356	1,44E-07	0,0022	-0,1921	Included	chr6	97914069	+		OpenSea				Yes
ce09187505	0,000112399	0,0405	0,1327	Included	chr6	106434429	-	chr6:106433984-106434459	Island				
ce17624536	6,66E-05	0,0324	0,1182	Included	chr6	106440910	-	chr6:106441986-106442912	N Shore				
cg01239717	5,47E-05	0,0297	-0,1052	Included	chr6	107077302	+		OpenSea	RTN4IP1;QRSL1;RTN4IP1	NM 032730;NM 018292;NM 03273	5'UTR;TSS200;1stExon	
cg19341652	3,84E-05	0,0254	-0,1552	Included	chr6	116600143	-	chr6:116600494-116601174	N Shore	DSE;TSPYL1	NM 001080976;NM 003309	TSS1500;1stExon	
ce26092983	1,53E-06	0,0060	-0,1127	Included	chr6	120533307	-		OpenSea				Yes
cg07617039	8,43E-05	0,0359	-0,1031	Included	chr6	127438746	+	chr6:127439265-127441072	N Shore	RSPO3	NM 032784	TSS1500	Yes
ce25075347	4,29E-05	0,0266	-0,2380	Included	chr6	133731801	-		OpenSea	EYA4:EYA4:EYA4	NM 172105:NM 172103:NM 00410	Body:Body:Body	
cg27021634	2,16E-05	0,0194	-0,1165	Included	chr6	133761614	+		OpenSea	EYA4;EYA4;EYA4;EYA4;EYA4	NM 004100;NM 172103;NM 00130	Body;Body;Body;Body;Body	
cg07224291	2,63E-10	0,0000	-0,1593	Included	chr6	133777802	-		OpenSea	EYA4;EYA4;EYA4	NM 172105;NM 172103;NM 00410	Body;Body;Body	
ci15276254	8,54E-05	0,0361	0,1353	Included	chr6	147972384	+		OpenSea				
ce20893956	9,37E-05	0,0373	-0,1011	Included	chr6	152126736	+	chr6:152128822-152129771	N Shelf	ESR1:ESR1	NM 001122742:NM 001122741	5'UTR:TSS200	
ce15390122	3,76E-05	0,0251	-0,1348	Included	chr6	152130188	+	chr6:152128822-152129771	S Shore	ESR1:ESR1:ESR1:ESR1:ESR1:ESR1	NM 001122740:NM 001291230:NM	Body:Body:Body:Body:Body:Body	
ci15626350	7,85E-05	0,0348	-0,1506		chr6	152130207	-	chr6:152128822-152129771	S Shore	ESR1;ESR1;ESR1;ESR1	NM 001122740;NM 001122741;NM	Body;Body;Body;Body	
cg18206764	8,89E-05	0,0368	0,1199	Included	chr6	152283837	-		OpenSea	ESR1;ESR1;ESR1;ESR1;ESR1;ESR1	NM 001122740;NM 001291230;NM	Body;Body;Body;Body;Body;Body	
ce06899237	6,22E-05	0,0317	0,1182	Included	chr6	153353519	-		OpenSea	RGS17	NM 012419	Body	
ce09612304	2,02E-05	0,0188	0,2203	Included	chr6	153588652	-		OpenSea				
cg12008779	1,78E-05	0,0180	0,1400	Included	chr6	163881737	+		OpenSea	QKI;QKI;QKI;QKI;QKI	NM 206855;NM 206854;NM 20685	Body;Body;Body;Body;Body	
cg08311646	8,70E-06	0,0129	-0,1599	Included	chr7	8402871	-		OpenSea				Yes
cg05517880	1,93E-05	0,0185	0,1541	Included	chr7	8431527	-		OpenSea				

cg05346619	0,000152344	0,0452	0,2760	Included	chr7	8857497	-			OpenSea				
cg00640055	3,53E-06	0,0090	-0,1427	Included	chr7	11665547	+			OpenSea	THSD7A	NM_015204	Body	
cg19800032	0.00014758	0.0445	-0.1221	Included	chr7	12134189	+			OpenSea				
cg16687095	2.27E-07	0.0024	0.1022	Included	chr7	27086742	-			OpenSea				Yes
cg20846872	1.20E-05	0.0151	-0.1112	Included	chr7	43004841	+			OpenSea				
cg03873694	0,000107783	0,0399	-0.1016	Included	chr7	43118627	+			OpenSea				
cg14251509	3,68E-05	0,0250	0,1346	Included	chr7	43239400	+			OpenSea	HECW1;HECW1	NM_001287059;NM_015052	5'UTR;5'UTR	
cg17800666	0.000127911	0.0424	-0.1121	Included	chr7	73456886	-			OpenSea	ELN:ELN:ELN:ELN:ELN:ELN:ELN:ELN:ELN:	NM_001278918:NM_001278939:NM	Bodv:Bodv:Bodv:Bodv:Bodv:Bodv:Bodv:B	
cg25670864	2.59E-05	0.0213	-0.1028		chr7	73457080	-			OpenSea	ELN:ELN:ELN:ELN:ELN:ELN:ELN:ELN:ELN:	NM_001278918:NM_001278939:NM	Bodv:Bodv:Bodv:Bodv:Bodv:Bodv:Bodv:B	
cg27367526	7,30E-06	0,0120	-0,1107	Included	chr7	89841692	+	chr7:89840813-89841491	S_Shore	STEAP2;STEAP2;STEAP2	NM_001040665;NM_001040666;NM	5'UTR;TSS1500;5'UTR		Yes
cg06489385	8,01E-06	0,0126	-0,1781		chr7	89842043	+	chr7:89840813-89841491	S_Shore	STEAP2-	NR_110029;NM_001040666;NM_152	TSS1500;TSS1500;5'UTR;5'UTR;5'UTR;5'UT		Yes
cg26424649	8,91E-05	0,0368	-0,1475	Included	chr7	90307521	-			OpenSea				
cg23810564	1.21E-06	0.0053	-0.1269	Included	chr7	90338935	-			OpenSea	CDK14:CDK14:CDK14:CDK14	NM_001287137:NM_001287136:NM	TSS200:TSS200:Bodv:Bodv	Yes
cg19704043	4.60E-06	0.0099	-0.2109	Included	chr7	93116447	+			OpenSea	CALCR:CALCR:CALCR	NM_001164738:NM_001164737:NM	5'UTR:Bodv:5'UTR	Yes
cg13900625	4,07E-05	0,0261	0,1195	Included	chr7	94430374	-			OpenSea				
cg22055479	1,30E-05	0,0157	-0,1191	Included	chr7	110082468	+			OpenSea				Yes
cg09453847	3,03E-05	0,0229	0,2266	Included	chr7	114492046	+			OpenSea				
cg09251068	1.78E-05	0.0180	0.1022	Included	chr7	117421001	+			OpenSea	CTTNBP2	NM_033427	Bodv	
cg18264932	2.40E-05	0.0205	-0.1521	Included	chr7	120414717	-			OpenSea				Yes
cg00029246	5,03E-06	0,0104	0,1198	Included	chr7	137223417	+			OpenSea	DGKI	NM_004717	Bodv	Yes
cg22846800	6,99E-06	0,0118	0,1035	Included	chr7	157004540	+			OpenSea	UBE3C	NM_014671	Bodv	
cg24237626	9.35E-05	0.0373	0.1043	Included	chr8	24540195	+			OpenSea				
cg05913846	3.22E-08	0.0011	0.1809	Included	chr8	50139926	+			OpenSea				
cg05137895	1.10E-07	0.0020	0.2022		chr8	50164320	-			OpenSea				Yes
cg06702849	5,23E-05	0,0294	0,1019	Included	chr8	52560007	+			OpenSea	PXDNL	NM_144651	Bodv	
cg14689479	7,45E-05	0,0341	-0,1251	Included	chr8	53326618	+			OpenSea				
cg02340116	1.61E-05	0.0172	0.1183	Included	chr8	54089593	+			OpenSea				
cg06674311	5.59E-06	0.0107	-0.1531	Included	chr8	58740949	+			OpenSea				
cg24542704	0.000127764	0.0424	0.1105	Included	chr8	64187670	+			OpenSea				
cg16342423	3,60E-06	0,0090	0,1629		chr8	75015350	+			OpenSea				
cg07571020	5,12E-07	0,0034	0,1300	Included	chr8	75015421	+			OpenSea				Yes
cg06997118	0.000174681	0.0481	0.1054	Included	chr8	75015687	+			OpenSea				
cg07146298	1.04E-05	0.0140	-0.1174	Included	chr8	80533246	-			OpenSea	STMN2:STMN2	NM_001199214:NM_007029	Bodv:Bodv	Yes
cg03961824	1.95E-05	0.0186	-0.1241	Included	chr8	82530967	+			OpenSea				
cg22718061	0,000102325	0,0389	0,1160	Included	chr8	84860061	+			OpenSea				
cg13002622	7,07E-06	0,0119	-0,1128	Included	chr8	87737054	+			OpenSea	CNGB3	NM_019098	Body	Yes
cg19496364	1.89E-05	0.0185	-0.1170	Included	chr8	94551463	+			OpenSea				Yes
cg24280820	0.000188429	0.0496	0.1021	Included	chr8	98226672	+			OpenSea	LOC101927066	NR_125390	Bodv	
cg21789008	3.17E-06	0.0084	-0.1185	Included	chr8	118764818	+			OpenSea				Yes
cg13539678	1,39E-06	0,0057	-0,1069		chr8	119394582	-			OpenSea	SAMD12;SAMD12;SAMD12	NR_109794;NM_001101676;NM_207	Body;Body;Body	
cg20519373	2,96E-07	0,0025	-0,2019		chr8	119456570	-			OpenSea	SAMD12;SAMD12	NM_001101676;NM_207506	Body;Body	
cg16692227	2.81E-05	0.0221	-0.1162	Included	chr8	119567541	-			OpenSea	SAMD12:SAMD12	NM_001101676:NM_207506	Bodv:Bodv	
cg11957261	8.27E-07	0.0044	-0.1195	Included	chr8	119727631	+			OpenSea				
cg14764944	9.93E-06	0.0138	0.1461		chr8	123146896	+			OpenSea				Yes
cg21390512	4,19E-05	0,0264	-0,1340		chr8	127568850	+	chr8:127568676-127570873	Island	FAM84B	NM_174911	Bodv		
cg02925049	8,95E-05	0,0369	-0,1186		chr8	127568854	+	chr8:127568676-127570873	Island	FAM84B	NM_174911	Body		
cg13636698	0.000133838	0.0433	-0.1089	Included	chr8	127569019	+	chr8:127568676-127570873	Island	FAM84B	NM_174911	Bodv		
cg08673945	2.63E-05	0.0214	0.1024	Included	chr9	20490677	-			OpenSea	MLLT3:MLLT3	NM_001286691:NM_004529	Bodv:Bodv	
cg02310457	3,31E-05	0,0236	-0,1376	Included	chr9	22682693	+			OpenSea	LINC01239;LINC01239	NR_038977;NR_038977	ExonBnd;Body	Yes
cg09236765	6,62E-05	0,0324	0,1026	Included	chr9	79145898	-			OpenSea				
cg06484220	1.59E-05	0.0171	-0.1091	Included	chr9	89900174	+			OpenSea				
cg05371159	0.000130281	0.0427	0.1287	Included	chr9	94342441	+			OpenSea				
cg20404850	8.19E-06	0.0126	0.1156		chr9	99374660	+			OpenSea	CDC14B:CDC14B	NM_003671:NM_033331	Bodv:Bodv	Yes
cg16107559	2,53E-06	0,0076	-0,1965		chr9	116225834	-	chr9:116225763-116226133	Island	RGS3;RGS3;RGS3	NM_017790;NM_001282923;NM_14	TSS200;TSS200;Body		
cg15823733	2,33E-07	0,0024	-0,1534	Included	chr9	116225992	+	chr9:116225763-116226133	Island	RGS3;RGS3;RGS3;RGS3;RGS3	NM_017790;NM_017790;NM_00128	5'UTR;1stExon;1stExon;5'UTR;Body		

Sample_Group	Cohort #	DYRK1A variant	SVM	SVM score
test	Ind #25	p.Gly168Asp	positive	0,7430
test	Ind #26	p.Arg255Gln	negative	0,0709
test	Ind #27	p.Asp287Val	positive	0,8478
test	Ind #28	p.Ile305Arg	positive	0,9347
test	Ruaud_#2	p.Ser311Phe	positive	0,8190
test	Ind #29	p.Ser324Arg	positive	0,9613
test	Ind #31	p.Tyr462His	negative	0,0242
test	Ind #32	p.Arg467Gln	positive	0,7874
test	Ind #33	p.Gly486Asp	GoF?	0,0008
test	Bronicki_#9	p.Thr588Asn	negative	0,0233
test	Ind #18	p.Ser660fs	positive	0,9275
test_rep	Ind #18_repl	p.Ser660fs_repl	positive	0,9247
KMT2A	-	-	negative	0,0849
KMT2A	-	-	negative	0,0822
KMT2A	-	-	negative	0,0590
KMT2A	-	-	negative	0,0365
KMT2A	-	-	negative	0,0216
KMT2A	-	-	negative	0,0162
KMT2A	-	-	negative	0,0137
KMT2A	-	-	negative	0,0080
ARID1B	-	-	negative	0,0254
ARID1B	-	-	negative	0,0166
ARID1B	-	-	negative	0,0104
ARID1B	-	-	negative	0,0092
Control	-	-	negative	0,1394
Control	-	-	negative	0,1052
Control	-	-	negative	0,0920
Control	-	-	negative	0,0892
Control	-	-	negative	0,0827
Control	-	-	negative	0,0720
Control	-	-	negative	0,0682
Control	-	-	negative	0,0657
Control	-	-	negative	0,0583
Control	-	-	negative	0,0563
Control	-	-	negative	0,0509
Control	-	-	negative	0,0504
Control	-	-	negative	0,0501
Control	-	-	negative	0,0495
Control	-	-	negative	0,0483
Control	-	-	negative	0,0439
Control	-	-	negative	0,0403
Control	-	-	negative	0,0391
Control	-	-	negative	0,0372
Control	-	-	negative	0,0353
Control	-	-	negative	0,0351
Control	-	-	negative	0,0349
Control	-	-	negative	0,0345
Control	-	-	negative	0,0343
Control	-	-	negative	0,0309
Control	-	-	negative	0,0292
Control	-	-	negative	0,0289
Control	-	-	negative	0,0286
Control	-	-	negative	0,0286
Control	-	-	negative	0,0277
Control	-	-	negative	0,0270
Control	-	-	negative	0,0260
Control	-	-	negative	0,0258
Control	-	-	negative	0,0254
Control	-	-	negative	0,0251
Control	-	-	negative	0,0240
Control	-	-	negative	0,0223

Control	-	-	negative	0,0218
Control	-	-	negative	0,0215
Control	-	-	negative	0,0214
Control	-	-	negative	0,0212
Control	-	-	negative	0,0210
Control	-	-	negative	0,0210
Control	-	-	negative	0,0204
Control	-	-	negative	0,0196
Control	-	-	negative	0,0196
Control	-	-	negative	0,0190
Control	-	-	negative	0,0190
Control	-	-	negative	0,0186
Control	-	-	negative	0,0184
Control	-	-	negative	0,0183
Control	-	-	negative	0,0177
Control	-	-	negative	0,0168
Control	-	-	negative	0,0167
Control	-	-	negative	0,0162
Control	-	-	negative	0,0162
Control	-	-	negative	0,0159
Control	-	-	negative	0,0158
Control	-	-	negative	0,0152
Control	-	-	negative	0,0148
Control	-	-	negative	0,0147
Control	-	-	negative	0,0142
Control	-	-	negative	0,0138
Control	-	-	negative	0,0137
Control	-	-	negative	0,0137
Control	-	-	negative	0,0125
Control	-	-	negative	0,0125
Control	-	-	negative	0,0120
Control	-	-	negative	0,0120
Control	-	-	negative	0,0119
Control	-	-	negative	0,0115
Control	-	-	negative	0,0114
Control	-	-	negative	0,0112
Control	-	-	negative	0,0112
Control	-	-	negative	0,0110
Control	-	-	negative	0,0110
Control	-	-	negative	0,0103
Control	-	-	negative	0,0103
Control	-	-	negative	0,0099
Control	-	-	negative	0,0099
Control	-	-	negative	0,0096
Control	-	-	negative	0,0092
Control	-	-	negative	0,0089
Control	-	-	negative	0,0089
Control	-	-	negative	0,0088
Control	-	-	negative	0,0083
Control	-	-	negative	0,0081
Control	-	-	negative	0,0073
Control	-	-	negative	0,0072
Control	-	-	negative	0,0069
Control	-	-	negative	0,0067
Control	-	-	negative	0,0061
Control	-	-	negative	0,0056
Control	-	-	negative	0,0049

Variant			*In silico*		*In vitro* studies				Individuals				Final classification	
Variant	Nb patients	Nb gnomad	CADD	Conserved[1]	Expression	AutoP	Localization	Results previously reported	Report	Clinical features (CS_{DYRK1A})	Inheritance	DNAm profil	ACMG/AMP criteria	Final classification
p.Ser660fs	1	0		NA	NA	NA	Aggr.	NA	*this report* Ind #18	poorly (7.5/20)	**dn**	positive		Lik Patho
p.Ala341Ser	0	89	24,9	midly	100%	100%	ns	NA	-	-	-	-	BS1, BS2, BS3, BP4	Benign
p.Gly168Asp	2	0	31	highly	<50%	0%	ns	NA	*this report* Ind #25	NA	dn	positive	PS2, PS3, PM2, PP3	Patho
									GeneDx (clinvar SCV00057310)	NA	NA	NA		
p.Arg255Gln	1	0	24	midly	100%	100%	ns	NA	*this report* Ind #26	poorly (5/15)	?	negative	BS3, BP4	Lik Benign
p.Asp287Val	3	0	28,9	highly	<25%	0%	ns	drastic decrease of autoP and kinase activity (1)	DDD (Decipher 258963)	highly [a]	dn	NA	PS2, PS3, PM2,PP3, PP4	Patho
									this report Ind #27 (Geneva Hospital, SCV000598121)	interm. (10/15)	dn	positive		
									Tubingen (clinvar SCV00144673)	intermediate [i]	NA	NA		
p.Ile305Arg	1	0	26,9	midly	<25%	0%	ns	NA	*this report* Ind #28	highly (16/20)	dn	positive	PS2, PS3, PM2, PP4	Patho
p.Ser311Phe	2	0	33	moderate	<50%	0%	ns	drastic decrease of autoP and kinase activity (1,2)	Ruaud_#2 (clinvar SCV000586742)	interm. (12,5/20)	dn	positive	PS2, PS3, PM2, PP3	Patho
									GeneDx (clinvar SCV000520979)	NA	NA	NA		
p.Ser324Arg	1	0	28 ,1	highly	80%	<25%	ns	NA	*this report* Ind #29 (SCV000902439)	interm. (10,5/20)	dn	positive	PS2, PS3, PM2, PP3	Patho
p.Glu366Asp*	1	0	35*	midly	100%	100%	ns	NA	*this report* Ind #30	highly (16/20)	dn	NA	PS2, PS3, PM2, PP4, PP3	Patho *
p.Tyr462His	1	0	29,6	midly	100%	100%	ns	NA	*this report* Ind #31	poorly (6,5/20)	dn	negative	PS2, PM2, BS3,	Lik Benign
p.Arg467Gln	4	0	33	highly	<50%	0%	ns	drastic decrease of autoP and kinase activity (1,2)	DDD (Decipher 270174)	poorly [b]	dn	NA	PS2, PS3, PM1, PM2, PP3	Patho
									Posey et al., 2016 (clinvar SCV000245477)	interm.[c]	dn	NA		
									GeneDx (clinvar SCV000534701)	NA	NA	NA		
									this report Ind #32	interm. (10.5/20)	dn	positive		
p.Gly486Asp	2	0	29 ,1	midly	100%	100%	ns	no decrease of kinase acti	Dang et al., 2018	NA	NA	NA	PS2, PM2, BS3	VUS
									this report Ind #33 (Geneva Hospital, SCV000747759)	poorly (2/15) [d]	dn	GoF?		
p.Thr588Asn	1**	0***	22 ,8	midly	100%	100%	ns	no effect on autoP and P	Bronicki_#9 (clinvar SCV000196065 = SCV000965705)**	highly (15.5/20)	dn	negative	PS2, PM2, PP4, BS3, BP4	Lik Benign
p.Arg158His	1	2	29,8	highly	100%	100%	NA	NA	DDD (Deciper _LikBenign)	NA[e]	dn	NA	PS2, PP3, BS2, BS3	Benign
p.Ala277Pro	2	0	28,9	midly	50%	0%	NA	drastic decrease of autoP	DDD (Deciper _Patho)	interm.[f]	dn	NA	PS2, PS3, PM2	Patho
									GeneDx (SCV000571206)	NA	NA	NA		
p.Gly171Arg	1	0	32	highly	50%	0%	NA	NA	Invitae (clinvar SCV000952112.2_LikelyPatho)	interm. [g]	dn	NA	PS2, PS3, PM2, PP3	Patho
p.Leu241Pro	1	0	29 ,7	highly	~50%	0%	NA	NA	EGL diagnostic (clinvar SCV000703832.2 _VUS)	NA	NA	NA	PS3, PM2, PP3	Lik Patho
p.Pro290Arg	1	0	28 ,3	highly	<50%	0%	NA	NA	Ambry (clinvar SCV000741841.1 _VUS)	interm. [h]	NA	NA	PS3, PM2, PP3	Lik Patho

Variant			*In silico*		*In vitro* studies	Individuals			Final classification	
Variant	Nb patients	Nb gnomad	CADD	Highly Conserved[1]	Results previously reported	Report	Clinical features (CS_{DYRK1A})	Inheritance	ACMG/AMP criteria	Final classification
His119Tyr	1	0	22.8	no	no effect on neurite outgrowth (Dang et al.)	Dang et al., 2018	intermediate [a]	NA	PM2, BS3	Lik benign
Lys188Ile	1	0	31	yes	drastic decrease of autoP and kinase activity (Arranz)	Ji et al., 2015 (clinvar SCV000206791_LikPatho)	highly (13/20)	dn	PS2,PS3, PM2, PP3, PP4	Patho
Ala195Thr	1	0	23,4	no	Increase kinase activity (Arranz et al.)?, no effect on neurite outgrowth (Dang et al.)	Dang et al., 2018	poorly [b]	NA	PM2, BS3, BP4	Lik benign
Leu207Pro	1	0	29,5	yes	drastic decrease of autoP and kinase activity (Arranz)	DDD (Decipher 259211_Patho)	intermediate[c]	dn	PS2,PS3, PM2, PP3	Patho
His223Arg	1	0	22 ,0	no	Increase kinase activity (Arranz) et al.?	GeneDx (clinvar SCV000620751_VUS)	NA	NA	PM2, BS3, BP4	Lik benign
Leu245Arg	2	0	29	yes	drastic decrease of autoP and kinase activity (Widowati et al.,Arranz et al.)	Ji et al., 2015 (clinvar SCV000206792_LikPatho)	highly (12/15)	dn	PS2,PS3, PM2, PP4, PP3	Patho
						Baylor college (clinvar SCV000807304_VUS)	intermediate [d]	dn		
Leu259Phe	1	0	24,8	no	Increase kinase activity (Arranz et al.) ?, no effect on neurite outgrowth (Dang et al.)	Dang et al., 2018	poorly [e]	NA	PM2, BS3, BP4	Lik benign
Asp287Tyr	1	0	32	yes	drastic decrease of autoP and kinase activity (Arranz et al;)	Zhang et al., 2015	intermediate [f]	dn	PS2,PS3, PM2, PP3	VUS
Leu295Phe	2	0	29 ,1	yes	slight decrease kinase activity (Widowati et al.,Arranz et al.)	Ji et al., 2015 = SCV000206793 (UCLA_LikPatho)	poorly (5.5/15)	dn	PS2,PS3, PM2, PP3	VUS
						GeneDx Clinvar SCV000321572_Patho)	NA	NA		
Phe308Val	1	0	29 ,1	yes	drastic decrease of autoP and kinase activity (Widowati et al., Arranz et al.)	Chicago Hospital (clinvar SCV000247240_LikPatho)	NA	NA	PS3, PM2, PM2, PP3	Lik patho
Gln313His	0	2	14,5	no	slight decrease kinase activity (Widowati et al.,Arranz et al.)	-	-	-	-	-
Arg325His	1	0	33	yes	drastic decrease of autoP and kinase activity (Arranz et al.)	GeneDx (clinvar SCV000574147_LikPatho)	NA	dn	PS2,PS3, PM2, PP3	Lik patho
Tyr327Cys	1	0	29 ,3	yes	drastic decrease of autoP and kinase activity (Arranz et al.)	BC Hospital (clinvar SCV000599256_LikPatho)	NA	dn	PS2,PS3, PM2, PP3	Lik patho
Arg328Trp	1	0	34	yes	drastic decrease of autoP and kinase activity (Arranz et al.)	GeneDx (clinvar SCV000492371_VUS)	NA	NA	PS3, PM2, PP3	Lik patho
Ser346Phe	1	0	32	yes	drastic decrease of autoP and kinase activity (Arranz et al.)	LMM Cambridge (Clinvar SCV000712522_LikPatho)	intermediate [g]	dn	PS2,PS3, PM2, PP3	Patho
Ser346Pro	2	0	29 ,7	yes	drastic decrease of autoP and kinase activity (Widowati et al.,Arranz et al.)	Bronicki et al., 2015 (Clinvar SCV000196060_LikPatho)	highly [h]	dn	PS2,PS3, PM2, PP3, PP4	Patho
						DDD (decipher 260956_Patho)	intermediate [i]	dn	PS2,PS3, PM2, PP3	Patho
Leu347Arg	1	0	31	yes	drastic decrease of autoP and kinase activity (Arranz et al.)	Trujillano et al., 2017	highly [j]	dn	PS2,PS3, PM2, PP3, PP4	Patho
Arg438His	1	1	33	no	sklight decrease in kinase activity (Arranz et al.)?	Wang et al., 2016	NA	dn	PS2, BS1, BS3	Lik benign
Arg458Met	1	0	32	no	Increase kinase activity (Arranz et al.)?	Dang et al., 2018	NA	NA	BS3, PM2	VUS
Arg528Trp	1	4	24	no	Increase kinase activity (Arranz et al.)?	Chicago Hospital (clinvar SCV000594478_VUS)	NA	NA	BS1, BS3, BP4	Benign

Name	Identifier	Classification	Inheritance	Clinical features
c.1726C>T p.Gln576*	Okamato et al. 2014	considered as disease causing	NA	poorly [a]
c.2040C>A p.Tyr680*	ClinVar (Genedx, SCV000779549.2)	Likely pathogenic	NA	poorly to intermediate [b]
c.2213_2218delinsAGAG p.Thr738fs	ClinVar (Genedx, SCV000570988.4)	Likely pathogenic	*de novo*	intermediate [c]